Jovan P. Šetrajčić
Stevo K. Jaćimovski
Siniša M. Vučenović

PHONON ENGINEERING THEORY OF CRYSTALLINE LAYERED NANOSTRUCTURES

Belgrade, 2016

PHONON ENGINEERING THEORY OF CRYSTALLINE LAYERED NANOSTRUCTURES

Jovan P. Šetrajčić, Stevo K. Jaćimovski, Siniša M. Vučenović

Publisher
ACADEMY OF CRIMINALISTIC AND POLICE STUDIES
196, Cara Dušana Street (Zemun)
Belgrade

Publisher representative
Professor DRAGANA KOLARIĆ, PhD
Acting Dean

Authors
Professor JOVAN ŠETRAJČIĆ, PhD
Professor STEVO JAĆIMOVSKI, PhD
Professor SINIŠA VUČENOVIĆ, PhD

Reviewers
Professor DEJAN RAKOVIĆ, PhD
Professor VJEKOSLAV SAJFERT, PhD

Editor
Professor RADOVAN RADOVANOVIĆ, PhD

Translated by
SLAĐANA ILIĆ

Cover
NEBOJŠA KUJUNDŽIĆ

Impression
100 copies

Printed by
Pekograf, Belgrade

ISBN 978–86-7020-370-9

Contents

I. INTRODUCTION

Over the last decade, we have witnessed a rapid development of nanotechnology, i.e. production technologies of structures with nanodimension [1–3]. The trend of rapid development of nanotechnologies is not accidental since nanostructures possess physical characteristics that are substantially different and qualitatively new from the physical characteristics of the structures which are larger in size. All of the abovementioned leads to the conclusion that nanomaterials can be a good basis for further development of Physics. In a way, nanostructure effects are connected to the effects in bulk structures, similarly to the relationship between quantum and classical effects. Therefore, further and even faster development of the science of nanostructure materials and nanotechnology is to be expected.

Science is nowadays very interested in low-dimensional systems, the dimensions of order of even few nanometers, which, in practical application, demonstrate exceptional characteristics in various fields. The need to minimize dimensions was imposed by a number of interrelated and mutually dependent requests of modern civilization, probably key to its further survival and sustainable development, which can generally be categorized as belonging to the fields of energy, health and ecology. In that sense, the subject of the research in this work will include nanomaterials in the field of biopharmaceutical technology for biomedical application [4–7].

Let us consider in what ways we can make contributions to research in the science. One approach is experimental, while the other is theoretical. There are big differences in the popularity of these approaches, yet both are said to have advantages and disadvantages.

There are two aspectsof theoretical approach. One uses computer resources, while the other uses analytics (literally speaking paper and pencil). The aim of our research group is that within materials science we understand the essential mechanisms of transport processes in low-dimensional systems, so we chose an analytical approach with the ambition that in the very near future, we study with the help of computer resources, too. Our method of choice is the Green's function which we use in the field of molecular crystals

The development of sophisticated techniques for the growth control of very thin layers caused intensive nano-crystalline structures research. One of the basic principles for their production is based on a process of self-construction [8–10], which is one of the "bottom-up" techniques, in which atoms or molecules arrange themselves into low-dimensional structures on the basis of mutual physical-chemical interactions. Improved knowledge of thermodynamics and kinetics of the nano-scale processes, with the advancement of characterization techniques and computer modeling, should lead to the development of complex systems.

Nanoscience continues to advance at a dramatic pace and is making revolutionary contributions in diverse fields, including quantum and optoelectronics, materials science, chemistry, and biology. The technologies needed to fabricate nanoscale structures and devices are advancing rapidly. These technologies have made possible the design and study of a vast array of novel devices, structures and systems confined dimensionally on the scale of 10 nm or less in one or more dimensions [11–13].

I.1. Nano science and phonon nano engineering

Application of nano-structures requires knowledge of their fundamental physical (mechanical, electromagnetic, optical, etc.) characteristics [14–16]. Thermodynamic properties associated with phonon displacements through the nano-samples are particularly interesting. Independent of the type of lattices, the thermodynamics of their subsystems (electrons, excitons, spin waves, etc.) is determined when the subsystem is in thermodynamic equilibrium with phonons [17–19]. Phonons are collective mechanical oscillations of molecules or atoms and represent the most important system of excitations. The reason is simple: phonons are present in all systems and their influence, more or less, changes behavior of all other objects or excitations of the system. The mentioned influence reflects primarily in the fact that they play the role of a thermostat of the system and determine its thermodynamics. Besides, the acoustical characteristics as well as conductive and superconductive properties etc. could not be realistically explained without phonons [20–23].

The main fact concerning phonon properties in nanostructures is absence of the so-called acoustical phonons, i.e. phonons whose energy tends to zero when phonon momentum tends to zero. An activation energy different from zero is necessary for exciting phonons in these structures. Such unexpected characteristics require revision of all conclusions obtained regarding bulk theories of phonons. Therefore, the contribution of phonon subsystems to thermodynamic analysis is the first step in a research of nanostructure properties.

This text describes a major aspect of the effort to understand nanostructures, namely the study of phonons and phonon-mediated effects in structures with nanoscale dimensional confinement in one or more spatial dimensions. During the last two decades there has been a steady effort to understand the optical and acoustic phonons in nanostructures such as the superlattice, quantum wires, nanotubes and quantum dots. The central theme of this paper is the description of the acoustic phonons of the optical type in these nanostructures. As a preliminary to describing the dispersion relations and mode structures for phonons in nanostructures, phonon amplitudes are quantized in terms of the harmonic oscillator approximation, and anharmonic effects leading to phonon decay are described in terms of the dominant phonon decay channels. These elastic and discontinued models are applied to describe the deformation potential and interactions in a variety of nanostructures including layered crystals, firstly – ultrathin films and superlattices. Finally, this paper describes how the dimensional confinement of phonons in nanostructures leads to modifications in the electronic, optical, acoustic, superconducting and thermodynamic properties of the quantum.

Research of the influence of phonons with quantum size and confinement effects in nanostructures is not new. It has been conducted for almost two decades. It is known [23–25] that acoustic phonons affect practically all electronic, thermal and optical properties of semiconductors. They are carriers of heat and together with optical phonons constrain the mobility of electrons in the areas of medium and high temperatures. Reduction of sizes in nanostructures leads to the so-called confinement of phonons due to which the phonon branches are quantized (dimensional quantization) and a substantive modification of their energy spectrum, group velocity and polarization occur. Due to the reflections from the inner surface of the structure, phonon modes hybridize and cease to be purely longitudinal

or purely transverse, and their group velocity is reduced compared to the case in the bulk structure. Dependence of energy on the wave vector is highly nonlinear and linear approximation of the laws of dispersion of phonons in small size nanostructures makes no sense. Changing the phonons dispersion law due to confinement severely affects the kinetic effects conditioned by the interaction of acoustic phonons with electrons, dotted defects, phonon-phonon interaction. Managing transport properties of acoustic phonons through the modification of their energy spectrum in nanostructures was named phonon engineering [26].

The concept of phonon engineering is based on the corresponding changes to the phonon spectrum in order to improve the electric and thermal transport properties of the given nanostructure. In homogeneous layers and nanowires, phonon engineering can be realized on the account of changes in the size of the nanostructure or changes in the quality of exterior surfaces. In this sense, the most advantageous are composite materials composed of layers with different phonon properties. In these structures, general hybridized phonon modes occur, which may originate from the phonon properties of the individual layers or as averaged modes of different layers. By changing the thickness of the layers as well as the types of materials that go into the composite, a different degree of hybridization of the phonon modes can be achieved and thus change thermal transport properties of the structure in a wide range.

A demonstration of phonon engineering is given in a series of papers for the three-layer film heterostructures [26–28]. There the phonon modes are divided into three groups: fluctuations in the inner layer of the coating and general oscillations as a whole. Redistribution of atom displacements between layers leads to attenuations of electron-phonon interaction and to the increase of the mobility of electrons in materials that are coated with other materials.

Unlike in the previous papers [29–31], here we will try to observe the difference between the characteristics of different nano-crystalline structures: ultrathin films and adequate composite films, i.e. superlattices, we were interested in whether the quantum size effects (quantum confinement), quantum (de)coherence and influence of boundary conditions, strengthen or weaken in nanosamples [31–33].

While the theoretical study of the structures which are larger in size generally requires solving differential equations with constant coefficients, difference equations appear in the research of nanostructures, but their coefficients depend on the spatial coordinates due to the necessity to introduce the boundary conditions and the breaking of spatial translational symmetry in the equation, as well as the impact of vacancies and impurities. The most commonly used mathematical structure in solving the problem of difference equations are translational operators [33–35], because their use enables the most efficient reaching of solutions.

The major part of this paper deals with the application of the mentioned methodology of solving difference equations and the problem of structures with broken symmetry along a single crystallographic direction. Furthermore, nanostructures that are translationally invariant in only one direction and structures that do not possess translational invariance have also been studied. The method of Green's functions is generally used here because this method is self-consistent i.e. it solves both the dynamic and thermodynamic sides of the problem. Other methods are used for either one or the other. For example, dynamic

characteristics of the problem can be determined by using the wave function, but in order to solve thermodynamics, one has to resort to methods of Statistical physics. Regardless of this, in some sections of the second part, structure problems were solved by using the wave functions of nanostructures.

Thermal properties of nanostructures have recently attracted a lot of attention. The influence of size effects on thermal conductivity is becoming extremely important for device design and reliability [26–28,32–35]. The problem of thermal management is even more severe for photonic devices such as vertical cavity surface emitting lasers. On the other hand, to improve performance of thermoelectric, one needs to achieve low thermal conductivity. These are two contradictory demands, but both can be approached with appropriate modification of phonon modes, e.g., phonon engineering.

On the basis of the calculated dispersion law and distribution of phonon states in nanoscopic crystals, free energy and entropy will be calculated. Internal energy, as well as heat capacitance, will also be analyzed. Low-temperature behavior of these quantities will be compared to the corresponding ones of bulk-structures. It was shown that heat capacitances of nano-layered structures in low-temperature region were higher than the same quantities of the corresponding bulk sample. In the middle and the highest temperature region, temperature behavior of the inverse: heat capacitance of layered structures was lower than those of the corresponding bulk ones. The consequences were discussed with relation to the better superconductive properties of nano-materials.

The thermal conductivity reduction, while having a negative effect on thermal management of electronic devices, has a positive effect on thermoelectric devices, which require materials with high electrical conductivity, the Seebeck's coefficient, low thermal conductivity and superconductivity [27].In [36,37] authorsreport on the experiments using a conventional semiconductor thin film, where thermal conductivity in planes decreases with decreasing thickness because the thermal transport in such structures is mostly limited by the phonon scattering from the film boundaries. An opposite dependence can be observed in few-layer graphenes where the transport is limited mostly by the lattice inharmoniousness [38–40].

I.1.1. *Nanotechology and nanostructures*

Nanotechnology [41–43] is multidisciplinary field based on the study of processes taking place at the nanometer scale, as well as the design, synthesis and application of materials of nanometric dimensions.It is, therefore, a technology that manipulates the individual atoms, small molecules or a single macromolecule.The development of nanotechnology began when it was found that the reduction of dimensions for the purpose of confinement of elementary excitations movement has the effect of completely altered physical properties of the observed material, compared to macroscopic pattern.

The term "crystal nanostructures" [43–45] means a low-dimensional crystalline systems whose dimensions are in one, two or all three crystallographic directions smaller than the average free path length of the physical properties of carriers in them (dimensions on the order of De Broglie wavelength). In such systems, quantum effects are expressed, resulting in the application of quantum-mechanical description of carriers movement required for the whole structure, and not only within the unit cell.

This reduction in size of the aforementioned structures to atomic scales of dimensions leads to the appearance of significantly different physical properties of the material, which can continuously be changed in a relatively simple manner (for example, by changing the thickness or composition of the material) in a rather wide range. These altered material properties are the result of the following several phenomena.

1. Quantum confinement – confinement of elementary excitations (phonons, charge carriers, exciton etc.) to the dimensions of the order of interatomic distances results in a quantization of energy and momentum, as well as reducing the density of their situation;
2. Quantum coherence – the phase difference of the wave function of carriers moving within these structures remain to some extent preserved, so that the interference must be taken into account. However, in nanostructures quantum coherence generally is not well preserved as it is the case with atoms and molecules, but is often more or less disturbed by structural defects. For this reason, in the analysis of the movement of carriers of these structures it is necessary to take into account coherent and decoherent effects, which greatly complicates the issue;
3. Impacts of boundary surface and interfaces, i.e. boundary layers – a considerable number of (sometimes even the majority) of atoms that make up the nanostructure is located at or near the surface or interfacial boundary – boundary layers. Mechanical, electrical, thermodynamic, magnetic, optical and chemical properties of these atoms can vary significantly from the properties of atoms inside the structure.This is caused by the fact that the atoms on the surface are connected with a smaller number of identical adjacent atoms or molecules from those of the interior. By reducing the dimensions of the structure, this difference is gaining in importance. For example [43], for the iron cube of volume 1 cm3 percentage of the surface in relation to the total number of atoms will amount to 5%.When the dimensions of a cube is reduced to 10 nm, the percentage of surface atoms will rise to 10%.In the iron cubes with the volume of 1 nm^3 each atom would be superficial.

The division of nanostructures is carried out in several ways, but most often based on the number of spatial dimensions along which the movement of carriers is confined [44]. In this sense, there are:

1. Quantum wells and thin crystalline plates – these are structures whose thickness in one direction of the order of nanometers, while the dimensions of the remaining two directions, conditionally speaking, are infinite (ie. very large). Elementary excitations (electrons, holes, phonons, etc. exciton.) are confined only in one direction, while the remaining two are free. Therefore, in these structures two-dimensional (2D) natural gas of carriers of physical propertiesis formed;
2. Quantum wires – in them layer dimensions are small in two directions, while the dimension in the third direction is infinite, so that in the quantum wires a one-dimensional (1D) gas of elementary excitationis is formed;
3. Quantum dots – here, all three dimensions are small, so that the carriers are completely confined and form zero-dimensional (0D) excitation gas.

Depending on the size of the removal of the closest neighbors we can distinguish:

1. Multiple quantum wells (wires, dots), in which the removal is large enough so that each of them can be considered in isolation;
2. Superlattices, where the removal is so small the entire structure must be analyzed uniquely.

I.1.2. *Nanofabrication*

Precise structuring of materials to the dimensions of the order of nanometers is of great importance for electronics, optoelectronics, high temperature superconductivity, biology, medicine, environmental protection and many other scientific and technological disciplines.Theoretical and experimental researches of properties of low dimensional systems (thin films, supelattices, quantum wires and quantum dots), have become very intense in recent decades, so it could be said to represent one of the striking research directions of Condensed Matter in modern physics.

The development of sophisticated techniques of controlled growth of very thin layers essentially caused the intensive study of nanocrystalline structure.One of the basic principles of their formation is based on a process of self-construction or self-assembly SA [45], which is one of the so-called"bottom-up" technique, where the atoms or molecules arrange themselves in a regulated low-dimensional structures on the basis of mutual physical-chemical interactions.Although the Self-Construction has been known for many years, its use in the industry is still in its infancy. Advanced knowledge of thermodynamics and kinetics of processes on the nanoscale, with progression ofcharacterized techniques and computer modeling, should lead to the development of complex systems.The most commonly used methods of deposition crystal layer and forming nanoparticles include molecular beam epitaxy, MOCVD technology, the hot wall epitaxy, atomic layer epitaxy and vacuum vapor deposition[46–48].

Although research in nanotechnology are based on well-known and proven achievements in physics, chemistry, materials science and engineering, researchers in this field are faced with many problems that are unique to nanostructures and nanomaterials.For example, the doping of the semiconductor is for macroscopic samples of virtually routine, ie. well trained proceedings. However, normal random fluctuations in the concentration of dopants at the nanometer scale are becoming extremely important and can not be tolerated.With a typical concentration of dopants of 1018 m^{-3}in the element with dimensions $10\times10\times10nm^3$ there would be only one dopant atom. Any distribution fluctuations of dopants in this range of dimensions would result in its completely altered features.

Furthermore, it is not all the same at which position within the sample the impurity atom is, considering the fact that its surface location would have had a different impact than if it had been inside the sample. To ensure a successful production and processing of nanomaterials and nanostructures the following problems must be overcome:

1. Overcome the huge surface energy, which is a result of enormous surface area or large surface area to volume ratio. We should bare in mind the fact that specific surface, and total surface energy accordingly, are negligible with macroscopic samples, but they become considerable for very small particle dimensions. When the size of particles changes from centimeter to nanometer scale, total size and surface energy change as much as seven orders of magnitude. Due to such huge total size, all materials of nanodimensions have large surface energy, which makes them thermodynamically unstable or metastable.
2. Ensure that nanomaterials have desired dimensions, uniform atom distribution in all directions, morphology, crystallinity, chemical composition, and microstructure.
3. Prevent nanomaterials and nanostructures from coarsening through either Ostwald ripening [46–48] or agglomeration as time evolutes.

I.1.3. *Spectroscopy of phonons*

An important tool which has stimulated research on Nanophysics and nanotechnology is a scanning tunneling microscope (STM) [49], whose working principle at the macroscopic and the atomic scale is based on a strong dependence of quantum-mechanical tunnel effect on the distance. Over the past few decades, STM has inspired the emergence of a large number of related scanning microscopic research instruments, which measure a multitude of properties with atomic resolution.By far the most important such a device is the interatomic force microscope (AFM) [50], which allows tests of poorly conductive surfaces, it was used to study the problems such as the forces necessary for the breakdown of individual protein molecules.While the STM probe tip does not touch the surface, the distance between the surface and the tip is realized through control of current tunneling electrons, with the AFM tip interacts with the surface of the sample. Considering that a force of this interaction does not depend on electrical conductivity of the test sample, using a microscope of interatomic force non-conductive samples can be tested.

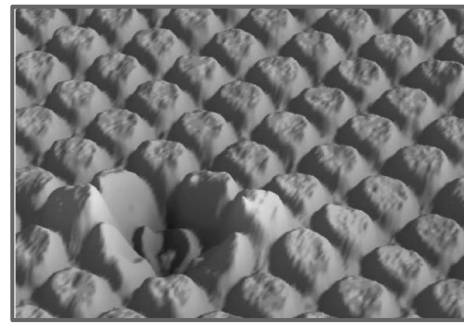

Figure 1: AFM recording of PdFePd thin film surface

The latter example also illustrates another important aspect of the following devices: apart from showing atoms from the surface of solids, it is possible for them to impact on individual atoms and molecules [51] and very attractive options for setting the atoms on the surface, but in predefined positions were provided. Research in nanotechnology is not limited only to the miniaturization of various devices, but also to the synthesis of new materials on the nanometer scale, which may exhibit excellent physical properties [52].The beginning of applying nanotechnology solutions in the field of materials dates back to 1985, when the first nanomaterial was received, now known as fullerene molecule (C60). In the domain of protection against UV radiation nanoparticles based on ZnO and TiO_2showed distinct advantages.

Generally, the nanoparticles provide up to ten times better chemical reaction than conventional materials, because the active surface on which the chemical reaction takes place is increased. Since the nanotubes are made first electronic switches and circuits for the purpose of nanoelectronics are made of the nanotubes, and cords whose tensile strength is 8 – 10 times higher than the product of the same material and the same size in mechanical engineering.The real revolution is on the horizon in the textile industry also, as it is being worked on the development of textile fibers that will be biocompatible and complementary with the skin, which in addition to the standard features that garments have, it will also have a role of biosensor systems. Considering the fact that the skin in the

so-called “trigger” zones represent functions of particular organs of the body, it will in the future be possible to make,, intelligent clothing" that will report to the provider or doctor about the health of the person.

I.1.4. *Significance and detection of phonons*

The theme of this monograph is concentrated on examining microscopic and macroscopic (thermodynamic) properties of thin layered (ultrathin films and superlattices) and low-dimensional (quantum wires and dots) crystal system and establishing a strict correlation between the nano-dimensions of these structures and quantum effects that occur in them at the macroscopic level. Special attention will be paid to the share in the phonon thermal transport through the low-dimensional systems.

Phonons represent elementary excitations in crystals [53–55] and the phonon subsystem in them is always present, regardless of whether the main carriers of the mechanisms that producecertain physical properties, phenomena and effects in the crystal structures occur electrons excitons , magnons, plasmons, polarons or other types of elementary excitation.The importance of phonons is reflected in the fact that they participate in the specific heat and thermal conductivity of the crystal, but equally important are their interactions with other energy excitations (scattering of electrons on the phonons is the cause of the occurrence of electrical resistance, a scattering of phonons– whatever the cause – limits thermal conductivity; also, phonon-phonon interactions are associated with thermal expansion of the crystal).

For all these reasons, testing of the share and influence of phonon subsystems on the physical characteristics of materials has great significance for the theory of solid state. However, the question is whether it is correct to observe phonon subsystem in crystals in isolation from all other elementary excitation.This approximation is obviously correct in the case of the insulator, but its justification can be questioned in metal samples. The theoretical foundation of the correctness of the applied method was formulated by Born-Oppenheimer (adiabatic) approximation, in which the electron-phonon interaction can subsequently be included, often with the help of perturbation theory.

The set goal of the monograph is to show the theoretical study of microscopic and macroscopic properties of thin layered and low-dimensional crystal structures within the phonon model of acoustic type. The methods of theoretical research, which interpret the mechanisms and patterns of behavior of microscopic systems and their repercussions on the macroscopic properties of samples, until recently, were only applicable to ideal space-time translationally invariant crystal structures.The development of modern mathematics (especially discrete) and software- computer techniques enabled the “adjustment” of these research methods on more realistic physical (in this case, crystal) systems [56–58].

In order to verify and assess theoretical methods and its results as correct and accurate, it is necessary to execute their experimental confirmation. One of the simplest and most reliable experimental methods for the characterization and testing of the phonon spectra in nanostructures is Raman scattering method [58–60], which is one of most frequently used spectroscopic methods.

Spectroscopic methods allow the determination of the position of the energy levels of different excitation (electronic, vibrational, rotational, or combinations thereof) in the

examined sample. All the phenomena discussed in spectroscopy are explained using several possible occurrences of the interaction of electromagnetic radiation with matter (Figure 2).

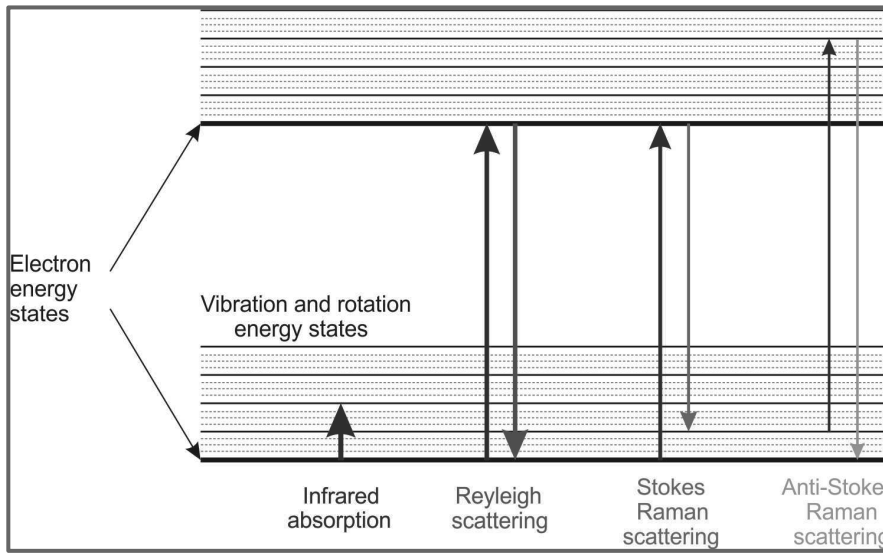

Figure 2: The basics of spectroscopic methods

1. Absorption of radiation – the system absorbs a photon, after which it remains in the excited state;
2. The emission of radiation (spontaneous or stimulated) – a system that is in an excited state returns to the ground state or an excited state of lower energy photon emission;
3. Rayleigh scattering – photon that is scattered in this way has the same energy as the incident photon, but it has a different direction. The system does not change its energy, which means that it is elastic scattering;
4. Raman scattering – photon leaving the system does not have the same energy as the incident photon, i.e. by Raman scattering the system gains or loses energy. The difference in the energy of the system before and after the Raman scattering corresponds to the difference between the energy of the incoming and outgoing photons. If the outgoing photon has lower energy than incoming photons (the system has got scattering energy), it is the Stokes scattering, while otherwise it is anti-Stokes scattering.

Raman scattering can be understood as the optical analog Compton scattering. Nonlinear Response of a transparent optical medium on the intensity of the light that passes through it is very fast, but not immediate. This delayed reaction of optically transparent medium is caused by vibrations of the crystal lattice. When these vibrations are connected with optical phonons, the effect is called Raman scattering, while the acoustic phonons are connected with Brillouin scattering.When, for example, two laser beams with different wavelengths (and usually with the same direction of polarization) move together through the Raman-active medium, the beam with a higher wavelength (ie. Stokes wave) may suffer optical amplification on account of the beam with a lower wavelength (Figure 3).In the process of Raman scattering an incident photon is transformed into photons of lower energy, a difference in the energies of the incident and outgoing photons carries the

phonon (energy quantum oscillations of the crystal lattice). In principle it is also possible that already existing phonon interacts with the incident photons giving one photon with higher energy which belongs to the anti-Stokes wave with a shorter wavelength.This process, however, is usually poor, especially at lower temperatures. It should, however, bear in mind that a strong anti-Stokes light can also occur by mixing four waves if the process is phase aligned.

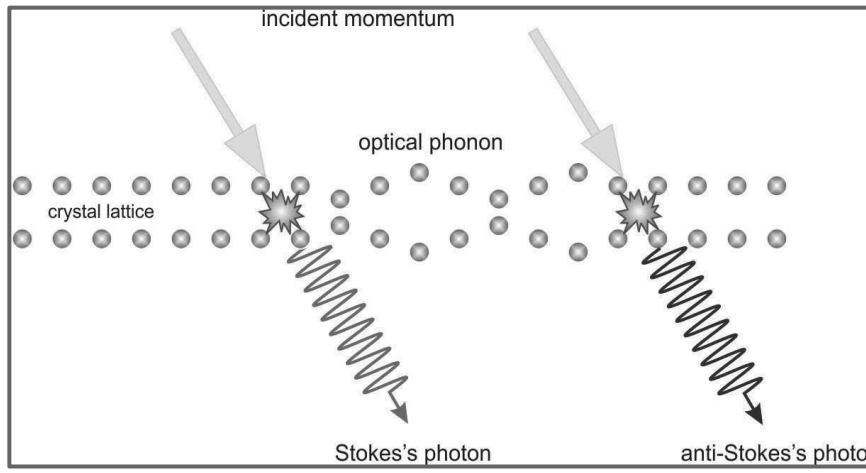

Figure 3: Schematic outline of the process of Raman scattering

Along with other forms of inelastic light scattering, Raman scattering is the most reliable and the most frequently used method in solid state physics for testing the elementary excitations (primarily phonons, but also magnon, exciton, and other elementary excitations) as well as for studying the electronic structure of materials.The most important topics of physics of semiconductors, which are taught by methods of inelastic light scattering, certainly include oscillations of the crystal lattice and the low-energy electronic excitations. Understanding these phenomena in elementary semiconductors and semiconductor compounds, as well as in artificial crystals obtained by molecular beam epitaxy and other techniques, the growth is very important both from fundamental and practical point of view.Controlled preparation of nanostructures such as superlattices and quantum wells, with currently realizable reliability of the order of quantityof monoatomic layer for separation of various materials, enables controlling and changing of physical parameters such as the width of the electronic gap, effective mass, dielectric or magnetic properties. On the one hand, this provides an opportunity for a systematic examination of physical phenomena that originate from changes of dimensionality, while on the other hand – the device features can be optimized and customized in this way.

Knowledge of the laws of the dynamics of the crystal lattice contributes significantly to our understanding of the structure of crystals. Phonon frequency, intensity and scattering selection rules, which can be defined by Raman spectroscopy, lead to conclusions which are related to microscopic parameters such as connection types and crystal structure, but also the degree of deviation from the ideal crystal lattice. These features also allow examination of the influence of external parameters, and – consequently – the implementation of the fundamental tests of theoretical models by which they can further improve.

I.2. Phonons in crystalline structures – Bulk samples

Phonon is a quantum of energy of a linear oscillator [61–63]. Phonon energy of the isolated oscillator is equal to the product of the Dirac constant $\hbar = 1.055 \cdot 10^{-34}$ Js, and the oscillator frequency, which depends on elastic forces under whose effect oscillation is done. If we have a set of oscillators which interact with each other, as with atoms in a crystal lattice, phonons are collective excitations of the system. The frequency of such a collective excitation depends on the interactions between the oscillating atoms and the wavelength of the waves of mechanical oscillations which extends through a set of interacting atoms. This dependence on the reciprocal wavelength, i.e. of the wave vector$k = 2\pi/\lambda$, is the dispersion law of phonons.

In crystals with a simple lattice and in the area of small wave vectors, phonons have a linear dispersion law: $\omega(k) \sim k$. These phonons are acoustic phonons. Depending on the polarization, acoustic phonons have three branches: one longitudinal, where polarization vector is directed alongthe wave propagation, and two transversal, where orthogonal polarization vectors are perpendicular to the direction of wave propagation.

In a complex crystal lattice consisting of σ sublattices, 3σ of phonon branches appear, of which three branches are acoustic phonons (their energy is equal to zero for $k = 0$), and 3σ– 3 branches of optical phonons whose energy is different from zero for $k = 0$. This means that the excitation of optical phonons requires energy. This excitation energy is called the threshold energy (energy gap) of optical phonons.

I.2.1. *Model of phonons*

The Hamiltonian of collective mechanical oscillations (phonons) in a crystal is obtained by developing the potential energy of crystals by small atomic displacements from the equilibrium positions$\vec{u}_{\vec{n}}$. Here $\vec{n}$ is the vector of the crystal lattice, which is through the vector of the crystal unit cell $\vec{a}_x, \vec{a}_y$ and $\vec{a}_z$ given with: $\vec{n} = n_x\vec{a}_x + n_y\vec{a}_y + n_z\vec{a}_z$, where n_x, n_y i $n_z$are integers. Since all the atoms, before they start to oscillate, are in equilibrium positions corresponding to the minimum interatomic interaction energy, during the development of the potential energy in a sum by displacements, partial derivatives $\left(\partial V_{\vec{l}} \big/ \partial u_{\vec{l}}^{s}\right)_{u_{\vec{l}}^{s}=0}$; $\vec{l} = \vec{n} - \vec{m}$; $s = (x,y,z)$ are equal to zero (balance condition), so during the development, as the first different from zero, there are members containing different sources of energy of interatomic interactions by projections $\left[\partial^2 V_{\vec{l}} \big/ \left(\partial u_{\vec{l}}^{s} u_{\vec{l}}^{s'}\right)\right]_{u_{\vec{l}}^{s}=0; u_{\vec{l}}^{s'}=0}$; $\vec{l} = \vec{n} - \vec{m}$; $s,s' = (x,y,z)$. These members represent Hooke's constants [61–63]. Further members of the development are discarded because they are proportionate to the product of three or more small atomic displacements.

The potential energy of the mechanical oscillations system is the second term in the development:

$$W = \frac{1}{2}\sum_{\vec{n},\vec{m}} V_{\vec{n}+\vec{u}_{\vec{n}}-(\vec{m}+\vec{u}_{\vec{m}})} = \frac{1}{2}\sum_{\vec{n},\vec{m}} V_{\vec{n}-\vec{m}} + \frac{1}{4}\sum_{s,s'}\left[\frac{\partial^2 V}{\partial u_{\vec{n}-\vec{m}}^{s} \partial u_{\vec{n}-\vec{m}}^{s'}}\right]_{\substack{u_{\vec{n}-\vec{m}}^{s}=0 \\ u_{\vec{n}-\vec{m}}^{s'}=0}} u_{\vec{n}-\vec{m}}^{s} u_{\vec{n}-\vec{m}}^{s'} . \qquad (1)$$

Diagonal second derivation in this term are Hooke's spring constants, while mixed expressions, i.e. Hooke's torsion constants, are significantly smaller than Hooke's spring constants, and therefore usually discarded in theory.

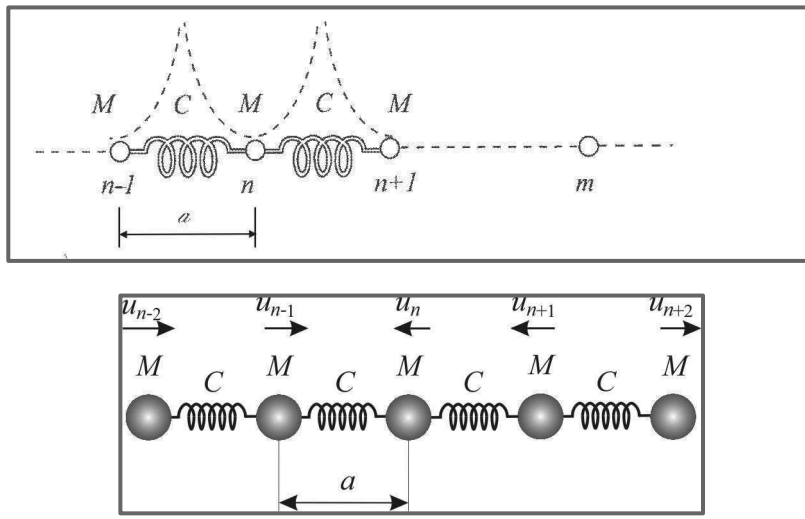

Figure 4: Model of 1D series of atoms of the same weight at equal equilibrium distances (above); Dynamic model of oscillation of 1D crystalline chain (below)

Kinetic energy is added to the potential energy of mechanical oscillations

$$T = \sum_{\vec{n}} \frac{p_{\vec{n}}^2}{2M}, \tag{2}$$

where M is the mass of the atoms, and p is the impulse given with $p_{\vec{n}} = M\,\dot{u}_{\vec{n}}$. Since phonons are quantum objects, values $u_{\vec{n}}$ and $p_{\vec{n}}$ are operators, where $u_{\vec{n}}$ is the multiplicative operator, and $p_{\vec{n}}$ differential operator. These operators satisfy the standard commutation relations [18–20]:

$$\left[u_{\vec{n}}^{s}, p_{\vec{m}}^{s'}\right] = i\hbar\,\delta_{\vec{n},\vec{m}}\,\delta_{s,s'}.$$

Phonons are boson-type excitations, so the operators u_n^s and p_n^s develop by straight waves, where the coefficients of the development are creation and annihilation Bose-operators $b_{\vec{k}}^{+}$ i $b_{\vec{k}}$. These developments are given [61–63] with:

$$\begin{aligned} u_{\vec{n}} &= \sum_{\vec{k},j} \vec{l}_j\left(\vec{k}\right)\sqrt{\frac{\hbar}{2MN\omega_j\left(\vec{k}\right)}}\left[b_j\left(\vec{k}\right)\mathrm{e}^{i\vec{k}\vec{n}-it\omega_j\left(\vec{k}\right)} + b_j^{+}\left(\vec{k}\right)\mathrm{e}^{-i\vec{k}\vec{n}+it\omega_j\left(\vec{k}\right)}\right]; \\ p_{\vec{n}} &= \frac{1}{i}\sum_{\vec{k},j} \vec{l}_j\left(\vec{k}\right)\sqrt{\frac{\hbar}{2MN\omega_j\left(\vec{k}\right)}}\left[b_j\left(\vec{k}\right)\mathrm{e}^{i\vec{k}\vec{n}-it\omega_j\left(\vec{k}\right)} - b_j^{+}\left(\vec{k}\right)\mathrm{e}^{-i\vec{k}\vec{n}+it\omega_j\left(\vec{k}\right)}\right]. \end{aligned} \tag{3}$$

In these expressions, $\vec{l}_j\left(\vec{k}\right)$ are polarization operators, and N is the number of atoms in a crystal sample. By substituting (3) in the Hamiltonian of mechanical oscillations: $H = T + W$, we obtain the Hamiltonian in a diagonal form by the operators of phonon number $\hat{n}_j\left(\vec{k}\right) = b_j^+\left(\vec{k}\right) b_j\left(\vec{k}\right)$, in the following form:

$$\hat{H} = \sum_{\vec{k},j} \hbar\omega_j\left(\vec{k}\right)\left[n_j\left(\vec{k}\right) + \frac{1}{2}\right]. \tag{4}$$

The second member of this formula does not depend on the number of phonons and is called the energy of zero oscillations, i.e. oscillations which atoms perform at the absolute zero.In the Debye theory [18–20], another member of the formula (4) is discarded: such Hamiltonian shows that the internal energy of the phonon system at low temperatures is proportional to the fourth degree of absolute temperature, while at high temperatures it is proportional to the first degree of absolute temperature.

Thermal capacity of the phonon system, which is defined with the derivation of the internal energy by temperature, at low temperatures is proportional to the third degree of absolute temperature [61–63], while at high temperatures it is constant and amounts to $3R$, where R is the universal gas constant. This last result is called the Dulong–Petit law.

In the Debye theory, the concept of the Debye frequency is introduced, which is determined by the maximum value of the wave vector in the first Brillouin zone: $k_\mathrm{D} = \pi\sqrt{3}/a$,for a crystal with simple cubic symmetry and with a lattice constant a. This maximum value of the wave vector corresponds to the Debye frequency $\omega_\mathrm{D} = ck_\mathrm{D}$, where c is the speed of sound in the crystal. Through the Debye frequency a corresponding frequency is introduced – the Debye temperature based on the energy relation: $k_\mathrm{B}T_\mathrm{D} = \hbar\omega_\mathrm{D}$, where $k_\mathrm{B} = 1.38 \cdot 10^{-23}$ J/K – Boltzmann constant. From here it follows:

$$T_\mathrm{D} = \frac{\hbar\omega_\mathrm{D}}{k_\mathrm{B}} = \frac{\hbar c\, k_\mathrm{D}}{k_\mathrm{B}} = \frac{\pi\sqrt{3}\,\hbar c}{a\, k_\mathrm{B}}, \tag{5}$$

this is of the order of 100 K.

In concluding this brief overview, we would like to emphasize that phonons are elementary excitations which are present in all the systems that are found on the absolute temperature different from zero, and as such influence the behavior of other elementary excitations, which can, together with phonons, occur in these systems. Accordingly, they are the main "factors" that determine all the characteristics and behavior of crystalline systems.

I.2.2. *Phonon's crystalline model*

Although in nature there is no pure isotropic crystal, nor can they be at today's level of technology produced, the study of ideal and unlimited structures is useful becausefor the basic physical phenomena their global features can be calculated and we get what is called a quality picture.The conclusions obtained in this way, as well as research methodology can be transferred to non-ideal structures, primarily at crystal structure with impaired translational symmetry [64-68]. Ideal infinite structures are the crystals with the property of translational invariance in three mutually incomplanar directions.These directions,

which are introduced in crystallography, do not have to be mutually orthogonal, and therefore in theoretical physics of condensed matter, Descartes introduces an additional system. Here will be observed only when the cubic crystal crystallographic directions of mutually orthogonal introduced and these problems no. Due to this, the Hamiltonian system on the approximation of nearest neighbors (4) can be written as

$$H = \sum_{\alpha;\vec{n}} \frac{p^2_{\alpha;\vec{n}}}{2M} + \frac{1}{4} \sum_{\alpha;\vec{n},\vec{\lambda}} C^{\alpha\alpha}_{\vec{n},\vec{\lambda}} \left(u_{\alpha;\vec{n}} - u_{\alpha;\vec{n}\pm\vec{\lambda}} \right)^2 , \tag{6}$$

where $p = M\,\dot{u}$ – is crystal momentum of the atom, a M – mass of these atoms.The second term on the right side of the sign of equality represents effective interatomic potential of interaction (V_{eff}).

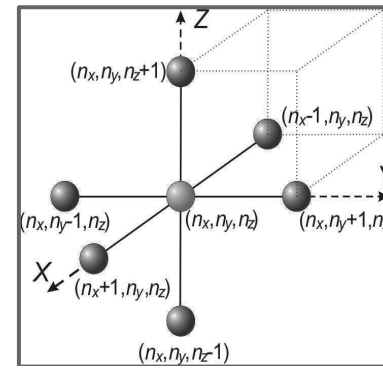

Figure 5: Atom with its nearest neighbors

To understand the beginning of the application of mathematical formalism Figure 4 is given, which shows the crystal atom surrounded by its nearest neighbors. For simplicity, it is assumed that it is a simple cubic structure with one atom per elementary cell (primitive cell).It can be seen that $|\vec{\lambda}|/a$ can only take the values: -1 and $+1$. In accordance with all this, the expression for phonon Hamiltonian (6) can be written in a more preferred (developed) forms:

$$H = T + V_{eff} , \tag{7}$$

where:

$$T = \sum_{\alpha;\vec{n}} \frac{p^2_{\alpha;\vec{n}}}{2M} , \tag{8}$$

$$\begin{aligned} V_{eff} = \sum_{\alpha;n_x,n_y,n_z} \frac{C_\alpha}{4} \Bigg[& \left(u_{\alpha;n_x+1\,n_y,n_z} - u_{\alpha;n_x,n_y,n_z} \right)^2 + \left(u_{\alpha;n_x-1\,n_y,n_z} - u_{\alpha;n_x,n_y,n_z} \right)^2 + \\ & + \left(u_{\alpha;n_x,n_y+1\,n_z} - u_{\alpha;n_x,n_y,n_z} \right)^2 + \left(u_{\alpha;n_x,n_y-1\,n_z} - u_{\alpha;n_x,n_y,n_z} \right)^2 + \\ & + \left(u_{\alpha;n_x,n_y,n_z+1} - u_{\alpha;n_x,n_y,n_z} \right)^2 + \left(u_{\alpha;n_x,n_y,n_z-1} - u_{\alpha;n_x,n_y,n_z} \right)^2 \Bigg] . \end{aligned} \tag{9}$$

Hooke's torsion constants $C^{\alpha\alpha}$ are disregarded in comparison to the tension constant $C_\alpha \equiv C^{\alpha\alpha}$ [69]. Operators $u_{\alpha\vec{n}}$ i $p_{\alpha\vec{n}} = M\,\dot{u}_{\alpha\vec{n}}$ meet the standards of commutation relation:

$$\left[u_{\alpha\vec{n}},\, p_{\beta,\vec{m}}\right] = i\hbar\,\delta_{\alpha,\beta}\,\delta_{\vec{n},\vec{m}}\,; \quad \left[u_{\alpha\vec{n}}, u_{\beta,\vec{m}}\right] = \left[p_{\alpha\vec{n}},\, p_{\beta,\vec{m}}\right] = 0\,. \tag{10}$$

I.2.3. *Dispersion law of phonons*

Energy spectra and conditions will be defined by the method of Green's functions. For this purpose, observe the two-time temperature Green's functions of movement – movement:

$$G^{\alpha}_{\vec{n},\vec{m}}(t-t') \equiv \langle\langle u_{\alpha;\vec{n}}(t)\,|\,u_{\alpha;\vec{m}}(t')\rangle\rangle = \Theta(t-t')\,\langle\left[u_{\alpha;\vec{n}}(t), u_{\alpha;\vec{m}}(t')\right]\rangle_0\,. \tag{11}$$

By double differentiation of this expression in time and slight rearranging, we get:

$$M\,\frac{d^2}{dt^2}\,G^{\alpha}_{\vec{n},\vec{m}}(t-t') = -i\hbar\,\delta_{\vec{n},\vec{m}}\,\delta(t-t') + \frac{\Theta(t-t')}{i\hbar}\,\langle\left[\left[p_{\alpha;\vec{n}}(t), H(t)\right], u_{\alpha;\vec{m}}(t')\right]\rangle_0\,.$$

Taking $t' = 0$ and by time Fourier tranformation $t \to \omega$, the last expression becomes:

$$\int_{-\infty}^{+\infty} d\omega\, \mathrm{e}^{-i\omega t}\left\{\frac{i\hbar}{2\pi}\,\delta_{\vec{n},\vec{m}} - M\omega^2 G^{\alpha}_{\vec{n},\vec{m}}(\omega) - \frac{1}{i\hbar}\,\langle\langle\left[p_{\alpha;\vec{n}}, H\right]\,|\,u_{\alpha;\vec{m}}\rangle\rangle_\omega\right\} = 0\,,$$

which is fulfilled for:

$$-M\omega^2 G^{\alpha}_{\vec{n},\vec{m}}(\omega) = -\frac{i\hbar}{2\pi}\,\delta_{\vec{n},\vec{m}} + \frac{1}{i\hbar}\,\langle\langle\left[p_{\alpha;\vec{n}}, H\right]\,|\,u_{\alpha;\vec{m}}\rangle\rangle_\omega\,. \tag{12}$$

Further procedure of determining the Green's functions, requires calculation of the commutator which exists in the higher Green's functions $\langle\langle\cdots|\cdots\rangle\rangle$ of the above equation:

$$\left[p_{\beta;m_x,m_y,m_z}, H\right] = \left[p_{\beta;m_x,m_y,m_z}, T\right] + \left[p_{\beta;m_x,m_y,m_z}, V_{eff}\right] = \left[p_{\beta;m_x,m_y,m_z}, V_{eff}\right] =$$

$$= \sum_{\alpha;n_x,n_y,n_z} \frac{C_\alpha}{4}\left\{2\left[p_{\beta;m_x,m_y,m_z}, \left(u_{\alpha;n_x,n_y,n_z} - u_{\alpha;n_x+1,n_y,n_z}\right)\right]\left(u_{\alpha;n_x,n_y,n_z} - u_{\alpha;n_x+1,n_y,n_z}\right) + \right.$$

$$+ 2\left[p_{\beta;m_x,m_y,m_z}, \left(u_{\alpha;n_x,n_y,n_z} - u_{\alpha;n_x-1,n_y,n_z}\right)\right]\left(u_{\alpha;n_x,n_y,n_z} - u_{\alpha;n_x-1,n_y,n_z}\right) +$$

$$+ 2\left[p_{\beta;m_x,m_y,m_z}, \left(u_{\alpha;n_x,n_y,n_z} - u_{\alpha;n_x,n_y+1,n_z}\right)\right]\left(u_{\alpha;n_x,n_y,n_z} - u_{\alpha;n_x,n_y+1,n_z}\right) +$$

$$+ 2\left[p_{\beta;m_x,m_y,m_z}, \left(u_{\alpha;n_x,n_y,n_z} - u_{\alpha;n_x,n_y-1,n_z}\right)\right]\left(u_{\alpha;n_x,n_y,n_z} - u_{\alpha;n_x,n_y-1,n_z}\right) +$$

$$+ 2\left[p_{\beta;m_x,m_y,m_z}, \left(u_{\alpha;n_x,n_y,n_z} - u_{\alpha;n_x,n_y,n_z+1}\right)\right]\left(u_{\alpha;n_x,n_y,n_z} - u_{\alpha;n_x,n_y,n_z+1}\right) +$$

$$\left. + 2\left[p_{\beta;m_x,m_y,m_z}, \left(u_{\alpha;n_x,n_y,n_z} - u_{\alpha;n_x,n_y,n_z-1}\right)\right]\left(u_{\alpha;n_x,n_y,n_z} - u_{\alpha;n_x,n_y,n_z-1}\right)\right\} =$$

$$= -i\hbar \sum_{\alpha;n_x,n_y,n_z} \frac{C_\alpha}{2} \delta_{\alpha\beta} \Big[\Big(\delta_{\vec{n},\vec{m}} - \delta_{n_x+1,m_x} \delta_{n_y,m_y} \delta_{n_z,m_z} \Big) \Big(u_{\alpha;n_x,n_y,n_z} - u_{\alpha;n_x+1,n_y,n_z} \Big) +$$

$$+ \Big(\delta_{\vec{n},\vec{m}} - \delta_{n_x-1,m_x} \delta_{n_y,m_y} \delta_{n_z,m_z} \Big) \Big(u_{\alpha;n_x,n_y,n_z} - u_{\alpha;n_x-1,n_y,n_z} \Big) +$$

$$+ \Big(\delta_{\vec{n},\vec{m}} - \delta_{n_x,m_x} \delta_{n_y+1,m_y} \delta_{n_z,m_z} \Big) \Big(u_{\alpha;n_x,n_y,n_z} - u_{\alpha;n_x,n_y+1,n_z} \Big) +$$

$$+ \Big(\delta_{\vec{n},\vec{m}} - \delta_{n_x,m_x} \delta_{n_y-1,m_y} \delta_{n_z,m_z} \Big) \Big(u_{\alpha;n_x,n_y,n_z} - u_{\alpha;n_x,n_y-1,n_z} \Big) +$$

$$+ \Big(\delta_{\vec{n},\vec{m}} - \delta_{n_x,m_x} \delta_{n_y,m_y} \delta_{n_z+1\, m_z} \Big) \Big(u_{\alpha;n_x,n_y,n_z} - u_{\alpha;n_x,n_y,n_z+1} \Big) +$$

$$+ \Big(\delta_{\vec{n},\vec{m}} - \delta_{n_x,m_x} \delta_{n_y,m_y} \delta_{n_z-1\, m_z} \Big) \Big(u_{\alpha;n_x,n_y,n_z} - u_{\alpha;n_x,n_y,n_z-1} \Big) \Big]$$

Commutation relations for the displacements and impulses (10), and the definition of the Kronecker symbol are used here:

$$\delta_{r,s} = \begin{cases} 1 & \text{za} \quad r = s\,, \\ 0 & \text{za} \quad r \neq s\,. \end{cases}$$

Considering that

$$G^{\alpha}_{\vec{n},\vec{m}} \equiv G^{\alpha}_{n_x,n_y,n_z;m_x,m_y,m_z} = \langle\langle u_{\alpha;n_x,n_y,n_z} \mid u_{\alpha;m_x,m_y,m_z} \rangle\rangle \tag{13}$$

and replacing obtained commutator into equation (12) it follows:

$$-M\omega^2 G^{\alpha}_{n_x,n_y,n_z;m_x,m_y,m_z} = -\frac{i\hbar}{2\pi} \delta_{n_x,m_x} \delta_{n_y,m_y} \delta_{n_z,m_z} - C_\alpha \Big(6\, G^{\alpha}_{n_x,n_y,n_z;m_x,m_y,m_z} -$$

$$- G^{\alpha}_{n_x+1,n_y,n_z;m_x,m_y,m_z} - G^{\alpha}_{n_x-1,n_y,n_z;m_x,m_y,m_z} - G^{\alpha}_{n_x,n_y+1,n_z;m_x,m_y,m_z} - \tag{14}$$

$$- G^{\alpha}_{n_x,n_y-1,n_z;m_x,m_y,m_z} - G^{\alpha}_{n_x,n_y,n_z+1;m_x,m_y,m_z} - G^{\alpha}_{n_x,n_y,n_z-1;m_x,m_y,m_z} \Big).$$

By applying spatial Fourier transformation ($\vec{n} \to \vec{k}$):

$$G^{\alpha}_{\vec{n},\vec{m}}(\omega) = \frac{1}{N} \sum\nolimits_{\vec{k}} \mathrm{e}^{-i(\vec{n}-\vec{m})\vec{k}}\; G^{\alpha}_{\vec{k}}(\omega)\,; \quad \delta_{\vec{n},\vec{m}} = \frac{1}{N} \sum\nolimits_{\vec{k}} \mathrm{e}^{-i(\vec{n}-\vec{m})\vec{k}}\,,$$

onto equation (14), after insignificant algebraic operations, it becomes:

$$\frac{M}{N} \sum_{\vec{k}} \mathrm{e}^{-i(\vec{n}-\vec{m})\vec{k}} \left\{ \frac{i\hbar}{2\pi M} - G^{\alpha}_{\vec{k}}(\omega) \Big[\omega^2 + \right.$$

$$\left. + 2\frac{C_\alpha}{M} \Big(3 - \cos a_x k_x - \cos a_y k_y - \cos a_z k_z \Big) \Big] \right\} = 0\,,$$

and it is fulfilled if:

$$\left[\left(\frac{\omega}{\Omega_\alpha}\right)^2 + 2\left(\cos a_x k_x + \cos a_y k_y + \cos a_z k_z - 3\right)\right] G_{\vec{k}}^{\alpha}(\omega) = \frac{i\hbar}{2\pi\, C_\alpha}. \tag{15}$$

Its solutions can be written in the following form:

$$G_{\vec{k}}^{\alpha}(\omega) = \frac{i\hbar}{4\pi M\ \omega_{\vec{k}}^{\alpha}}\left(\frac{1}{\omega - \omega_{\vec{k}}^{\alpha}} - \frac{1}{\omega + \omega_{\vec{k}}^{\alpha}}\right). \tag{16}$$

Here, obviously, the poles of Green's functions are obtained when the denominator of expression in brackets equate to zero. After solving this condition under $\omega \equiv \omega_\alpha(\vec{k})$ the required dispersion law of phonons is obtained:

$$E_\alpha(\vec{k}) \equiv \hbar\,\omega_{\vec{k}}^{\alpha} = 2\,E_\alpha \sqrt{\sin^2\frac{a_x k_x}{2} + \sin^2\frac{a_y k_y}{2} + \sin^2\frac{a_z k_z}{2}}\,, \tag{17}$$

whereis $E_\alpha = \hbar\Omega_\alpha = \hbar\sqrt{C_\alpha/M}$.

In approximation of small vawe vectors (for simple cubic structure $a_x = a_y = a_z \equiv a$ and with $k = \sqrt{k_x^2 + k_y^2 + k_z^2}$), relation (17) comes down to:

$$E_\alpha(\vec{k}) = a\,k\,, \tag{18}$$

which represents typical and known [70–73]expression for dispersion law of acustic phonons.

Careful considerations show that there are several types of spreading out of wave disturbances in the crystal, which differ by the movement of atoms within the unit cell. Each type of phonon is characterized by a specific dependence of energy on quasi-impulses. For the string with three degrees of freedom, there are three modes of oscillation: one along the direction of the string and two mutually normal in the planes, orthogonal to the axis of the string. In such systems the possibility of spreading of two types of waves arises: longitudinal and transversal, which follows from the condition of standardization.In longitudinal wave motion vector $\vec{u}(\vec{k})$ is directed along the carbon chain and coincides with the direction of wave propagation $\vec{e}_1 \parallel \vec{k}$. In transverse waves, polarization vector $\vec{e}_2$ is vertical to the axis of the chain and perpendicular to the wave vector $\vec{k}$, $\vec{e}_2 \perp \vec{k}$. For small values $\vec{k}$ the dispersion laws of longitudinal and transverse waves have the same form:

$$\omega_{\parallel} = v_{\parallel} k\,; \omega_{\perp} = v_{\perp} k\,.$$

In crystals with a simple elementary cell of all three components the frequency of mechanical waves $\omega_\alpha(k)$ tend to zero when $k \to 0$. Such quantum mechanical excitations with a linear dispersion law are called acoustic phonons. If in a similar way complex crystal structures with σ sublattices per elementary cell are analized, then for the

permissible frequency solutions 3σ are obtained, of which three frequencies always tend to zero when $k \to 0$ and they correspond to acoustic phonon branches, while for other branches $(3\sigma - 3)$ it is $\lim_{k\to 0} \omega(k) \neq 0$, mechanical oscillations with this property are called the optical phonons.

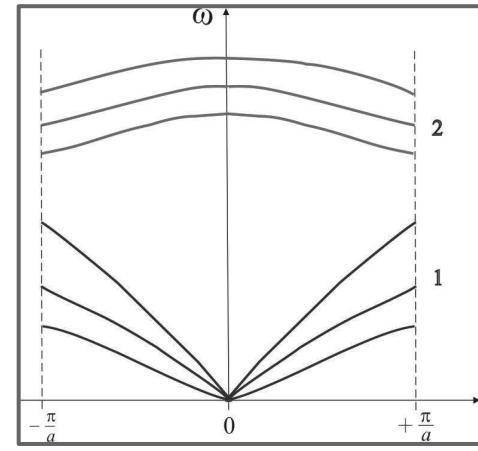

Figure 6: Dispersion curve of phonons for crystalline latticewith twoatomic basis (1 – acousticbranches; 2 – opticalbranches)

These considerations relate to the phonon spectra within a single elementary cell. A three-dimensional crystal with N elementary cells and σ sublattices has $3N\sigma$ degrees of freedom. Phonon spectrum, then always make 3 acoustic and $3N\sigma - 3$ optical branches[1].

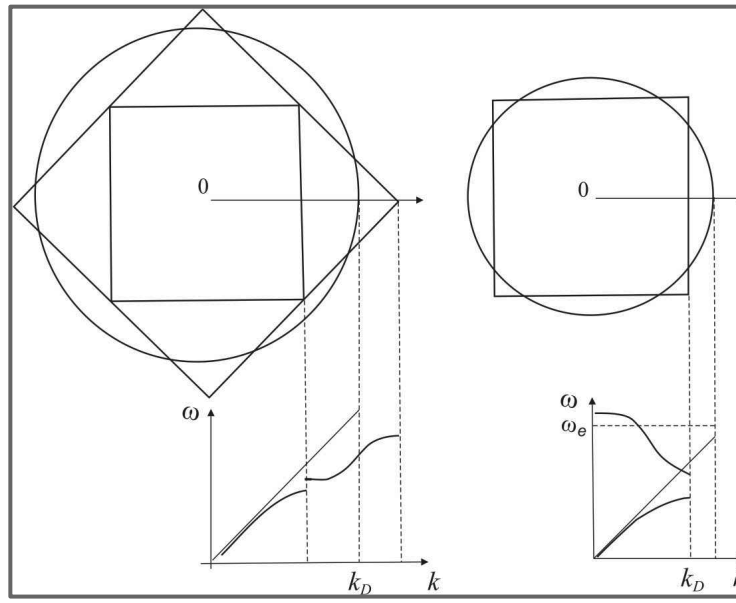

Figure 7: Approximation of acoustic and optical phonon branches [73]

[1]It should be noted that in simple crystalline structures only acoustic phononsoccur, while in the complex, besides the acoustic, optical phonons occur also. [64–68]

I.3. Phonon's thermodynamics

The behavior of gases and phonon gas being gas of quasiparticles is identical in thermodynamic sense. Using gaseous thermodynamics, we shall analyze the concept of entropy which is connected with many opened questions [74–76].

I.3.1. *Entropy of the system*

The main thermodynamic process consists in the fact that thermal energy brought to the system increases internal energy of the system and produces the work of the system, i.e.

$$\delta Q = C_V\, dT + p\, dV\,, \tag{19}$$

where C_V is molar heat at $V = const$, p is the pressure of the system. Substituting pressure from ideal gas equation $p\,V = RT$, we reduce (19) to

$$\delta Q = C_V\, dT + \frac{RT}{V} dV\,.$$

Since $\frac{\partial C_V}{\partial V} = 0$, while $\frac{\partial}{\partial T}\left(\frac{RT}{V}\right) = \frac{R}{V}$, it is seen that brought thermal energy δQ is not total differential. The main goal of thermodynamics was to translate δQ to total differential and these attempts have given to the concept of entropy. It is obvious that by means of integration factor which is function of T and V it can be done. Multiplying (7) with λ we obtain:

$$\lambda\,\delta Q = \lambda C_V\, dT + \lambda \frac{RT}{V} dV$$

and taking requirement

$$\frac{\partial}{\partial V}\left(\lambda C_V\right) = \frac{\partial}{\partial T}\left(\lambda \frac{RT}{V}\right),$$

we obtain a partial differential equation

$$\left(\gamma - 1\right) V \frac{\partial \lambda}{\partial V} - \frac{1}{T}\frac{\partial \lambda}{\partial T} = \lambda\,, \tag{20}$$

where $\gamma \equiv C_p/C_V$, and C_p is molar heat at constant pressure. The system of equations of usual differential equations following from (20)

$$\frac{dV}{\left(\gamma - 1\right) V} = -\frac{dT}{T} = \frac{d\lambda}{\lambda}\,, \tag{21}$$

has solutions

$$\lambda T = C_1\,; \quad T V^{\gamma - 1} = C_2$$

and the general solution for integration factor gets the form:

$$\lambda(T,V)=\frac{1}{T}f\left(TV^{\gamma-1}\right), \tag{22}$$

where f is arbitrary function of argument $TV^{\gamma-1}$. In thermodynamics was taken that $TV^{\gamma-1}=1$, so that integration factor (24) becomes:

$$\lambda(T,V)=\frac{1}{T}. \tag{23}$$

In this case the term $T^{-1}\,\delta Q$ goes over to total differential dS, where S is entropy of the system.

From the above analysis it is clear that translation of δQ to the total differential can be done more generally (multiplying δQ with function $T^{-1}f(TV^{\gamma-1})$. It means that entropy has a series of expressions different from T^{-1} which is used in thermodynamics. Only in adiabatic process (where $TV^{\gamma-1}=const$) remains thermodynamic definition: $dS=T^{-1}\delta Q$.

The use of different expressions of λ translating δQ to dS has to be subject of serious discussions. In connection with this, we would like to point out that Eigen explained the transition from non-animated to animated matter by some disturbances of entropy from monotonous behavior. These disturbances and oscillations entropy could be explained by the general formula (22) and (23) obtained.

I.3.2. *Thermodynamical characteristics*

In the crystal in the quantum state $|ks\rangle$ any number ν_{ks} – of phonons can be excited. Accordingly, the phonons form a "gas" of quasiparticles, which behaves according to Bose-Einstein statistics. Due to interactions between phonons, conditioned by anharmonic effects, the number of phonons in the crystal is not maintained and they are redistributed by various states, so that thermal equilibrium occurs when the crystal is at a certain temperature.For the calculation of average value of energy phonons in thermodynamic equilibrium, the laws of statistical physics are used. The state of the system in thermodynamics is obtained by describing with wave function, statistical operator or density matrix. The density matrix, for systems at constant temperature and pressure, is determined by the expression:

$$\rho=\exp\left(\frac{\Phi-H-\mu N}{\theta}\right), \tag{24}$$

where $N-$ is the number of particles operator, $H-$Hamilton operator, μ – chemical potential (related to one particle), Φ – the thermodynamic potential of variables μ and $\theta=k_BT$. The density matrix (24) describes a system that can exchange energy and particles with the environment at a constant temperature and pressure (grand canonical ensemble). Thermodynamic potential is determined from the condition of norming the density matrix:

$$1=\mathrm{Sp}(\rho)=\sum_s\langle s\,|\,\rho\,|\,s\rangle$$

(summation is carried out at the complete set $|s\rangle$ of state of the system and depends on the energy and number of particles in the system) and equality

$$\Phi = -\theta \ln\left[\mathrm{Sp}\left(\mathrm{e}^{\frac{\mu N - H}{\theta}}\right)\right]. \tag{25}$$

Chemical potential of the system μ is determined by the condition:

$$\mu = \left(\frac{\partial \Phi}{\partial N}\right)_{\theta,p}. \tag{26}$$

Using the density matrix (24) it is possible to calculate the mean value of the operator A of any physical value A: $\langle A\rangle = \mathrm{Sp}(\rho A)$, so the mean number of particles in the system is defined as:

$$\langle N\rangle = \mathrm{Sp}(\rho N). \tag{27}$$

If the number of particles in the system is maintained, then the condition (27) defines, in an implicit form, the chemical potential of the system. However, if the number of particles in the system is not maintained, the equilibrium state of the system is determined by the condition of minimum thermodynamic potential of any change in relation to the number of particles:

$$\mu = \left(\frac{\partial \Phi}{\partial N}\right)_{\theta,p} = 0. \tag{28}$$

In that way, at equilibrium state, the system with a variable number of particles (phonons system) has a chemical potential equal to zero [3]. In that case the free energy of the system F coincides with the thermodynamic potential, i.e. $F = \Phi + \mu N$ because for $\mu = 0$ it follows:

$$F = -\theta \ln\left[\mathrm{Sp}\left(\mathrm{e}^{-H/\theta}\right)\right]. \tag{29}$$

Knowing the expression for the free energy, mean value of the internal energy of the system can be calculated, ie.

$$U = F - \theta \frac{\partial F}{\partial \theta} = -\theta^2 \frac{\partial}{\partial \theta}\left(\frac{F}{\theta}\right). \tag{30}$$

If the state of particles in a system are characterized by quantum numbers s with the operators H and N as : $H = \sum_s H_s$; $N = \sum_s N_s$ then the thermodynamic potential can be written as:

$$\Phi = \sum_s \Phi_s\,; \quad \Phi_s = -\theta \ln\left[\mathrm{Sp}\left(\mathrm{e}^{\frac{\mu N_s - H_s}{\theta}}\right)\right] = \theta \ln\left(1 - \mathrm{e}^{\frac{\mu - E_s}{\theta}}\right), \tag{31}$$

where E_s i ν_s – are eigenvalues of the corresponding operators

$$H_s\,|\nu_s\rangle = E_s\,|\nu_s\rangle\,; \quad N_s\,|\nu_s\rangle = \nu_s\,|\nu_s\rangle\,.$$

Mean population number of particles (bosons) in the state s is then:

$$\langle \nu_s\rangle = -\frac{\partial \Phi_s}{\partial \mu} = \left(\mathrm{e}^{\frac{E_s - \mu}{\theta}} - 1\right)^{-1}. \tag{32}$$

The states of phonons in the crystal are characterized by wave vector and a branch of oscillations α. If you reject the energy of the ground state E_0, energy operators and the number of phonons can be written as:

$$H = \sum_{\alpha,\vec{k}} \hbar\omega_\alpha(\vec{k})\, \hat{b}^+_{\alpha,\vec{k}} \hat{b}_{\alpha,\vec{k}} + H^1; \quad N = \sum_{\alpha,\vec{k}} \hat{b}^+_{\alpha,\vec{k}} \hat{b}_{\alpha,\vec{k}}, \tag{33}$$

where H^1 – is operator of anharmonic corrections. The operator brings a small contribution to energy phonons, but provides the establishment of thermodynamic equilibrium in the system and is responsible for non-preservation of phonons number.This member is taken into account only when $\mu = 0$ to apply statistical physics formulas for equilibrium. So if $\mu = 0$ and by using the expression (29) to (33) we get the following expressions for the mean number of phonons in the state $|\nu_{\alpha\vec{k}}\rangle$:

$$\langle \nu_{\alpha,\vec{k}} \rangle = \left[\mathrm{e}^{\frac{\hbar\omega_\alpha(\vec{k})}{\theta}} - 1 \right]^{-1}, \tag{34}$$

as well as for the free energy of the crystal:

$$F = \Phi = \sum_{\alpha,\vec{k}} \Phi_{\alpha,\vec{k}} = \theta \sum_{\alpha,\vec{k}} \ln\left[1 - \mathrm{e}^{-\frac{\hbar\omega_\alpha(\vec{k})}{\theta}} \right]. \tag{35}$$

On the basis of thermodynamic relations (30) and expression (35), the internal energy of the crystal is:

$$U = \sum_{\alpha,\vec{k}} \hbar\omega_\alpha(\vec{k}) \left[\mathrm{e}^{\frac{\hbar\omega_\alpha(\vec{k})}{\theta}} - 1 \right]^{-1}. \tag{36}$$

Thermal capacitance of the lattice per unit volume and entropy are defined through a standard expression:

$$C_v = \frac{\partial U}{\partial T} = k_B \frac{\partial U}{\partial \theta}, \quad S = -\frac{\partial F}{\partial T} = -k_B \frac{\partial F}{\partial \theta}. \tag{37}$$

Thermodynamic behaviors of almost all the characteristics of a crystal are determined by phonons. Therefore, it is necessary to see their share in the thermal capacitance of solid bodies, ie thermal capacitance of that crystal (because the calculation is made by the elementary cell of the observed crystal). Experimental facts relating to thermal capacitances are as follows [77,78].

- In the area of indoor temperature thermal capacitance value of almost all solid bodies are close to $3Nk_B$ where N is the number of atoms
- At lower temperatures the heat capacity decreases and tends to zero as T^3 in dielectrics, and as T in metals; if the sample becomes a superconductor the declining is even faster.

Based on the presented theory and experimental facts presented, it can be relatively easy to calculate the free energy of isotropic crystals in two boundary cases at low and high temperatures. Thermodynamic analysis in the field of medium temperature creates a small difficulty. In this area the two approximate approachesare are used [77,78]: Debye's and Einstein's.

Debye's approximation

This approximation consists of the following:

- only acoustic branches of phonons (crystal with a primitive cell) are observed and
- Brillouin zone, whithin whose limits are the permissible values of the vector *k*, are replaced by the sphere of the same volume in reciprocal space:

$$N = \frac{V}{8\pi^3}\frac{4}{3}\pi k_D^3; \quad k_D = \sqrt[3]{6\pi^2\frac{N}{V}}; \quad \omega_D = \frac{v}{a}\sqrt[3]{6\pi^2}. \tag{38}$$

Debey's temperature is determined by the relation $\hbar\omega_D = k_B T_D$ and for the values $k_D \sim 10^8\ \text{cm}^{-1}$ and $\omega_D \sim 10^{13}\ \text{s}^{-1}$, we get the order of the value $T_D \sim 10$ K. Debye's temperatures ($T < 10$ K) are such that it can be assumed that the acoustic branches with energy proportional to the wave vector are:

$$\hbar\omega_\alpha(\vec{k}) = \hbar v_\alpha k \quad \text{for} \quad ak_{max} \gg 0.1, \tag{39}$$

where v_α –is the speed of sound of the corresponding branch of oscillation, on the order of $v_\alpha \sim (10^3 \div 10^5)$ m/s, if $a \approx 10^{-10}$ m.

Free energy is, for the acoustic branch of the spectrum and given dispersion law, expressed as:

$$F_{ak} = \sum_{\alpha=1}^{3}\sum_{\vec{k}} \ln\left[1 - \mathrm{e}^{-\frac{\hbar\omega_\alpha(\vec{k})}{\theta}}\right]. \tag{40}$$

By switching from sum to the integral by the rule [70–72]:

$$\sum_{\alpha\vec{k}} \to 3\frac{V}{2\pi^2\overline{v}^3}\int_0^{\omega_D}\omega^2 d\omega,$$

where $\frac{3}{\overline{v}^3} = \frac{2}{v_T^3} + \frac{1}{v_L^3}$ is averaged velocity of phonons by branches and direction. The boundary frequency ω_D is determined from the conditions of standardizing [70]:

$$N = 3\frac{V}{2\pi^2\overline{v}^3}\int_0^{\omega_D}\omega^2 d\omega = \frac{V\omega_D^3}{6\pi^2\overline{v}^3}. \tag{41}$$

With the introduction of the change $x = \frac{\hbar\omega}{\theta}$ we finally get the expression for the free energy:

$$F_{ak} = 9Nk_BT\left(\frac{T}{T_D}\right)^3\int_0^{T_D/T} x^2\ln\left(1-\mathrm{e}^x\right)dx. \tag{42}$$

• High temperatures

If the inequality $\hbar\omega_\alpha(\vec{k}) \ll \theta$ is satisfied for all phonons, i.e. if $x \ll 1$, an approximation $1-\mathrm{e}^{-x} \simeq 1-(1-x) = x$ may be used. Then the free energy is calculated from (42) and from it internal energy, thermal capacitance and entropy [70]:

$$\begin{aligned} F_{ak} &= 3Nk_BT\left(\ln\frac{T_D}{T}-1\right); \qquad U = 3Nk_BT, \\ C_v &= 3Nk_B; \qquad\qquad S = 3Nk_B\left(\ln\frac{T}{T_D}+\frac{4}{3}\right). \end{aligned} \tag{43}$$

• Low temperatures

In the case of low temperatures, ie.when $x \gg 1$ the expression for the free energy can be written as:

$$F_{ak} = 9Nk_BT\left(\frac{T}{T_D}\right)^3 \int_0^\infty x^2 \ln\left(1-\mathrm{e}^x\right)dx.$$

The upper limit can now be expanded on ∞ so that the integral in the expression for the free energy can be expressed through the Riemann ζ function [79], ie

$$\int_0^\infty x^2 \ln\left(1-\mathrm{e}^x\right)dx = -2\sum_{n=1}^{\infty}\frac{1}{n^4} = -2\zeta(4) = -2\frac{\pi^2}{90}.$$

For this case thermodynamic functions are expressed as follows:

$$\begin{aligned} F_{ak} &= -\frac{\pi^4 Nk_BT}{5}\left(\frac{T}{T_D}\right)^3; \qquad U = \frac{3\pi^4 Nk_BT}{5}\left(\frac{T}{T_D}\right)^3, \\ C_v &= \frac{12\pi^4 Nk_B}{5}\left(\frac{T}{T_D}\right)^3; \qquad S = \frac{4\pi^4 Nk_B}{5}\left(\frac{T}{T_D}\right)^3. \end{aligned} \tag{44}$$

• General case

Free energy of acoustic phonons can be calculated:

$$\begin{aligned} F_{ak} &= 9N\,k_BT\left(\frac{T}{T_D}\right)^3 \int_0^{\omega_{max}} \omega^2 \ln\left(1-\mathrm{e}^{-\frac{\hbar\omega}{\theta}}\right)d\omega = \\ &= VN\theta\left[3\ln\left(1-\mathrm{e}^{-\xi}\right)-D(\xi)\right], \end{aligned} \tag{45}$$

where $\xi = T_D/T$ and $D(\xi) \equiv \frac{3}{\xi^3}\int_0^\xi \frac{x^3dx}{\mathrm{e}^x-1}$ – is Debye's function [79,80], which has the following boundary values:

$$D(\xi)=\begin{cases} 1-\dfrac{3}{8}\xi+\dfrac{1}{20}\xi^2, & \text{for} \quad \xi \ll 1, \\ \dfrac{\pi^4}{5}\xi^{-3}+O\left(\mathrm{e}^{-\xi}\right), & \text{for} \quad \xi \gg 1. \end{cases}$$

Applying the same approximations in the two extreme cases the same expressions for thermodynamic functions and size are obtained as in (44) and (45).The simplicity of Debye's approach consists in the fact that the whole thermodynamic aspect of the phonons in the crystal is expressed through a single parameter $\theta_D = k_B T_D$. Debye's temperature plays an important role in the theory of oscillations of the crystal lattice. It separates the low-temperature region, where it quantum statistics has to be used from hightemperature region where classical statistical mechanics must be applied. For the different bodies θ_D is different [70–72].If it is calculated with reduced Debye's temperatures, ie. T / T_D for all the bodies the same dependence of thermal capacity and entropy is obtained of this reduced temperature.

Debye temperature can be determined by measuring the thermal capacitance at low temperatures.

Despite the approximations Debye's theory agrees with the experiments [81]. As in Einstein's model, in the high temperature limes good agreement with the results of conventional thermal capacitance is obtained. At low temperatures, heat capacity and entropy behave $\sim T^3$. By that quantum theory has explained the deviation from the classical theory of the experiment.

Einstein's approximation

When observing lattice with complex (complex) basis optical branches of oscillation must be taken into consideration. Their frequencies slightly depend on the wave vector and, therefore, Einstein's approximation is applied at which the same frequency is attributed to all oscillations.

When calculating the contribution to free energy of optical branches oscillation phonons, the dependence of their frequency on the wave vector is ignored, ie. $\omega_\alpha(\vec{k}) = \omega_A$ is taken. Then:

$$F_{op} = \theta N \sum_{\alpha=4}^{3\sigma-3} \ln\left(1-\mathrm{e}^{-\frac{\hbar\omega_A}{\theta}}\right),$$

where summation is stretched to $(3\sigma-3)$ brances of optical oscillations of the crystal.After the summation it follows

$$F_{op} = 3\theta N(\sigma-1)\ \ln\left(1-\mathrm{e}^{-\frac{\hbar\omega_A}{\theta}}\right), \tag{46}$$

and the total internal energy is expressed then, using (30)

$$U = 3N(\sigma - 1)\frac{\hbar\omega_A}{e^{\frac{\hbar\omega_A}{\theta}} - 1}. \tag{47}$$

Based on that and on the definition (37) the expression for thermal capacitance is determined:

$$C_V = 3(\sigma - 1)Nk_B\left(\frac{\frac{\hbar\omega_A}{\theta}}{e^{\frac{\hbar\omega_A}{\theta}} - 1}\right)^2 e^{\frac{\hbar\omega_A}{\theta}}, \tag{48}$$

which can be "extended" within the observed temperature areas.

The expression for entropy using (38) it takes the form:

$$S = 3(\sigma - 1)Nk_B\left[\frac{\frac{\hbar\omega_A}{\theta}}{e^{\frac{\hbar\omega_A}{\theta}} - 1} - \ln\left(1 - e^{-\frac{\hbar\omega_A}{\theta}}\right)\right]. \tag{49}$$

• High temperatures

Approximative development: $\frac{\hbar\omega_A}{\theta} \ll 1$; $e^{\hbar\omega_A/\theta} - 1 \gg \frac{\hbar\omega_A}{\theta}$ is used, and by $\frac{\hbar\omega_A}{\theta} \ll 1$; $e^{\hbar\omega_A/\theta} - 1 \gg \frac{\hbar\omega_A}{\theta}$, and by arranging it, the following expressions are obtained:

$$\begin{aligned} F_{op} &= -3N\theta(\sigma - 1)\ln\frac{\theta}{\hbar\omega_A}; & U &= 3N\theta(\sigma - 1), \\ C_v &= 3Nk_B(\sigma - 1); & S &= 3(\sigma - 1)k_B\ln\frac{\theta}{\hbar\omega_A}. \end{aligned} \tag{50}$$

• Low temperatures

The following approximation: $\frac{\hbar\omega_A}{\theta} \gg 1, e^{\hbar\omega_A/\theta} - 1 \gg e^{\hbar\omega_A/\theta}$ is used here. Thermodynamical values are of the following form:

$$\begin{aligned} F_{op} &= -3(\sigma - 1)Nk_B e^{\frac{\hbar\omega_A}{\theta}}; & U &= 3(\sigma - 1)N\hbar\omega_A e^{-\frac{\hbar\omega_A}{\theta}}, \\ C_v &= 3(\sigma - 1)Nk_B\left(\frac{\hbar\omega_A}{\theta}\right)^2 e^{-\frac{\hbar\omega_A}{\theta}}; & S &= 3(\sigma - 1)Nk_B\left(\frac{\hbar\omega_A}{\theta} + 1\right)e^{-\frac{\hbar\omega_A}{\theta}}. \end{aligned} \tag{51}$$

By reducing the temperature all calculated values tend toward zero.In Einstein's model, the third law of thermodynamics is met. At low temperatures the thermal energy is much smaller than the phonon quantum $\hbar\omega_A$, so harmonic oscillators remain at the lowest energy levels. At high temperatures, the results of Einstein's approximation exceed the

experimentally proven classical expressions. However, the agreement with the practice is not completely at lower temperatures.However, the agreement with the practice is not completely at lower temperatures. From expression for C_V it can be seen that when $T \to 0$, and $C_V \to 0$ exponentially, while measurements indicate that $C_V \sim T^3$.

The temperature T_A, at which heat capacity starts to decrease rapidly, Einstein temperature is characteristic. It is one of the most important variables that characterize the crystal. At temperatures that are lower than the characteristic temperature $T \ll T_A$, quantum approach is necessary, and in $T \gg T_A$ classical approach can be used.

• Middle temperatures

In this part the behavior of the thermal capacitance is similar to the Debye's model, an approximately linear (Figure 8).In this area [73]is used and the general expression (49). For crystals with polyatomic basis, optical branches of the spectrum correspond to higher values ω, and acoustic – to lower values.Debye's model is used when the energy spectrum possesses, exclusively, three acoustic branches. In more complex cases Einstein's approximation can be used, in which the frequency of optical branches do not depend on k, and are equal ω_A. Characteristic features of Einstein's expression for thermal capacitance are as follows

• At temperatures much higher than Einstein's, each optical mode gives a constant share in the expression for thermal capacitance, as Dulong Petit law predicts.

• At temperatures much lower than Einstein's, the share of the optical mode to thermal capacitance decreases exponentially indicating the difficulty of thermal excitation of optical modes at low temperatures.

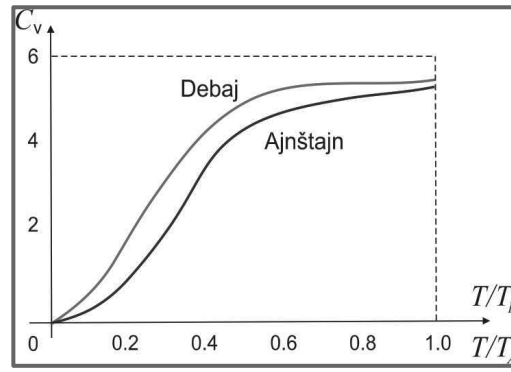

Figure 8: The thermal capacitance of the crystal

I.3.3. *Phonon states density*

Function of spectral phonon density gives the distribution of the number of phonons with different energies on the frequency scale [70–73]:

$$D_\alpha(\omega) \equiv \frac{dn_\alpha}{d\omega}; \qquad D(\omega) = \sum_{\alpha=1}^{3\sigma} D_\alpha(\omega), \tag{52}$$

(where n_α is the number of states in all the branches of the spectrum, acoustic and optical for a given frequency, and V is the volume) and in the general case it can be expressed as:

$$D(\omega) = V \sum_{\alpha=1}^{3\sigma} \int \frac{d\vec{k}}{(2\pi)^3} \delta(\omega - \omega_\alpha(\vec{k})) = V \sum_{\alpha=1}^{3\sigma} \int \frac{dS}{(2\pi)^3} \frac{1}{|\nabla \omega_\alpha(\vec{k})|}, \tag{53}$$

where the last integral is taken on the surface of I Brillouin zone, on which $\omega_\alpha(\vec{k}) =$ const. Density of state can always be calculated if one knows the law of dispersion $\omega = \omega_\alpha(\vec{k})$. The points at which the group velocity is zero are called Van Hove's singularities [70–73]. In these points peaks on the curve $D(\omega)$ appear.

Using the expression for the density of phonon state, Debye approximation (in the previous paragraph) and its limitations can compactly be formulated. Let all three branches of the acoustic spectrum are characterized by linear dispersion law $\omega_\alpha(k) = v\,k$ in longwave approximation. It is also considered that the phonon wave vectors lie in the sphere of radius k_D, and not in I Brillouin's zone. Then the expression (53) becomes simpler:

$$\begin{aligned} D_D(\omega) &= \frac{3V}{(2\pi)^3} \int_0^\pi \sin\theta\, d\theta \int_0^{2\pi} d\phi \int_0^{k_D} k^2\, dk\, \delta(\omega - vk) = \\ &= \begin{cases} \dfrac{3V}{2\pi^2} \dfrac{\omega^2}{\overline{v}^3}, & \text{for} \quad \omega < \omega_D, \\ 0, & \text{for} \quad \omega > \omega_D, \end{cases} \end{aligned} \tag{54}$$

where $3\,\overline{v}^{-3} = v_L^{-3} + 2v_T^{-3}$. If the observed sample comprises N elementary cells then the total number of states of acoustic phonons is equal to N, a Debye frequency is determined from the condition of standardization:

$$N = \int_0^{\omega_D} D_D(\omega)\, d\omega = \frac{V \omega_D^3}{6\pi^2 v^3}; \quad V = Na^3; \quad \omega_D = k_D v$$

(number of lattice nodes is equal to the number of phonon states), from which:

$$\omega_D = \frac{v}{a} \sqrt[3]{6\pi^2}. \tag{55}$$

Although the actual density of state is very far from Debye, estimation of the maximum frequency is the correct size on the order. Replacing the actual density of states $D(\omega)$ by Debye's is possible, if the crystal is with a primitive elemental cell.

In the context of Einstein's model, where the crystal is treated as a collection $3N$ of independent quantum oscillators (see preceding paragraph) which oscillate with their own frequency $\omega_\alpha(\vec{k}) = \omega_A$, the expression for density state of optical phonons is:

$$D_A(\omega) = \int \frac{d\vec{k}}{(2\pi)^3} \delta(\omega - \omega_A) = N\,\delta(\omega - \omega_A)\,. \tag{56}$$

The number of those oscillatorsis $3(\sigma - 1)N$, where σ is number of sublattices in the cell.

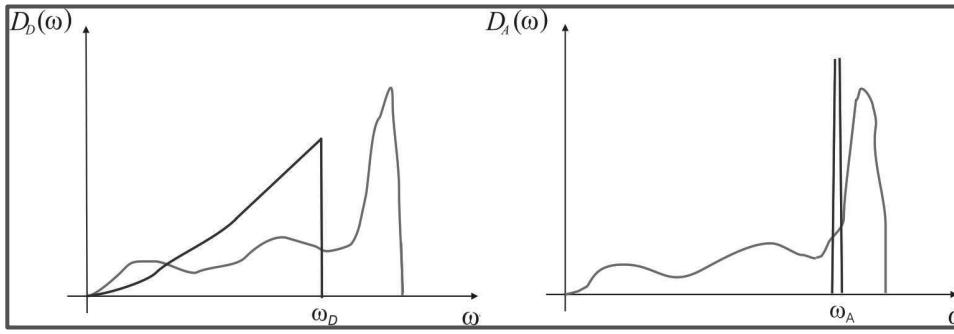

Figure 9: Debye (left) and Einstein (right) approximation of phonon statesdensity [73]

Calculation, in general, is a very complex task. However, knowledge of the exact shape, and in particular the situation of the maximum of this function on a frequent scale, is very important in the interpretation of various physical effects and the interpretation of experimental results in the solid body (eg. in the study of magnet-acoustic resonance, volt-ampere characteristic of the tunnel crossing in Mossbauer spectroscopy, superconductivity, etc.). [77,81–83].

I.3.4. *The heat conductivity*

In the thermal excitations of a crystal phonons are formed in it. They are spread through the crystal at the speed of sound and transfer (heat) energy. Heat flow *J*, developed in the area of low temperature *T* is determined by Fourier law [84–86]:

$$\vec{J} = -\kappa \,\mathrm{grad}\, T = -\kappa \left(\frac{\partial T}{\partial n} \right)_n , \tag{56}$$

where κ – is coefficient of thermal conductivity and $\left(\frac{\partial T}{\partial n} \right)_n$ temperature gradient along the normal to the isothermal surface.

The law of conservation of impulse is fulfilled in every interaction if the interaction between phonons does not exist or is realized without flashover process, so-called U process (Umklapprozesse).In this case phonons transmit energy without temperature gradient, i.e. thermal resistance is absent. The state of thermal resistance indicates that, in the processes of interaction of phonons, the law of conservation of impulse is violated, i.e. leap processes are realized.However, leap processes are only possible in an interaction of phonons with energy $\hbar\omega$, which exceeds a critical energy E_0. At low temperatures, the mean number of these phonons and thermal resistance are proportional $\exp\left(-E_0 / k_B T\right)$, and thermal conductivity $\exp\left(E_0 / k_B T\right)$.Such a temperature dependence was observed in

Berman's experiments [87] for diamond crystal $E_0 \sim \theta_D / 2.6$ and solid helium $E_0 \sim \theta_D / 2.3$, where $\theta_D = k_B T_D$ and T_D – Debye temperature.

The coefficient of thermal conductivity as a result of the solutions of the Boltzmann transport equation in relaxation time approximation is given in the expression

$$\kappa = \frac{1}{(2\pi)^3} \sum_n \int \left(\vec{v}_{k,n} \cdot \vec{e}\right)^2 \tau_{\vec{k},n} C_{ph}\left(\vec{k},n\right) d\vec{k}. \tag{57}$$

Summation is performed through all of the phonon modes *n*, $\vec{e}$ is the unit vector along the gradient of the temperature, $\vec{k}$ is the wave vector. C_{ph} is the specific heat capacity per frequency ω phonon mode, and $\vec{v}_{\vec{k},n}$ is the speed of phonons in the n^{th} mode with the wave vector $\vec{k}$.

The specific heat is given as

$$C_{ph} = \frac{\hbar^2 \omega^2}{k_B T} \frac{\exp\left(\hbar\omega / k_B T\right)}{\left[\exp\left(\hbar\omega / k_B T\right) - 1\right]^2}. \tag{58}$$

In isotropic case $\left(\vec{v}_{\vec{k},n} \cdot \vec{e}\right)^2 = \frac{1}{3} v_{\vec{k},n}^2$:

$$\kappa = \frac{4\pi}{3} \frac{1}{(2\pi)^3} \sum_n \int v_{\vec{k},n}^2 \tau_{\vec{k},n} C_{ph}\left(\vec{k},n\right) g\left(\vec{k},n\right) d\vec{k}, \tag{59}$$

where $g\left(\vec{k},n\right)$ – is density of phonon states and can be written as $g\left(\vec{k},n\right) d\vec{k} = \left(\omega^2 / v^3\right) d\omega$ in so-called Debye's case, i.e. when $\omega = vk$. It follows that the thermal conductivity

$$\kappa = \frac{1}{3} \frac{1}{2\pi^2} \sum_n \int_0^{\omega_{max,n}} \frac{\tau_{\omega,n}}{v_{\omega,n}} C_{ph}\left(\omega,n\right) \omega^2 d\omega. \tag{60}$$

Here, $\omega_{nax,n}$ is maximum frequency of phonons in the spectrum for the appropriate mode*n*.

This is a general expression for thermal conductivity. Specific heat, which depends on the law of dispersion of phonons, as well as the time relaxation response depending on the relaxation mechanisms, will be discussed.

I.3.5. *Specific heat*

It is known that the phonons Bose quasiparticles with the function of the distribution in the form of

$$f_{\text{B}}\left(\omega,T\right) = \left[\exp\left(\hbar\omega_{n.k} / k_B T\right) - 1\right]^{-1}. \tag{61}$$

The internal energy of certain branches of phonon system is given as

$$U_{n.k} = \hbar\omega_{n,k} \left[\frac{1}{2} + f_{\text{B}}\left(\omega,T\right)\right], \tag{62}$$

and total internal energy

$$U_{\text{tot}} = \sum_{n,k} U_{n,k}(\omega, T). \tag{63}$$

As the specific heat is defined as $C_V = \left(\frac{\partial U}{\partial T}\right)_V$ it follows that

$$C_V = \sum_{n,k} \frac{\hbar^2 \omega^2}{k_B T} \frac{\exp(\hbar\omega / k_B T)}{\left[\exp(\hbar\omega / k_B T) - 1\right]^2}. \tag{64}$$

Now so called Einstein's model of the dispersion law of phonons will be analyzed in which the so-called optical branches of the phonon spectrum that are considered to have a constant frequency value $\omega = \omega_E$ are discussed

$$\begin{aligned} U_{\text{tot}} &= \sum_{n,k} U_{n,k}(\omega, T) = 3N\hbar\omega_E \left[f_{\text{B}}(\omega_E, T) + \frac{1}{2} \right] = \\ &= 3N \frac{\hbar\omega_E}{\left(\exp(\hbar\omega_E / k_B T) - 1\right)} + 3N \frac{\hbar\omega_E}{2}. \end{aligned} \tag{65}$$

Here N is the total number of atoms in the system. From this expression for the internal energy is easy to obtain expression for specific heat at Einstein's model

$$C_V = \frac{\partial U_{\text{tot}}}{\partial T} = 3N \frac{\hbar^2 \omega_E^2}{k_B T} \frac{\exp(\hbar\omega_E / k_B T)}{\left[\exp(\hbar\omega_E / k_B T) - 1\right]^2}. \tag{66}$$

In temperature limit when $T \to 0$:

$$C_{V,ph} \approx \exp(-\hbar\omega_E / k_B T). \tag{67}$$

In this model, specific heat decreases exponentially at low temperatures, which is not in accordance with the experimental data which show that the specific heat behaves depending on the temperature as T^3.

If we take into consideration Debye's model for 3-dimensional isotropic crystal, then the expression for density of phonon state is the following:

$$D(\omega) d\omega = \frac{\int d^3k}{\Delta^3 k} = \frac{\int d^3k}{(2\pi / a)^3} = \frac{a^3}{2\pi^2} \frac{k^2}{d\omega / dk} d\omega$$

(a is the constant of the crystal lattice). As $\omega = vk$ final expression for the density of phonon state of Debye's model is as follows:

$$D(\omega) = \frac{a^3 \omega^2}{2\pi^2 v^3}. \tag{68}$$

The internal energy and specific heat in general form for Debye's model are given as

$$U_{\text{tot}} = \int \hbar\omega \left[\frac{1}{2} + f_{\text{B}}(\omega, T) \right] D(\omega) d\omega ;$$

$$C_{V,ph} = \frac{\partial}{\partial T} \int \hbar\omega f_{\text{B}}(\omega, T) D(\omega) d\omega =$$

$$= \frac{1}{2\pi^2 v^3} \int_0^{\omega_D} \frac{\hbar^2 \omega^4}{k_B T^2} \frac{\exp(\hbar\omega / k_B T)}{\left[\exp(\hbar\omega / k_B T) - 1 \right]^2} d\omega = \tag{69}$$

$$= 9Nk_B \left(\frac{T}{\theta} \right)^3 \int_0^{x_D} \frac{x^4 e^x}{\left(e^x - 1 \right)^2} dx.$$

In a case when $T \to 0$ temperature dependence of the specific heat is

$$C_{V,ph} = \frac{12\pi^4}{5} Nk_B \left(\frac{T}{\theta} \right)^3 \approx T^3 \tag{70}$$

at which: $\theta = \frac{\hbar\omega_D}{k_B} = \frac{\hbar}{k_B} \sqrt[3]{6\pi^2 N}$; $x_D = \frac{\hbar\omega_D}{k_B T}$.

Klemens model

In Klemens model [88] thermal conductivity is calculated separately for each mechanism of relaxation and then the total thermal conductivity is obtained as

$$\frac{1}{\kappa} = \sum_i \frac{1}{\kappa_i}. \tag{71}$$

In this model relaxation time in a collision of the type phonon- point defects (defects with different mass as isotopes, impurities, etc.) Is given as:

$$\frac{1}{\tau_{i,j}} = \frac{\pi}{6} V' \Gamma g(\omega) \omega^2 = \frac{V' \Gamma}{4\pi v_j^3} \omega^4 ;$$

$$\Gamma = \frac{\sum_i (c_i M_i)^2 - \left(\sum_i c_i M_i \right)^2}{\left(\sum_i c_i M_i \right)^2}, \tag{72}$$

where $\tau_{i,j}$ is the relaxation time of the j[th] phonon branch; V is the atomic volume; Γ parameter of mass fluctuations in collisions of phonons and point defects; c_i and M_i respectively, are concentration and mass point defects (isotopes and impurities); $g(\omega)$ is the density of phonon state of Debye's model, while v_j is the group velocity of each phonon branch in the spectrum of phonons. At low temperatures and scattering of phonons at the boundaries of crystal thermal conductivity and behaves as $\sim T^3$ and reflection factor is determined by the geometry of the sample and the sample surface detail. Speed scattering is given by the relation:

$$\tau^{-1} = \frac{\overline{v}}{L_0}, \tag{73}$$

whereL_0 is effective mean free path of phonons, which depends on many factors (sample geometry, focus of phonons, mirror (diffusion) reflection from the surface, etc.).

Experimental is the fact that the level of impurities significantly affects the thermal conductivity of the sample. For example highly enriched germanium $^{70}\mathrm{Ge}\left(99{,}99\%\right)$ has 14 times higher thermal conductivity than sample $^{70/76}\mathrm{Ge}\left(43\%\ ^{70}\mathrm{Ge};\ 48\%\ ^{76}\mathrm{Ge};\right.$ $\left.9\%\ \text{other impurities}\right)$. [89]

Callaway'smodel

Joseph Callaway has developed a model to calculate the coefficient of phonon thermal conductivity that is valid in the temperature range from 2,5K to 100K [84,90]. In this model we analyze Debye's isotropic phonon dispersion law, ie. No distinction is made between the longitudinal and transverse phonon branches in the spectrum of phonons and Debye's density of phonon states. The mechanisms of relaxation are as follows:

1. Collisions of phonons with isotopes in the crystal lattice and dotted admixture According to Klemens relaxation time in collisions of phonons with isotopes is given as $\tau^{-1} = A\,\omega^4$, where A is a parameter which is determined by fitting and which depends on the mass fluctuations in collision of the isotope with the phonons as well as on the speed of of phonons.
2. Collisions of phonons with the boundaries of crystals
   $\tau^{-1} = \frac{\overline{v}}{L_0}$, where $\overline{v}$ is the average speed of phonons, and L_0 the characteristic length of the sample (crystal). It is assumed that the scattering at the boundaries is purely diffusional and that the mean velocity of phonons is the same for all branches of the phonon spectrum.
3. Three-phonon normal collisions,
   $\tau_N^{-1} = B_2\,T^3\,\omega^2$,where B_2 is the parameter which is obtained by fitting and which depends on the speed of phonons and Grinajzenove constants. The expression for relaxation time was found by Hering for collision of longitudinal phonons at low temperatures, with the condition of maintaining phonons momenta.
4. Collisions of phonons in the U processes
   $\tau_U^{-1} = B_1\,T^3\,\omega^3$, where B_1 is the parameter which is determined by fitting and depends, according to Pailler, on the temperature as $\exp\left(-\theta / bT\right)$, on the speed of phonons, Gruneisen's constant and Debye's temperature. U processes in Callaway model are related neither to low nor high temperatures. However, this model is limited to low temperature, i.e. where the U processes are negligible.

Total relaxation time is given by Matthiessen's rule [71–73]:

$$\tau = \left(\frac{\overline{v}}{L_0} + B_1 T^3 \omega^2 + A\,\omega^4 + B_2 T^3 \omega^2 \right)^{-1}, \tag{74}$$

so the thermal conductivity is given in the

$$\kappa = \frac{1}{2\pi^2 \overline{v}} \int_0^{\omega_D} \frac{\hbar^2 \omega^4 k_B T^{-2}}{\overline{v} / L_0 + B_1 T^3 \omega^2 + A\omega^4 + B_2 T^3 \omega^2} \times \\ \times \frac{\exp\left(\hbar\omega / k_B T\right)}{\left[\exp\left(\hbar\omega / k_B T\right) - 1\right]^2} d\omega. \tag{75}$$

This model describes the thermal conductivity at low temperatures well $\left(\leq 0.1\,\theta\right)$ where the phonon spectrum is well approximated and where the dominant collisions of phonons with isotopes / admixtures and with the boundaries of the sample.

Holland's model

Unlike Klemens and Callaway model and the analysis of thermal conductivity at Holland's model explicitly considers the contribution of transverse and longitudinal phonons [91].

1. Collisions with isotopes and admixtures

$$\tau^{-1} = A\omega^4. \tag{76}$$

2. Collision with boundaries

$$\tau^{-1} = \frac{\overline{v}}{F L_0}, \tag{77}$$

where $\overline{v}^{-1} = \frac{1}{3}\left(2v_T^{-1} + v_L^{-1}\right)$, and F is reflection parameter, introduced due to the partial diffusion scattering at the boundaries of the crystal. Thus, in this model collisions of phonons with the boundaries are not entirely diffusive. Holland's model tries to explain the behaviour of thermal conductivity at higher temperatures $\left(T > 0.1\,\theta\right)$.

3. The expression for relaxation time of phonon-phonon collision for three-phonon collisions at so called. normal processes has been modified in relation to the Callaway's model

$$\tau_{N,T}^{-1} = B_T \omega T^4 \quad \text{for} \quad 0 \leq \omega < \omega_1; \\ \tau_{N,L}^{-1} = B_L \omega^2 T^3 \quad \text{for} \quad 0 \leq \omega < \omega_3. \tag{78}$$

Unlike Callaway'smodel where we consider only longitudinal phonons in Holland's model the transverse phonons are considered also.

4. With U phonon collision, relaxation time is

$$\tau_{U,T}^{-1} = \frac{B_{U,T}\omega_2}{\sinh\left(x\right)} \quad \text{for} \quad \omega_1 \leq \omega \leq \omega_2; \\ \tau_{U,T}^{-1} = 0 \quad \text{for} \quad \omega < \omega_1, \tag{79}$$

where $x = \frac{\hbar\omega}{k_B T}$.

In Holland's model, in U processes, only transverse phonons are analyzed. Also, for $\omega \leq \omega_1$ $\left(\text{or } \theta \leq \theta_1\right)$ U processes are absent.

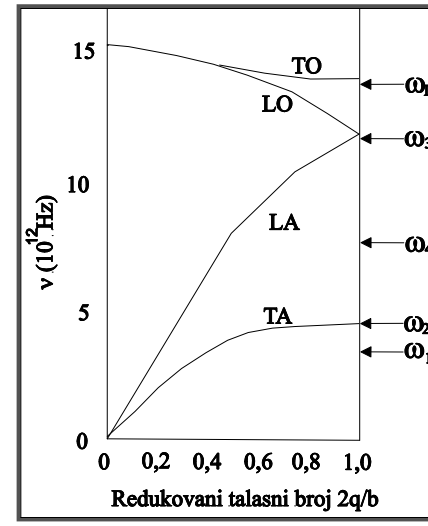

Figure 10: Phonon branches depending on the reduced wave vector [91]

Combining terms for longitudinal and transverse modes of phonons it follows that: $\kappa = \kappa_T + \kappa_L$, i.e.

$$\kappa = \frac{2}{3}\int_0^{\theta_T/T} \frac{C_T T^3 x^4 \mathrm{e}^x \left(\mathrm{e}^x - 1\right)^{-2} dx}{\tau_T^{-1}} + \frac{1}{3}\int_0^{\theta_L/T} \frac{C_L T^3 x^4 \mathrm{e}^x \left(\mathrm{e}^x - 1\right)^{-2} dx}{\tau_L^{-1}} =$$

$$= \frac{2}{3}\int_0^{\theta_1/T} \frac{C_1 T^3 x^4 \mathrm{e}^x \left(\mathrm{e}^x - 1\right)^{-2} dx}{\overline{v}/FL_0 + Am^4 x^4 T^4 + B_{N,T} mx T^5} +$$

$$+ \frac{2}{3}\int_{\theta_1/T}^{\theta_2/T} \frac{C_2 T^3 x^4 \mathrm{e}^x \left(\mathrm{e}^x - 1\right)^{-2} dx}{\overline{v}/FL_0 + Am^4 x^4 T^4 + \dfrac{B_{U,T} m^2 x^2 T^2}{\sinh(x)}} + \tag{80}$$

$$+ \frac{1}{3}\int_0^{\theta_L/T} \frac{C_L T^3 x^4 \mathrm{e}^x \left(\mathrm{e}^x - 1\right)^{-2} dx}{\overline{v}/FL_0 + Am^4 x^4 T^4 + B_{N,L} m^2 x^2 T^5};$$

$$i = T, L; \quad x = \hbar\omega / k_B T; \quad \theta_i = k_B \omega_i / \hbar;$$

$$C_i = \left(k_B / 2\pi^2 v_i\right)\left(k_B / \hbar\right)^3; \quad m = k_B / \hbar.$$

In Holland's model it is assumed that transverse phonon modes have three constant velocity values that depend on the field of phonons frequency, i.e. have a constant speed at low frequencies $\omega < \omega_1$, then the speed which rapidly decreases and remains constant between ω_1 and ω_2. For phonons with a frequency above ω_2 the speed of phonons is zero.

Generally speaking, Holland'smodel explains the behavior of thermal conductivity at higher temperatures better than Callaway model.

References

[1] G.Cao, Nanostructures & Nanomaterials, Synthesis, Properties & Applications*, Imperial College Press*, London 2004.

[2] R.P.Agarwal, Difference Equations and Inequalities: Theory, Methods and Applications, *MarcelDekker*, New York 2000.

[3] V.D.Sajfert, B.S.Tošić, The Research of Nanoscience Progress,*J.Comput.Theor.Nanosci*. **7**/1, 15–84 (2010).

[4] K.J.Morrow, R.Bawa, C.Wei: Recent Advances in Basic and Clinical Nanomedicine, *Med.Clin.N.Am.* **91,** 805-843 (2007).

[5] Y.Pathak, D.Thassu: Drug Delivery Nanoparticles – Formulation and Characterization, *Informa*,New York 2009.

[6] H.E.Schaefer: Nanoscience –The Science of the Small in Physics, Engineering,Chemistry, Biology and Medicine, *Springer*, Berlin 2010.

[7] J.P.Šetrajčić, D.Lj.Mirjanić, A.J.Šetrajčić-Tomić, S.Armaković, I.J.Šetrajčić, Core-Shell Nanomodels for Biomedical Applications, *Proceedings –International Conference – New face of TMCR: Modern Technologies, Quality and Innovation (ModTech'11)*, 545(2011).

[8] Nanoscale Assembly – Chemical Techniques, Ed. W.T.S.Huck, *Springer*, New York 2005.

[9] Self-Organized Nanoscale Materials, Eds. M.Adachi, D.J.Lockwood, *Springer*, New York 2006.

[10] J.P.Šetrajčić, S.K.Jaćimovski, V.D.Sajfert, Phonon Contribution to Heat Capacitanceof Nanolayered Crystalline Structures, *Mod.Phys.Lett.*B **29**/4, 1550008 (2015); doi: 10.1142/S0217984915500086.

[11] A.N.Cleland, Foundations of Nanomechanics, ISBN 978-3-642-07821-7; *Springer*, Berlin 2003.

[12] M.A.Stroscio, M.Dutta, Phonons in Nanostructures, ISBN 0-521-79279-7; *University Press*, Cambridge 2004.

[13] O.Manasreh, Semiconductor Heterojunctions and Nanostructures, *McGraw-Hill*, New York 2005.

[14] C.Delerue, M.Lannoo, Nanostructures -- Theory and Modelling, *Springer*, Berlin 2009.

[15] H.E.Schaefer, Nanoscience – The Science of the Small in Physics, Engineering, Chemistry, Biology and Medicine, *Springer*, Berlin 2010.

[16] M.C.Tringides, M.Jałochovski, E.Bauer, Quantum Size Effect in Metallic Nanostructures, *Physics Today*, April 2007, pp. 50–54.

[17] M.G.Cottam, D.R.Tilley, Introduction to Surface and Superlattice Excitations, *University Press*, Cambridge, 1989.

[18] C.Kittel, Quantum Theory of Solids, *Wiley*, New York 1963.

[19] G.D.Mahan, Condensed Matter in a Nutshell, *University Press*, Princeton 2011.

[20] J.M.Ziman, Electrons and Phonons: The Theory of Transport Phenomena in Solids, *Oxford University Press*, New York 2001.

[21] F.Marsiglio and J.P.Carbotte: Electron-Phonon Superconductivity, http://arxiv.org/find/cond-mat/, No: 0106143 (2001).

[22] A.K.Saxena, High-Temperature Superconductors, *Springer*, Berlin – Heidelberg 2010.

[23] J.P.Šetrajčić, V.M.Zorić, N.V.Delić, D.Lj.Mirjanić, S.K.Jaćimovski, Phonon Participation in Thermodynamics and Superconductive Properties of Thin Ceramic Films, Ch.15, pp.317-348, In Thermodynamics, Ed. M.Tadashi, *InTech*, Vienna 2011.

[24] A.A.Balandin, K.L.Wang, Significant Decrease of the Lattice Thermal Conductivity due to Phonon Confinement in a Free-Standing Semiconductor Quantum Well, *Phys.Rev*.B **58**/3, 1544 (1998);

[25] A.A.Balandin, E.P.Pokatilov, D.L.Nika, Phonon Engineering in Hetero- and Nanostructures, *J.Nanoelect.Optoelect*. **2**, 140 (2007).

[26] D.L.Nika, N.D.Zincenco and E.P.Pokatilov, Engineering of Thermal Fluxes in Phonon Mismatched Heterostructures, *J.Nanoelect.Optoelect*. **4**, 180 (2009).

[27] A.A.Balandin, D.L.Nika, Phononics in Low-Dimensionals Materials, *Materials Today***15**/6, 266 (2012).

[28] D.L.Nika, E.P.Pokatilov, A.A.Balandin, Phonon-Engineered Mobility Enhancement in the Acoustically Mismatched Silicon/Diamond Transistor Channels, *Appl.Phys.Lett*. **93**, 173111 (2008).

[29] J.P.Šetrajčić, S.K.Jaćimovski, D.Raković, D.I.Ilić, Phonon Spectra in Crystalline Nanostructures, in Electrical and Computer Engineering Series: Advances in Simulation, Systems Theory and Systems Engineering, Eds. N.E.Mastorakis, V.V.Kluev, Dj.Koruga, *WSEAS Press*, 2003; pp. 146-151.

[30] D.Popov, S.K.Jaćimovski, B.S.Tošić, J.P.Šetrajčić, Kinetics of Thin Films Mechanical Oscillations, *Physica* A **317**, 129-139 (2003).

[31] S.K.Jaćimovski, J.P.Šetrajčić, B.S.Tošić, V.D.Sajfert, Thermodynamics of Mechanical Oscillations in Superlattices, *Materials Science Forum***453-454**, 33-36 (2004).

[32] S.K.Jaćimovski, B.S.Tošić, J.P.Šetrajčić, V.M.Zorić, V.D.Sajfert, D.I.Ilić, Thermodynamics of Mechanical Oscillations in Crystalline Superlattices, *Int.J.Mod.Phys.*B **21**(6), 917-930 (2007).

[33] S.K.Jaćimovski, J.P.Šetrajčić, M.S.Jaćimovski and V.V.Stojanović, Phonon Contribution in Thermodynamics and Transport Properties of Ultrathin Ceramic Films, *Acta Phys.Pol.* A **126**/3, 811 (2014).

[34] J.P.Šetrajčić, V.D.Sajfert, D.Lj.Mirjanić, S.M.Vučenović, Operator Method for Solving the Difference Equations, *Proceedings 5th WSEAS International Conference on Applied Mathematics*, **488**/148, 1-4 (2004).

[35] J.P.Šetrajčić, S.K.Jaćimovski, V.D.Sajfert, I.J.Šetrajčić, Specific Quantum Mechanical Solution of Difference Equation of Hyperbolic Type, *Commun.Nonlinear Sci.Numer.Simulat*. **19**/5, 1313 (2014).

[36] J.W.Kim, Ho-S.Yang, Y.Ha Jun, K.Ch.Kim, Interfacial effect on thermal conductivity of diamond-like carbon films, J Mech.Sci.Technol. **24**/7, 1511-1514 (2010).

[37] W.Liu, M.Asheghi, Thermal Conductivity Measurements of Ultra-Thin Single Crystal Silicon Layers, *J.Heat Transfer128*, 75 (2006).

[38] G.Zhang, H.Zhang, Thermal Conduction and Rectication in Few-Layer Graphene Y Junctions, *Nanoscale***3**, 4604 (2011).

[39] D.L.Nika, A.I.Cocemasov, A.A.Balandin, Specific Heat of Twisted Bilayer Graphene, *Appl.Phys.Lett.***105**, 031904 (2014).

[40] S.K.Jaćimovski, M.Bukurov, J.P.Šetrajčić, D.I.Raković, Phonon Thermal Conductivity of Graphene, Superlattices and Microstructures, http://dx.doi.org/10.1016/j.spmi.2015.09.027 – In Press (2015).

[41] C.P.Poole Jr, F.J.Owens: Introduction To Nanotechnology, *John Wiley &Sons Ltd*, New Jersey 2003.

[42] E.L.Wolf: Nanophysics and Nanotechnology, *Wiley-VCH*, Weinheim 2006.

[43] R.W.Kelsall, I.W.Hamley, M.Geoghegan (Eds.): Nanoscale Science and Technology, *John Wiley &Sons Ltd*, Chichester 2005.

[44] M.Adachi, D.J.Lockwood (Eds.): Self-Organized Nanoscale Materials, *Springer Science+Business Media, Inc.*, New York 2006.

[45] W.T.S.Huck (Ed.): Nanoscale Assembly – Chemical Techniques, *Springer Science+Business Media,Inc.*, New York 2005.

[46] E.Knystautas (Ed.): Engineering Thin Films and Nanostructures with Ion Beams, *CRC Press*, Boca Raton, FL (USA) 2005.

[47] C.N.R.Rao, P.J.Thomas, G.U.Kulkarni: Nanocrystals: Synthesis, Properties and Applications, *Springer-Verlag*, Berlin Heidelberg 2007.

[48] A.G.Davies, J.M.T.Thompson (Eds.): Advances in Nanoengineering – Electronics, Materials and Assembly, *Imperial College Press*, London 2007.

[49] W.Zhou, Z.L.Wang (Eds.): Scanning Microscopy for Nanotechnology, *Springer Science+Business Media, LLC*, New York 2006.

[50] P.Eaton, P.West: Atomic Force Microscopy, *University Press*, Oxford, 2010.

[51] M.F.Crommie, C.P.Lutz and D.M. Eigler: Confinement of electrons to quantum corrals on a metallic surface, *Science* **262**, 218-220, 1993.

[52] E.Roduner: Nanoscopic Materials – Size-dependent Phenomena, *RSC Publishing*, Cambridge 2006.

[53] M.T.Dove: Introduction to Lattice Dynamics, *University Press*, Cambridge 1993.

[54] J.M.Ziman: Electrons and Phonons, *Oxford Science*, Oxford 1996.

[55] J.P.Wolfe: Imaging Phonons – Acoustic Wave Propagation in Solids, *University Press*, Cambridge 1998.

[56] M.A.Stroscio, M.Dutta: Phonons in Nanostructures, *University Press*, Cambridge 2004.

[57] B.K.Ridley: Electrons and Phonons in Semiconductor Multilayers, *University Press*, Cambridge 2009.

[58] J.P.Šetrajčić, D.I.Ilić, B.Markoski, A.J.Šetrajčić, S.M.Vučenović, D.Lj.Mirjanić, B.Škipina, S.Pelemiš: Adaption and Application of the Green Function Method to Research on Molecular Ultrathin Film Optical Properties, *Physica Scripta* T135 014043 (4 pp) 2009.

[59] C.S.S.R.Kumar (Ed.): Raman Spectroscopy for Nanomaterials Characterization, *Springer-Verlag*, Berlin Heidelberg 2012.

[60] P.J.Larkin: Infrared and Raman Spectroscopy, *Elsevier*, 2011.

[61] C.Kittel, Introduction to Solid State Physics, *Wiley*, New York 1986.

[62] H.Ibach, H.Lüth, Solid–State Physics: An Introduction to Principles of Material Science, *Springer*, Berlin 2003.

[63] N.N.Bogolyubov, Problems of the Dynamic Theory in Statistical Physics, *Nauka*, Moscow 1946.

[64] G.Strobl, Condensed Matter Physics: Crystals, Liquid Crystals, and Polymers, *Springer*, Berlin 2004.

[65] W.Harrison, Solid state theory, *DoverPubl*., New York 1979.

[66] B.S.Tošić, Statistička fizika, *PMF*, Novi Sad 1978.

[67] B.J.McClelland, Statistical Thermodynamics, *Chapman*, London 1973.

[68] E.S.R.Gopal, Statistical Mechanics and Properties of Matter, *Wiley*, New York 1974.

[69] B.S.Tošiić, J.P.Šetrajčić, R.P.Djajić-Jovanović, D.Lj.Mirjanić, *Phys.Rev.* B **36**, 9094 (1987).

[70] I.Supek, Teorijska fizika i struktura materije, *Školska knjiga*, Zagreb 1977.

[71] W.Harrison, Solid State Theory, *Dover Publ.*, New York 1979.

[72] W.Jones, N.H.March, Theoretical solid state physics (I and II), *Dover*, New York 1985.

[73] N.W.Ashchroft and N.D.Mermin, Solid State Physics, Holt, New York (1976)

[74] N.N.Bogolyubov, Problems of the Dynamic Theory in Statistical Physics, *Nauka*, Moscow 1946.

[75] I.Prigogine, Non-Equilibrium Statistical Mechanics, *Wiley*, New York 1962.

[76] D.N.Zubarev, NonequilibriumStatistical Thermodynamics, *Consultants Bureau*, New York 1974.

[77] A.O.E.Animal, Intermediate Quantum Theory of Crystalline Solids, *Prentice-Hall*, New Jersey 1977.

[78] Lj.Ristovski, Teorija kondenzovanog stanja, *Fizički fakultet*, Beograd 1994.

[79] I.S.Gradshtein i I.M.Ryzhik, Tablyci integralov, summ, ryadov i proizvodenii, *Fizmatgiz*, Moskva 1962.

[80] D.S.Mitrinović, Uvod u specijalne funkcije, *Gradjevinska knjiga*, Beograd 1972.

[81] N.B.Brandt i S.M.Chudinov, Elektrony i fonony v metalah,*MGU*, Moskva 1980.

[82] S.K.Jaćimovski: Kolektivno mehaničko oscilovanjei termodinamičke osobine superprovodnih filmova (MRteza), *ETF*, Beograd 1997.

[83] Ž.Kovačevićc: Uticaj primjesa na elektronsku strukturu CuO2 ravni visokotemperaturskih superprovodnika, *PMF Podgorica* i *Fizički fakultet Beograd*, Podgorica 2000.

[84] J.Callaway, Quantum Theory of the Solid State,*Academic Press*, New York 1974.

[85] L.Kantorovich, Quntum Theory of the Solid Ttate: An Introduction, *Springer science and Business Media*, Berlin 2004.

[86] Fuxiang Han, A Modern Course in the Quantum Theory of Solids, *Worl Scientific*, New Yersey 2013.

[87] B.S.Tošić, J.P.Šetrajčić, R.P.Đajić, D.Lj.Mirjanić, Phonons in Broken-Symmetry Structures, *Phys.Rev.* B **36**, 9094 (1987).

[88] P.G.Klemens, The thermal conductivity of dielectric solids at low temperatures, *Proc. Royal. Soc.*, -ser. A, **208**, 108 (1951).

[89] Asen-Palmer et al., Thermal conductivity of germanium crystals with different isotopic compositions, *Phys. Rev*. B**56**, 9431 (1997).

[90] J.Callaway, Model for lattice thermal conductivity at low temperatures, *Phys. Rev*. **113**, 1046 (1959).

[91] M.G.Holland, Analysis of lattice thermal conductivity, *Phys. Rev*. **132**, 2461 (1963).

II. PHONONS IN NANOSTRUCTURES

Application of nano-structures requires knowledge of their fundamental physical (mechanical, electro-magnetic, optical, etc.) characteristics. Thermodynamic properties associated with phonon displacements through the nano-samples are particularly interesting. Independent of the type of lattices, the thermodynamics of their subsystems (electrons, excitons, spin waves, etc.) is determined when the subsystem is in thermodynamic equilibrium with phonons. Besides, the acoustical characteristics as well as conductive and superconductive properties etc. could not be realistically explained without phonons. The fact which must be especially pointed out is that the role of phonons in nanostructures is much more impressive than in bulk structures. The main fact concerning phonon properties in nanostructures is the absence of the so-called acoustic phonons: for the exciting of phonons in nanostructures activation energy different from zero is necessary. These unexpected characteristics require revision of all conclusions obtained by bulk theories of phonons. Therefore, the contribution of phonon subsystems to thermodynamic and energy transferring analysis is the first step in a research of nanostructure properties.

This – second partof the monographdescribes a major aspect of the effort to understand nanostructures, namely the study of phonons and phonon-mediated effects in structures with nanoscale dimensional confinement in one spatial dimension. During the last two decades, there has been a steady effort to understand the optical and acoustic phonons in crystalline layered nanostructures such as ultrathin films and composite films, i.e. superlattices, as well as in nanorods and quantnum dots [1–5]. The central theme of this part of the monograph is the description of the acoustic phonons of the optical type in these nanostructures. In this moment we will try to observe the difference between the characteristics of this two different nano-crystalline structures, we were interested in whether the quantum size effects (quantum confinement), quantum (de)coherence and influence of boundary conditions, strengthen or weaken in nanosamples. Finally, this monograph describes how the dimensional confinement of phonons in nanostructures leads to modifications in the electronic, optical, acoustic, superconducting and thermodynamic properties of quantum [6–10].

II.1. Phonons in 1D systems

II.1.1. *Coupled oscillators*

We will analyze small horizontal (longitudinal) oscillation systems of connected beads here (Figure 1), ignoring all resistances and taking the fact that in equilibrium all springs are unstrained.

The beads are acted upon by elastic (restitution) force of the springs: $\vec{F}_i = F_i\vec{e}_x; i = 1,2$, whose intensity is proportional to the elongation / shortening of the corresponding springs. Thus, the intensity of the forces acting on the beads 1 and 2 (Figure 1b), respectively:

$$\begin{aligned} F_1 &= -k(x_1 - a) + k(x_2 - x_1 - a)\,, \\ F_2 &= -k(x_2 - x_1 - a) - k(x_2 - 2a)\,. \end{aligned} \tag{1}$$

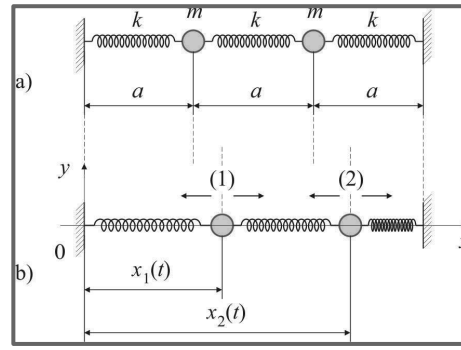

Figure 1: A system of coupled oscillators

By observing only a small disturbance around the equilibrium position:

$$\begin{aligned} u_1(t) &= x_1 - a = x_1(t)\,; \\ u_2(t) &= x_2 - 2a = x_2(t)\,, \end{aligned} \tag{2}$$

and by using Newton's second law $m\ddot{u}_i = F_i$we get a system of homogeneous linear differential equations of second order with constant coefficients:

$$\begin{aligned} \ddot{u}_1 + \Omega^2(2\ u_1 - u_2) &= 0\,, \\ \ddot{u}_2 + \Omega^2(2\ u_2 - u_1) &= 0\,, \end{aligned} \tag{3}$$

where$\Omega^2 \equiv k/m$.By applying the Laplace transformations$t \to \omega$ [11], i.e. $L\{u_i(t)\} = f_i(\omega)$, to both equations with defined initial conditions: $u_i(0) = a_i$; $\dot{u}_i(0) = b_i$; $i = 1{,}2$, the system of differential equations (3) becomes a system of linear algebraic equations:

$$\begin{aligned} (\omega^2 + 2\Omega^2)f_1 - \Omega^2 f_2 &= pa_1 + b_1\,, \\ -\Omega^2 f_1 + (\omega^2 + 2\Omega^2)f_2 &= pa_2 + b_2\,. \end{aligned} \tag{4}$$

This system has nontrivial and nonsingular solutions of the form:

$$\begin{aligned} f_{1,2}(\omega) = \frac{1}{2}\Big[&\frac{\omega}{\omega^2+\Omega^2}\Big(a_1 + a_2 + \frac{b_1+b_2}{\omega}\Big) \pm \\ &\pm \frac{\omega}{\omega^2+3\Omega^2}\Big(a_1 - a_2 + \frac{b_1-b_2}{\omega}\Big)\Big]\,. \end{aligned} \tag{5}$$

By Laplace's inversion: $\omega \to t$, tj. $L^{-1}\{f_i(\omega)\} = u_i(t)$, we get the required time displacements of tied beads – oscillators:

$$\begin{aligned} u_{1,2}(t) &= \frac{a_1+a_2}{2}\cos\Omega t + \frac{b_1+b_2}{2\Omega}\sin\Omega t \pm \\ &\pm \Big(\frac{a_1-a_2}{2}\cos\sqrt{3}\Omega t + \frac{b_1+b_2}{2\sqrt{3}\Omega}\sin\sqrt{3}\Omega t\Big) \equiv \\ &\equiv \mathcal{A}\sin(\Omega t + \alpha) \pm \mathcal{B}\sin(\sqrt{3}\Omega t + \beta)\,; \end{aligned} \tag{6}$$

$$\mathcal{A} \equiv \frac{a_1+a_2}{2}\sqrt{1+\frac{1}{\Omega^2}\left(\frac{b_1+b_2}{a_1+a_2}\right)^2}\ ;$$
$$\mathcal{B} \equiv \frac{a_1-a_2}{2}\sqrt{1+\frac{1}{3\Omega^2}\left(\frac{b_1-b_2}{a_1-a_2}\right)^2}\ ; \tag{7}$$
$$\alpha \equiv \arctan\left(\Omega\frac{a_1+a_2}{b_1+b_2}\right)\ ;$$
$$\beta \equiv \arctan\left(\sqrt{3}\Omega\frac{a_1-a_2}{b_1-b_2}\right)\ .$$

From the form of the solution (6) we can see that beads movement has oscillatory character with discreet normal frequencies:$\omega_1 = \Omega$ i $\omega_2 = \sqrt{3}\Omega$. By introducing normal coordinates of the system:

$$q_1(t) = \mathcal{A}\sin(\Omega t + \alpha)\ ;$$
$$q_2(t) = \mathcal{B}\sin(\sqrt{3}\Omega t + \beta)\ , \tag{8}$$

solutions for the oscillatory movement of tied oscillators can be written as:

$$u_1(t) = q_1(t) + q_2(t)\ ;$$
$$u_2(t) = q_1(t) - q_2(t)\ . \tag{9}$$

Interesting is analysis of the normal mode (the way) of oscillation of the observed system of elastically tied beads [12]. Two special cases can be observed.

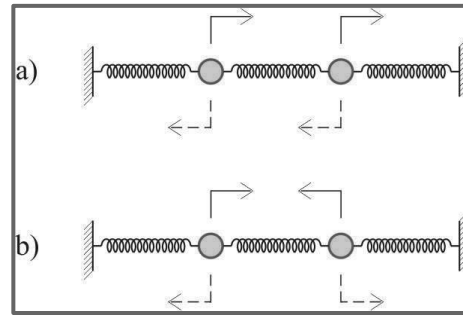

Figure 2: Normal oscillation modes

If the initial conditions are such that$\mathcal{B} = 0$, and that is when $a_1 = a_2$ i $b_1 = b_2$, ie. when at the initial moment both beads move the same distance: $u_1(0) = u_2(0)$and they are announced the same (by direction, way or intensity) initial impulse: $m\dot{u}_1(0) = m\dot{u}_2(0)$, then:

$$u_1^{(1)}(t) = u_2^{(1)}(t) \equiv q_1(t) = \mathcal{A}\sin(\Omega t + \alpha)\ . \tag{10}$$

Then both oscillators move simultaneously and identically. They have the same amplitude and move parallel (figure 2a) with the frequency $\omega_1 = \Omega$. It is said that the oscillation is in the phase!

If the initial conditions are such that$\mathcal{A} = 0$,and that is when$a_2 = -a_1$ and$b_2 = -b_1$, ie. when at the initial moment both beads move the same distance, but in different directions: $u_2(0) = -u_1(0)$and they are announced the opposite (the same by way, intensity, but the opposite direction) initial impulse: $m\dot{u}_2(0) = -m\dot{u}_1(0)$,then it is:

$$u_1^{(2)}(t) = -u_2^{(2)}(t) \equiv -q_2(t) = -\mathcal{B}\sin(\sqrt{3}\Omega t + \alpha)\,. \tag{11}$$

In this case, both move simultaneously of the oscillator, but in the opposite way, ie. They have the same amplitude and move toward each other or from each other (Figure 2b) with frequency$\omega_1 = \Omega$. Oscillation is then in antiphase!

This system of two identical tied oscillators, ultimately, can be treated as a very spatially-limited (crystalline) chain of identical motifs (atoms, ions, molecules), ie with a simple elementary cell, or without sublattice. And there are no conditions with$\omega_k = 0$, ie, wth $k = 0$, but there are only two disrete energy states: $\omega_1 = \Omega$ i $\omega_2 = \sqrt{3}\Omega$.

But here is the simplest phonon case!

II.1.2. *Phonons in crystalline chair*

Formation of model

In solving the problem of the mechanical oscillation, ie. undulations of atom / ion / molecule crystal lattice, we start from the simplest one-dimensional (1D) model [13] - longitudinal oscillation of number of identical motifs (the material point with mass M) identically connected by elastic springs (elastic coefficient C). Figure 3 shows a part of this system of elastically coupled oscillators - 1D crystal model, so called. ideal crystalline chain.

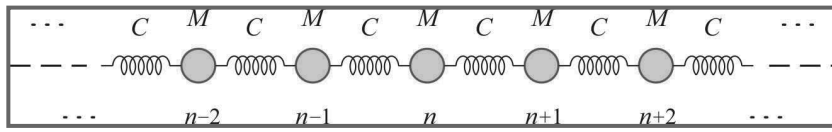

Figure 3: Model of unlimited crystalline chain

In equilibrium state of the system (motives still, spring unstrained) distance between the motif is *a* (constant crystal lattice). In dynamic state of the system the movement of any motif along the chain direction (left-right in the picture) is influenced by the elastic forces which connect it with neighboring motifs. The intensity of the resulting force at the nth motif is:

$$F_n = C(u_{n+1} - u_n) + C(u_{n-1} - u_n), \tag{12}$$

where$u_i$are small movements of i^{th} motif from the equilibrium position.

It is necessary to analyze the possibility of forming a longitudinal mechanical waves (sound) in this system.The kinetic energy of oscillation of the nth motive is:

$$T_n = \frac{1}{2}M\dot{u}_n^2 \equiv \frac{p_n^2}{2M}, \tag{13}$$

and potential (elastic deformation / interaction is conservative):

$$U_n = -\int F_n du_n = \frac{C}{2}[(u_{n+1} - u_n)^2 + (u_{n-1} - u_n)^2]. \tag{14}$$

Hamilton's function of the whole system is [12], $H = \sum_n E_n \equiv \sum_m T_m + U_m$, is then:

$$H = \frac{1}{2M}\sum_m p_m^2 + \frac{C}{2}\sum_m [(u_{m+1} - u_m)^2 + (u_{m-1} - u_m)^2]. \quad (15)$$

This expression is derived for later quantum-mechanical redefinition of this oscillatory movement – in the second quantization the concept of *phonon* is introduced – energy quantum of mechanical oscillation of the crystal lattice atom [14,15].

Equations for dinamic movement of certain motif, and here, each motif is identical and behaves in the same way, is obtained either directly – using II Newton's law ($M\ddot{u}_n = F_n$), or indirectly – by combining Hamilton'sequations ($\dot{p}_n = -\partial H/\partial u_n$ i $\dot{u}_n = \partial H/\partial p_n$):

$$\ddot{u}_n - \Omega^2(u_{n+1} - 2u_n + u_{n-1}) = 0\,, \quad (16)$$

where$\Omega^2 = C/M$is characteristic frequency of the system.Equation (15) is a homogeneous linear differential-difference equations of second order with constant coefficients.It must be noted that movement$u_m$is actually time function$u_m \equiv u_m(t)$, but at certain place in the space(distance between the motif and the coordinate beginning is$L_m(t) = ma + u_m$). Due to homogeneity and isotropy of time (in classical physics) and its continuity and unlimitness, Fourier-transformation $(t \leftrightarrow \omega)$ can be done in the form:

$$u_m(t) = \frac{1}{\sqrt{2\pi}}\int_{-\infty}^{+\infty} d\omega \mathrm{e}^{-i\omega t} u_m(\omega)\,, \quad (17)$$

By applying this transformation equation (16) becomes "pure" difference equation:

$$u_{n+1} + \rho u_n + u_{n-1} = 0 \quad (18)$$

(homogeneous, linear, second order with constant coefficients), where $\rho = \frac{\omega^2}{\Omega^2} - 2$.

This equation describes the displacement of the n^{th} motif in the observed chain and can be applied to a given – specific situation with set – known initial/ boundary conditions. We will applied it to the analysis of behavior, ie. the movement of atoms in the crystalline chain of unlimited length and chain of the final length.

Phonons in unbounded crystalline chair

In this case, nummeration of the crystalline chain motif is$n \in \left[-\frac{N_\mathrm{i}}{2}, +\frac{N_\mathrm{i}}{2}\right]$, where$N_\mathrm{i} \sim 10^8$atom motifs per cm, which in the theoretical solid state physics mean: $n \in [-\infty, +\infty]$.Based on the the multitude of particles theory, methods of quantum field theory (continuum) for this – translationally invariant systems can be successfully applied. This means that, here in the equation (18) which is the same for each of the$n$ ($\in [-\infty, +\infty]$) identical motifs, Fourier's transformation"space–impulse" [11] can be applied in the form:

$$u_m(\omega) = \frac{a}{\sqrt{2\pi}}\int_{-\infty}^{+\infty} dk \mathrm{e}^{-iakm} u_k(\omega) \quad (19)$$

(this Fourier transformation is actually: $m \leftrightarrow \kappa = ak$, where$k = 2\pi/\lambda$ – wave vector intensity), from which follows

$$u_{n\pm1}(\omega) = \frac{a}{\sqrt{2\pi}}\int_{-\infty}^{+\infty} dk \mathrm{e}^{-iakn} u_k(\omega)\mathrm{e}^{\mp iak}\,, \quad (20)$$

and whereupon that equation turns into the conditions of existence of non-trivial solutions by $u_k(\omega)$:

$$\int_{-\infty}^{+\infty} dk \mathrm{e}^{-iakn}(\rho + 2\cos ak)\; u_k(\omega) = 0\,. \quad (21)$$

This system of equations is met for$\rho = -2\cos ak$, i.e. with$\rho + 2 = (\omega/\Omega)^2$, for:

$$\omega \equiv \omega(k) = 2\Omega \left|\sin\frac{ak}{2}\right|. \tag{22}$$

This expression – in modern theoretical physics known as the law of dispersion or energy spectrum phonon, and represents possible, ie. allowed energy (energy balance) of phonons: $E_k = \hbar\omega_k \equiv h\nu_k$,can be written in non-dimensional form:

$$E_i(k) \equiv \frac{\hbar\omega(k)}{\hbar\Omega} = 2\left|\sin\frac{ak}{2}\right| \tag{23}$$

and represented graphically as in figure 4a. In this figure the wave vector$k$ – function argument$E_i$taken within boundaries of the right(positive) half of the first Brouillen's zone ($k \in [0, \pi/a]$), because from (23) we can "see" that for the left (negative) side ($k \in [-\pi/a, 0]$) this spectrum is the same, i.e. it is symetrical. Index$i$indicates that it is about an ideal – spatially unlimited structure.

The most interesting physical event is one that occurs at low intensities phonon wave vector *k*. In longwave approximation ($k = 2\pi / \lambda$) is:

$$E_i(k) \approx \hbar\Omega ak = cp \equiv E_i(p)\,, \tag{24}$$

where$p = \hbar k$ – quasiimpuls of phonons, and$c$ – speed of propagation of observed longitudinal mechanical disorders along the direction of crystal chain. It is evident that the velocity of longitudinal mechanical waves depends on the fundamental physical properties of the system: $c = a\Omega \equiv a\sqrt{C/M}$,and therefore it is the property of the material. This means that in this single (atomic)-motivesystem there are so called. acoustic phonons - phonons with a linear dispersion law (Figure 4b).

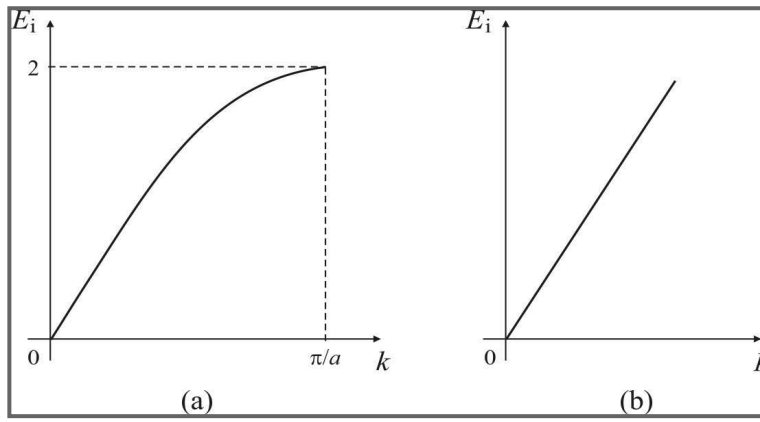

Figure 4: Phonon spectrum of space-unlimited chain

Phonons in bounded crystalline chair

In the case of crystalline chain of strictly limited length ($L = N_f a$ – short chain; Figure 5) motif nummeration is$n \in [0, N_f]$, ali je $N_f \leq 10^1 \ll 10^8 = N_i$motifs per cm, so it is not possible to conduct Fourier–transformation space-impulse of the equation (18), since the boundaries of the integration with Fourier space-impulse complex transformation are: $(-\infty, +\infty)$.

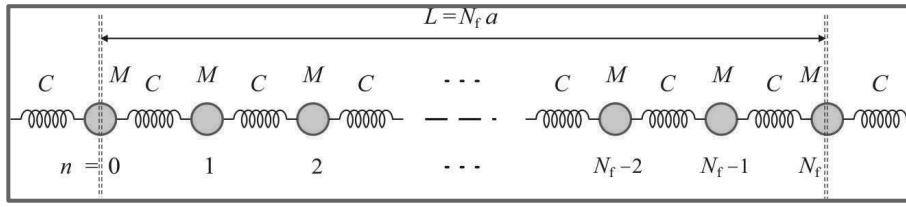

Figure 5: Limited/bounded crystalline chain model

This means that the system of infinitely many identical equations of the same form (18), in this case turns into final countable system of equations. The equations of this system due to the absence of displacement of the subject (and the very motives) outside the chain, i.e.

$$u_m = 0 \qquad za: \quad \begin{cases} m < 0\,, \\ m > N_\mathrm{f}\,, \end{cases} \tag{25}$$

are not the same as (18), but have the following form:

$$\begin{array}{ll} n = 0 & u_1 + \rho u_0 = 0 \\ n = 1 & u_2 + \rho u_1 + u_0 = 0 \\ n = 2 & u_3 + \rho u_2 + u_1 = 0 \\ \cdots & \cdots\cdots \\ \cdots & \cdots\cdots \\ \cdots & \cdots\cdots \\ n = N_\mathrm{f} - 2 & u_{N_\mathrm{f}-1} + \rho u_{N_\mathrm{f}-2} + u_{N_\mathrm{f}-3} = 0 \\ n = N_\mathrm{f} - 1 & u_{N_\mathrm{f}} + \rho u_{N_\mathrm{f}-1} + u_{N_\mathrm{f}-2} = 0 \\ n = N_\mathrm{f} & \rho u_{N_\mathrm{f}} + u_{N_\mathrm{f}-1} = 0 \end{array} \tag{26}$$

This system of$N_\mathrm{f} + 1$ differentequations (homogenous and linear, of the second order and with constant coeficients) also has nontrivial solutions –provided that the determinant of this system:

$$\Delta(\rho) = \begin{pmatrix} \rho & 1 & 0 & 0 & \cdots & 0 & 0 & 0 & 0 \\ 1 & \rho & 1 & 0 & \cdots & 0 & 0 & 0 & 0 \\ 0 & 1 & \rho & 1 & \cdots & 0 & 0 & 0 & 0 \\ 0 & 0 & 1 & \rho & \cdots & 0 & 0 & 0 & 0 \\ \vdots & \vdots & \vdots & \vdots & \ddots & \vdots & \vdots & \vdots & \vdots \\ 0 & 0 & 0 & 0 & \cdots & \rho & 1 & 0 & 0 \\ 0 & 0 & 0 & 0 & \cdots & 1 & \rho & 1 & 0 \\ 0 & 0 & 0 & 0 & \cdots & 0 & 1 & \rho & 1 \\ 0 & 0 & 0 & 0 & \cdots & 0 & 0 & 1 & \rho \end{pmatrix} \tag{27}$$

identically equal to zero, i.e. $\Delta(\rho_\mu) = 0, \quad \mu = 1, 2, 3, \ldots, N_\mathrm{f} + 1.$

This is met in famous Chebyshev polynomials provided real/regular solveablesystem of equations (26):

$$\rho_\mu = 2\cos\zeta_\mu\,; \quad \zeta_\mu = \frac{\mu\,\pi}{N_\mathrm{f}+2}; \quad \mu = 1, 2, 3, \ldots, N_\mathrm{f} + 1. \tag{28}$$

Modern quantum and statistical physics of condensed state knows unrealistic / irregular – imaginary solutions to this equation: $\rho > 2\cos ak$when the wave vector k takes imaginary values of $k \to \mathrm{i}\kappa$, ie. $\cos ak \to \cosh a\kappa$. This is physically interpreted as so called spatially-localized states – Tamm's states system, when observed excitations "retreat" in a

certain part of the area (mostly in the surface layer or "bind" for defects in the crystal structure). These conditions are of special physical character, a typical example – a natural phenomenon known as the skin-effect.

Based on this and the previous marking, with introducing renumeration: $\mu \to \nu = N_\mathrm{f} + 2 - \mu$; $\nu = 1, 2, 3, \ldots, N_\mathrm{f} + 1$, i.e. $\zeta_\mu \to \zeta_\nu = \pi - \frac{\nu\,\pi}{N_\mathrm{f}+2}$, phonon dispersion law in a very space-bounded 1D crystal systems – ultra-short crystalline chains, in form receives the same form as (23) or (24), and with spatially unlimited system the same crystal structure:

$$E_\mathrm{f}(k) = 2\left|\sin\frac{a k_\nu}{2}\right|; \qquad E_\mathrm{f}(p) \approx c\,p_\nu, \tag{29}$$

where $p_\nu \equiv \hbar\,k_\nu$, $k_\nu = \frac{\pi}{a}\frac{\nu\,\pi}{N_\mathrm{f}+2}$ (and makes sensein the case $N_\mathrm{f} \leq 10$). When $N_\mathrm{f} \to \infty$, i.e. $N_\mathrm{f} \leq 10^8$ mot/cm, expression (29) turn into (23) and (24), which represents the "control" of applied theoretical methodology. Unlike continuous zone (curve – Figure 4a, and straight line– Figure 4b), the dispersion law can be represented in the form of a discrete state (Figure 6a), even in longwave approximation (Figure 6b). Finally, it should be noted that, even when 1D crystal system has two ideal boundary surfaces, dispersion law of basic mechanical excitations – phonons, acquires two (new / different) characteristics:

• strict discretion of energy levels,

• appearance of energy gaps (*b*) or energy gaps – these are non-zero, and the lowest energy levels. Under the same name could be called the energy interval – values below those of the highest in the spectrum, those in the present case – illegal. In contrast to previous – bottom, these are as so called. the upper gaps (*l*):

$$\begin{gathered} b \equiv \left|E^\mathrm{f}_{k_\mathrm{min}} - E_i(k_\mathrm{min})\right| \equiv \\ \equiv \left|E^\mathrm{f}_k(\nu_\mathrm{min} = 1) - E_i(k_\mathrm{min} = 0)\right| = \frac{\pi}{N_\mathrm{f}+2}, \\ l \equiv \left|E_i(k_\mathrm{max}) - E^\mathrm{f}_{k_\mathrm{max}}\right| \equiv \\ \equiv \left|E_i\left(k_\mathrm{max} = \frac{\pi}{a}\right) - E^\mathrm{f}_k(\nu_\mathrm{max} = N_\mathrm{f}+1)\right| = \frac{\pi}{N_\mathrm{f}+2}, \end{gathered} \tag{30}$$

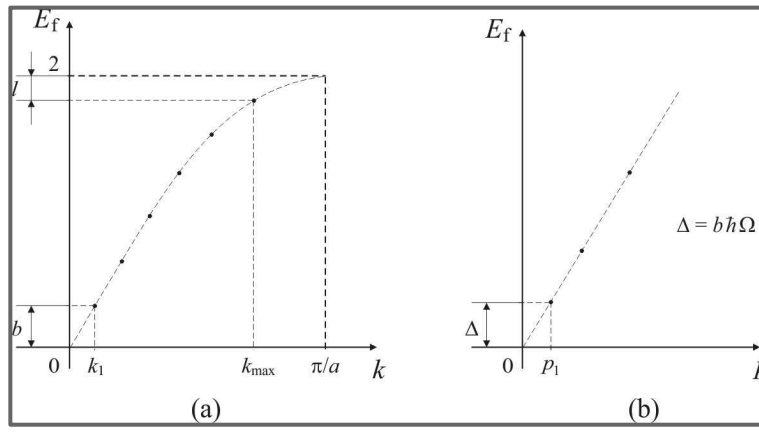

Figure 6: Phonon spectrum of spatially-limited/bounded chain

These special features (discretion and energy gaps as a result of the presence of spatial constraints) which redefine (narrow and / or extend and "split") zone of permitted energy

states of phonons in the observed crystal system, you may have a fundamental role in the explanation of various interesting physical effects – experimentally detected, and theoretically unanswered. Among them, certainly the most important position is one exotic natural phenomenon – the phenomenon of high-temperature superconducting ceramic based on copper-oxide materials [15–20].

Phonon thermodynamics of unbounded crystalline chair

In this part the 1D crystal lattice with one atom per elementary cell is analyzed. The nearest neighbor interaction within harmonic approximation is included. For such a model the dispersion relations are well known. Thermodynamic functions, such as specific heat of lattice and phonon thermal conductivity, are expressed via phonon density of states. In most simple cases, Einstein and Debye approximations are used for phonon density of states. In Einstein approximation the phonon density of states is expressed via Dirac δ function, while in Debye approximation the phonon density of states is of the ω^{d-1} type, where d is a dimension of the system. For the assumed 1D structure, it is useful to find thermodynamic characteristics by applying exact relation for phonon density of states and compare them with the results obtained by using Debye approximation. Such analysis of 1D structures can have both theoretical and practical implications for Q1D structures.

• Specific heat

We shall consider 1D crystal lattice with one atom per elementary cell, consisting of N identical atoms of mass m positioned on average interatomic distance a, with interatomic forces characterized by elastic constant γ. Within harmonic approximation the dispersion relation is well known [21]:

$$\omega = \omega_m \left| \sin \frac{ka}{2} \right|, \tag{21}$$

where $\omega_m = \sqrt{\gamma / m}$. By inserting dispersion relation (21) into general expression for phonon density of states [22]:

$$g(\omega) = \frac{Na}{\pi} \left| \frac{dk}{d\omega} \right|, \tag{22}$$

one obtains

$$g(\omega) = \begin{cases} \dfrac{2N}{\pi \sqrt{\omega_m^2 - \omega^2}}; & \omega < \omega_m, \\ 0; & \omega > \omega_m. \end{cases} \tag{23}$$

Then, by inserting phonon density of states (23) into expression for specific heat (per elementary cell) [23]:

$$C_v = k_B \int_0^{\infty} \left(\frac{\hbar\omega}{k_B T} \right)^2 \frac{e^{\frac{\hbar\omega}{k_B T}}}{\left(e^{\frac{\hbar\omega}{k_B T}} - 1 \right)^2} g(\omega)\, d\omega. \tag{24}$$

one obtains

$$C_v = \frac{2Nk_B}{\pi}\int_0^{\omega_m}\left(\frac{\hbar\omega}{k_BT}\right)^2 \frac{e^{\frac{\hbar\omega}{k_BT}}}{\left(e^{\frac{\hbar\omega}{k_BT}}-1\right)^2}\frac{1}{\sqrt{\omega_m^2-\omega^2}}d\omega. \tag{25}$$

Further on, by applying substitutions $x = \hbar\omega / k_BT;\ \omega_m = k_BTx_m / \hbar;\ \hbar\omega_m = k_B\theta;\ x_m = \theta / T$ where θ is Debye temperature, expression (25) is transformed into:

$$C_v = \frac{2Nk_B}{\pi}\int_0^{\frac{\theta}{T}} x^2 \frac{e^x}{(e^x-1)^2}\left[\left(\frac{\theta}{T}\right)^2 - x^2\right]^{-1/2} dx. \tag{26}$$

Expression (26) can be analytically solved for asymptotic low and high temperatures. In the case of asymptotic high temperatures $\theta << T$ one obtains:

$$\lim_{x\to 0}\left\{x^2\frac{e^x}{(e^x-1)^2}\frac{1}{\sqrt{x_m^2-x^2}}\right\} = \frac{1}{x_m};$$

$$C_v = \frac{2Nk_B}{\pi x_m}\int_0^{x_m} dx = \frac{2Nk_B}{\pi} = \text{const} \tag{27}$$

in accordance with Dulong-Petit law.

It is known empirically [24] that low-temperature dependence of the specific heat has the form $C_v \sim T^d$. So, it is interesting to find analytical expression for C_v at low temperatures in the case of 1D structures by applying exact expression for phonon density of states.

In the case of asymptotic low temperatures $\theta >> T$ it can be shown [25]that specific heat is linear function of temperature. By introducing function:

$$f(x, x_m) = \frac{2}{\pi}\left[\frac{x/2}{\sinh(x/2)}\right]^2 \frac{1}{\sqrt{x_m^2-x^2}}, \tag{28}$$

the expression for specific heat can be written as:

$$C_v = Nk_B(I_1 + I_2); \qquad \begin{aligned} I_1 &= \int_0^{qx_m} f(x, x_m)\,dx; \\ I_2 &= \int_{qx_m}^{x_m} f(x, x_m)\,dx; \end{aligned} \qquad 0 < q < 1. \tag{29}$$

In expressions (9), integral I_2 exponentially tends to zero when $x \to \infty$, while integral I_1 becomes:

$$I_1 = \frac{4T}{\pi x_m}\int_0^{\infty}\left[\frac{x/2}{\sinh(x/2)}\right]^2 dr = \frac{2}{3}\pi^2\frac{T}{x_m},, \tag{30}$$

so specific heat finally obtains the form

$$C_v = \frac{\pi N k_B^2}{3\hbar}\sqrt{\frac{m}{\gamma}}T. \tag{31}$$

For wider temperature range the expression (6) can be solved numerically, by adopted values of the parameters [26]:

$$N = 10^{24}; \quad a = 4\cdot 10^{-10}\,\text{m}; \quad v = 3{,}5\cdot 10^{3}\,\text{m/s}; \quad \omega_m = \frac{2v}{a} = 1{,}75\cdot 10^{13}\,1/\text{s}; \quad \theta = 134\,\text{K}$$

It is interesting to compare values obtained for specific heat (6) with the values obtained for specific heat in Debye approximation. In the case of 1D structure the phonon density of states in Debye approximation is given by [22]:

$$g(\omega) = \frac{Na}{\pi v} \tag{32}$$

and in this case the specific heat can be found by numerical solving of equation

$$C_v^D = \frac{Nak_B^2}{\pi\hbar v} T \int_0^{\frac{\theta}{T}} x^2 \frac{\mathrm{e}^x}{(\mathrm{e}^x - 1)^2} dx. \tag{33}$$

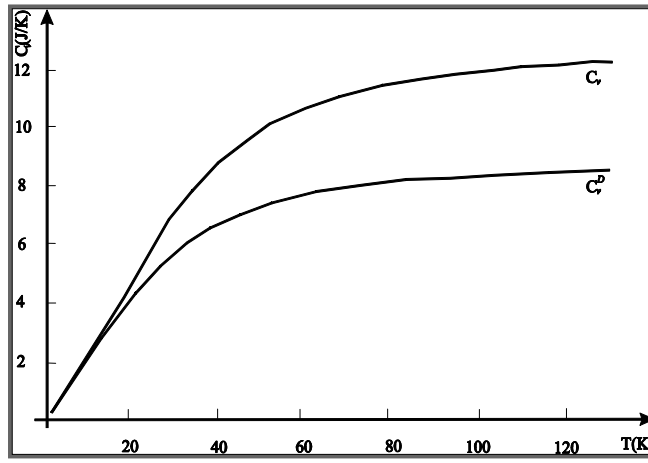

Figure7: Comparative presentation of specific heats

From Figure 7 it can be seen that specific heat calculated by using exact phonon density of states is above the one calculated in Debye approximation.

• Thermal conductivity

The heat conductivity tensor in most general case can be found by using Kubo formula, which is an even correlation function on the operator of heat flux. In the first approximation, finding of the heat conductivity tensor can be reduced on solving Boltzmann transport equation.

In analysis of experimental data for heat conductivity of crystal lattice Callaway model is most frequently used [26], which takes into account various relaxation phonon processes.

In this model for 3D case [27] a lot of approximations are made, restricting its application to low-temperature range:

- Debye approximation for describing phonon spectra is used;
- only mean sound velocity is taken into account;
- phonon scattering on the surface is diffused (not mirror-like);
- normal tree-phonon scattering processes are realized for low frequency longitudinal phonons;
- relaxation time of U-processes is described similarly to relaxation time of normal processes;
- relaxation times of various relaxation phonon processes are considered additive;
- neither crystal anisotropy nor phonon polarization is not taken into account (difference between longitudinal and transversal phonons is not made).

In the case of 1D structure, we are starting from the expression for thermal conductivity (per unit volume) obtained from kinetic theory [28]:

$$\kappa = \frac{1}{3}\int_0^{\frac{\theta}{T}} v_s^2 C_v(x)\,\tau(x)\,dx, \tag{34}$$

where v_s is phonon mean velocity, and τ is phonon relaxation time, which is a function of temperature and frequency.

Specific heat is given by expression (25), while phonon relaxation time has the form [26]:

$$\tau^{-1}(T,\omega) = \frac{v_s}{L} + A\omega^4 + BT^3\omega^2. \tag{35}$$

Fist term represents phonon relaxation time due to scattering on boundaries, second term represents phonon relaxation time due to scattering on dopants, and third term represents phonon relaxation time due to phonon-phonon scattering.

If we adopt substitution $x = \hbar\omega / k_B T$, expression (34) on the basis of (25) and (35) becomes:

$$\kappa = \frac{2Nk_B v_s^2}{3\pi}\int_0^{x_m} x^2 \frac{\mathrm{e}^x}{(\mathrm{e}^x-1)^2}\frac{1}{\sqrt{x_m^2 - x^2}}\left(\frac{v_s}{L} + Dx^4 + Ex^2\right)^{-1} dx, \tag{37}$$

where

$$D = A(k_B T/\hbar)^4; \qquad E = BT^3(k_B T/\hbar)^2. \tag{38}$$

In the limiting case the expression for thermal conductivity can be found in analytic form. In the limit of high temperatures when $\theta << T$, one obtains:

$$\kappa = \frac{2Nk_B L v_s}{3\pi\theta} T. \tag{19}$$

In the limit of low temperatures when $\theta >> T$, expression (37) tends to zero. This means that contribution to thermal conductivity is negligible when phonon energy is much higher than $k_B T$[29,30].

In the general case, the expression for thermal conductivity in wide temperature range can be found numerically.

The adopted values of the parameters are

$$A = 2.57\cdot10^{-44}\mathrm{s}^3;\ B = 2.77\cdot10^{-23}\ \mathrm{s/K};\ L = 1.8\cdot10^{-3}\ \mathrm{m}$$

while other parameters are the same as in previous part.

If thermal conductivity is calculated by using Debye approximation for phonon density of states, one obtains:

$$\kappa^D = \frac{Nak_B^2 v_s}{3\pi\hbar} T \int_0^{\frac{\theta}{T}} x^2 \frac{\mathrm{e}^x}{(\mathrm{e}^x - 1)^2} \frac{dx}{v_s / L + Dx^4 + Ex^2}. \tag{40}$$

Numerically calculated thermal conductivities are presented in Figure 2.

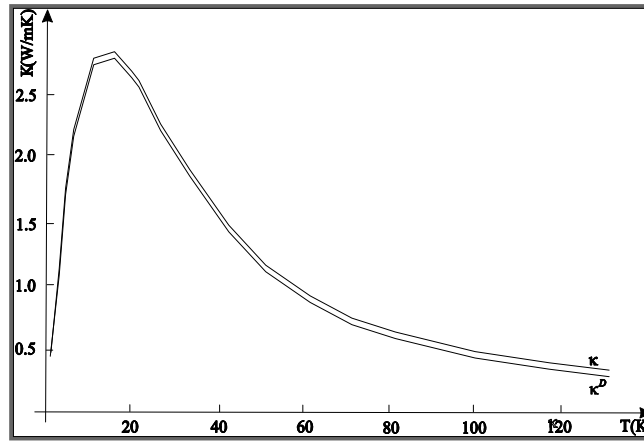

Figure 8: Comparative presentation of thermal conductivities

From Figure 8 it can be seen that thermal conductivities, calculated in Debye approximation and by using exact phonon density of states, respectively, are surprisingly compatible, which suggests that relaxation processes are dominating in thermal conductivity and that influence of phonon density of states is not so significant, and hence in this case Debye approximation is quite correct.

All numerical calculations were done by using program package *Mathematica 7.0.*

In the case of most simple 1D structures, specific heat calculated in Debye approximation is underestimated in respect to that one calculated for the exact phonon density of states. On the other hand, thermal conductivities calculated in these two cases are surprisingly compatible, which suggests that influence of phonon density of states is not so significant and that relaxation processes are dominating in thermal conductivity. In further research, this idea will be examined on 2D and 3D structures.

II.2. Phonons in ultrathin films

This part describes a major aspect of the effort to understand nanostructures, namely the study of phonons and phonon-mediated effects in structures with nanoscale dimensional confinement in one or more spatial dimensions. The central theme of this monograph is the description of the acoustic phonons of the optical type in these nanostructures. As a preliminary to describing the dispersion relations and mode structures for phonons in nanostructures, phonon amplitudes are quantized in terms of the harmonic oscillator approximation, and anharmonic effects leading to phonon decay are described in terms of the dominant phonon decay channels. Research of the influence of phonons with quantum size and confinement effects in nanostructures is not new. It has been conducted for almost two decades. It is known [31] that acoustic phonons affect practically all electronic, thermal and optical properties of semiconductors. They are carriers of heat and together with optical phonons constrain the mobility of electrons in the areas of medium and high temperatures. Reduction of sizes in nanostructures leads to the so-called confinement of phonons due to which the phonon branches are quantized (dimensional quantization) and a substantive modification of their energy spectrum, group velocity and polarization occur. Due to the reflections from the inner surface of the structure, phonon modes hybridize and cease to be purely longitudinal or purely transverse, and their group velocity is reduced compared to the case in the bulk structure.

Dependence of energy on the wave vector is highly nonlinear and linear approximation of the dispersion laws of phonons in small size nanostructures makes no sense. Changing the phonons dispersion law due to confinement severely affects the kinetic effects conditioned by the interaction of acoustic phonons with electrons, dotted defects, phonon-phonon interaction. Managing transport properties of acoustic phonons through the modification of their energy spectrum in nanostructures was named phonon engineering [32].

The concept of phonon engineering is based on the corresponding changes to the phonon spectrum in order to improve the electric and thermal transport properties of the given nanostructure. In homogeneous layers and nanowires, phonon engineering can be realized on the account of changes in the size of the nanostructure or changes in the quality of exterior surfaces. In this sense, the most advantageous are composite materials composed of layers with different phonon properties. In these structures, general hybridized phonon modes occur, which may originate from the phonon properties of the individual layers or as averaged modes of different layers. By changing the thickness of the layers as well as the types of materials that go into the composite, a different degree of hybridization of the phonon modes can be achieved and thus change thermal transport properties of the structure in a wide range. A demonstration of phonon engineering is given in a series of papers for the three-layer film heterostructures and coated nanowires [33]. In these structures, the phonon modes are divided into three groups: fluctuations in the inner layer of the coating and general oscillations as a whole. Redistribution of atom displacements between layers leads to attenuations of electron-phonon interaction and to the increase of the mobility of electrons in materials that are coated with other materials [31–33]. Another direction of development of phonon engineering is the optimization of thermal transport at the nanolevel. By targeted changing of the phonon spectra, density of states and group velocity of phonons, thermal conductivity of nanostructures can be increased or decreased. Depending on what material is used as a coating, thermal conductivity can be altered [32].

Phonon design will change radically under nanotechnology and for nano-engineers or nano-designers, respectively; a broad knowledge will become even more important in the future. Nanotechnology makes design the most important part of any development process. With nanotechnology the amount of design work increases enormously due to its complexity. Planning for the widespread change, each nano-design could make design planning incredibly important [34].As long as we are still far away from the realization of complex nanotechnological applications, nano-engineering and nano-design almost exclusively take place on computers. Computational nano-engineering is an important field of research aimed at the development of nanometer scale modeling and simulation methods to enable and accelerate the design and construction of realistic nanometer scale devices and systems [35]. Therefore, the intention of this paper is to give an introduction and basic theoretical methods and models for procedures, techniques, problems and difficulties arising with computational phonon nano-engineering and design [36]. For the sake of simplicity, the focus is laid on the molecular dynamics method which is well suited to explain the topic with just a basic knowledge of phonon physics.

It should be noted that the theory of nanoparticle systems lags quite behind the results of experimental research. This situation is justified by the inadequacy and lack of adaptability of mathematical apparatus which should follow theoretical assumptions regarding nanosystems. Theoretical physicists can define the basic equations of motion of the appropriate physical quantities and phenomena in nanosystems, as well as boundary conditions depending on the type of models, but the method of difference equations [36–38] is still insufficiently applicable or insufficiently flexible with respect to the requirements which lead to the solving of theoretical tasks. The purpose of this part is in accordance with the following: to make the basic settings in the way of solving some simple (for example, ultrathin films), but also some more complicated models of nano-patterns (e.g. nanorods and quantum dots), not engaging in the complexity or completeness of solutions, but simply in the development of an adequate theoretical research.We will mention here a unique example: the problem of applying the method of Green's functions, as a very efficient way of solving tasks of statistical physics, analogous to, for example, the methodology of the use of wave functions and the Schrödinger equation.

For better understanding of nanostructure physics it is necessary to emphasize their main feature: the physical characteristics of these very small samples are spatially dependent. This spatial dependence is the consequence of non-equivalency spatial distribution of their crystallographic points. As far as we know, this obvious fact was not theoretically reproduced. The formal reason for the need for the existence of theory of broken symmetry structures is the lack of procedures for calculating the Green's functions which depend on two spatial coordinates. In the theory of broken symmetry structures, up to now, Green's functions have been used depending on the difference of two spatial coordinates [39–41] (this approach is correct only in the case of ideal structures) or the Green's functions with diagonal spatial coordinates. In this work the calculation techniques for the Green's functions depending on two spatial coordinates are developed separately. These unique correct techniques of calculation immediately reproduced the expected physical result, i.e. the spatial dependence of the broken symmetry structure properties. In this paper this will be demonstrated on the set of examples. Apart from the confirmation of spatially dependent physical properties, some very interesting effects of structure deformation are ascertained, as well.

Unlike in the previous papers [1–11], here we will try to observe the difference between the characteristics of different nano-crystalline structures: ultrathin films, composite films, i.e. superlattices, nanorods and quantum dots, we were interested in whether the quantum size effects (quantum confinement), quantum (de)coherence and influence of boundary conditions, strengthen or weaken in nanosamples. While the theoretical study of the structures which are larger in size generally requires solving differential equations with constant coefficients, difference equations appear in the research of nanostructures, but their coefficients depend on the spatial coordinates due to the necessity to introduce the boundary conditions and the breaking of spatial translational symmetry in the equation, as well as the impact of vacancies and impurities. The most commonly used mathematical structure in solving the problem of difference equations are translational operators [42], because their use enables the most efficient reaching of solutions.

The major part of this paper deals with the application of the mentioned methodology of solving difference equations and the problem of structures with broken symmetry along a single crystallographic direction. Furthermore, nanostructures that are translationally invariant in only one direction and structures that do not possess translational invariance have also been studied. The method of Green's functions is generally used here because this method is self-consistent i.e. it solves both the dynamic and thermodynamic sides of the problem. Other methods are used for either one or the other. For example, dynamic characteristics of the problem can be determined by using the wave function, but in order to solve thermodynamics, one has to resort to methods of statistical physics. Regardless of this, in some sections of the second part, structure problems were solved by using the wave functions of nanostructures.It should be noted that the methodology for calculating the Green's function [43] in the conditions of broken symmetry has already been developed, where such a breaking of symmetry can be along one, two directions and along all three spatial directions. When the problem of calculating the Green's functions for structures with broken symmetry is concerned, there are a lot of inconsistencies today because of the fact that in such structures Green's functions depend on individual spatial variables, rather than on their difference, as is the case with the structures with ideal symmetry.

Thermal properties of nanostructures have recently attracted a lot of attention. The influence of size effects on thermal conductivity is becoming extremely important for device design and reliability [44–46]. The problem of thermal management is even more severe for photonic devices such as vertical cavity surface emitting lasers. On the other hand, to improve performance of thermoelectrics, one needs to achieve low thermal conductivity. These are two contradictory demands, but both can be approached with appropriate modification of phonon modes, e.g., phonon engineering.

On the basis of the calculated dispersion law and distribution of phonon states in nanoscopis crystals, free energy and entropy will be calculated. Internal energy, as well as heat capacitance, will also be analyzed. Low-temperature behavior of these quantities will be compared to the corresponding ones of bulk-structures. It was shown that heat capacitances of nano-layered structures in low-temperature region were higher than the same quantities of the corresponding bulk sample. In the middle and the highest temperature region, temperature behavior of the inverse: heat capacitance of layered structures was lower than those of the corresponding bulk ones. The consequences were discussed with relation to the better superconductive properties of nano-materials.

II.2.1. *Phonon ultrathin ideal film model*

Our model of ideal (on boundary planes – nonperturbed) ultrathin film represents a crystalline structure with broken space-translational symmetry. Here we will consider aultrathin film, which is infinite in *XY* planes having finite (nano-small) thickness in *z*-direction. It means that symmetry break appears on surfaces in *z*-direction (Figure9).

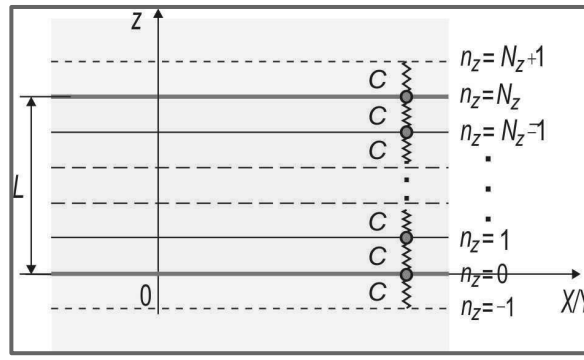

Figure 9: Cross section of the thin crystalline film model

The main consequence of symmetry break is spatial dependence of physical properties of the system. In the considered case, physical properties will depend on index n_z = 0,1,2,…,N_z; 2 ≤N_z≤ 10, labeling layers of the film in *z*-direction. Spatial dependence is determined by boundary conditions. Here the simplest boundary conditions will be taken consisting in the absence of layers labeled with $n_z = -1$ and $n_z = N_z + 1$ [47–49].

The analysis of the film-properties will be carried out with the help of Green's functions [50–52] of displacement as well as momentum types and their spectral intensities will be used for determination of some relevant kinetic and thermodynamic characteristics of the film. [53]

II.2.2. *Green's function of the displacement type*

The calculation procedure will be done in two steps. Firstly, the equation defining Green's function of the ideal system will be found. Thereafter, this equation will be translated into the system of equations accordingly to boundary conditions.

The Hamiltonian of mechanical oscillations in the system, in which the torsion effects are neglected, taken in the nearest-neighbors approximation is of the form [10,51–53]:

$$H = \frac{1}{2M}\sum_{\vec{n}} p_{\vec{n}}^2 + \frac{C}{2}\sum_{\vec{n}}\left[\left(u_{\vec{n}} - u_{\vec{n}-\vec{a}_x}\right)^2 + \left(u_{\vec{n}} - u_{\vec{n}-\vec{a}_y}\right)^2 + \left(u_{\vec{n}} - u_{\vec{n}-\vec{a}_z}\right)^2\right]. \tag{41}$$

In this formula *M* is mass of the atom, *C* is the Hook's constant, *u*are the atom displacements and *p* are the corresponding momenta $\left(p = M\dot{u}_n\right)$. The symbol $\vec{n} \pm \vec{a}_x$ has to be read as follows: $u_{\vec{n}\pm\vec{a}_x} \equiv u_{n_x\pm1,n_y,n_z}$ and the other symbols of the quoted type are similar.

The Green's function of the type displacement-displacement is given by:

$$\Psi_{\vec{n},\vec{m}}(t) \equiv \Psi_{n_x,n_y,n_z;m_x,m_y,m_z}(t) \equiv << u_{\vec{n}}(t) \left| u_{\vec{m}}(0) \right. >> = \Theta(t) < \left[u_{\vec{n}}(t), u_{\vec{m}}(0) \right] >, \tag{42}$$

where $\Theta(t)$ is Heaviside step-function: $\Theta(t) = 1$, for $t > 0$ and $\Theta(t) = 0$, for $t < 0$.Differentiating (2) with respect to time and using the equations of motions we obtain:

$$\frac{d}{dt}\Psi_{\vec{n},\vec{m}}(t) = \frac{1}{M}\Theta(t) < \left[p_{\vec{n}}(t), u_{\vec{m}}(0) \right] >= \frac{1}{M} << p_{\vec{n}}(t) \left| u_{\vec{m}}(0) \right. >>, \tag{43}$$

After differentiating with respect to time the Green's function $\frac{d}{dt} << p_{\vec{n}}(t) \left| u_{\vec{m}}(0) \right. >>$ and the use of equations of motions, we obtain:

$$\begin{aligned} \frac{d}{dt} << p_{\vec{n}}(t) \left| u_{\vec{m}}(0) \right. >> = -i\hbar\delta_{\vec{n},\vec{m}}\,\delta(t) + C\Big[\Psi_{\vec{n}+\vec{a}_x,\vec{m}}(t) + \Psi_{\vec{n}-\vec{a}_x,\vec{m}}(t) + \\ + \Psi_{\vec{n}+\vec{a}_y,\vec{m}}(t) + \Psi_{\vec{n}-\vec{a}_y,\vec{m}}(t) + \Psi_{\vec{n}+\vec{a}_z,\vec{m}}(t) + \Psi_{\vec{n}-\vec{a}_z,\vec{m}}(t) - 6\Psi_{\vec{n},\vec{m}}(t) \Big]. \end{aligned} \tag{44}$$

Carrying out the Fourier time-frequency transformations:

$$\Psi_{\vec{n},\vec{m}}(t) = \int_{-\infty}^{+\infty} d\omega\, \mathrm{e}^{-i\omega t}\Psi_{\vec{n},\vec{m}}(\omega); \quad \delta(t) = \int_{-\infty}^{+\infty} d\omega\, \mathrm{e}^{-i\omega t}, \tag{45}$$

in(43) and (44) and by combining these transformed equations, we obtain:

$$\begin{aligned} \omega^2\Psi_{\vec{n},\vec{m}}(\omega) = \frac{i\hbar}{2\pi}\frac{1}{M}\delta_{\vec{n},\vec{m}} - \frac{C}{M}\Big[\Psi_{\vec{n}+\vec{a}_x,\vec{m}}(\omega) + \Psi_{\vec{n}-\vec{a}_x,\vec{m}}(\omega) + \Psi_{\vec{n}+\vec{a}_y,\vec{m}}(\omega) + \\ + \Psi_{\vec{n}-\vec{a}_y,\vec{m}}(\omega) + \Psi_{\vec{n}+\vec{a}_z,\vec{m}}(\omega) + \Psi_{\vec{n}-\vec{a}_z,\vec{m}}(\omega) - 6\Psi_{\vec{n},\vec{m}}(\omega) \Big]. \end{aligned} \tag{46}$$

Keeping in mind that translational invariance in x and y directions are conserved we introduce the following space-momentum Fourier transformations:

$$\begin{aligned} \Psi_{\vec{n},\vec{m}}(\omega) &= \frac{1}{N_x N_y}\sum_{k_x,k_y} \mathrm{e}^{ik_x a_x(n_x-m_x)+ik_y a_y(n_y-m_y)} A_{n_z,m_z}(k_x,k_y,\omega); \\ \delta_{\vec{n},\vec{m}} &\equiv \delta_{n_x,m_x}\delta_{n_y,m_y}\delta_{n_z,m_z} = \frac{\delta_{n_z,m_z}}{N_x N_y}\sum_{k_x,k_y} \mathrm{e}^{ik_x a_x(n_x-m_x)+ik_y a_y(n_y-m_y)}. \end{aligned} \tag{47}$$

After the application of the last two formulas, the equation (46) reduces to

$$A_{n_z+1,m_z} + A_{n_z-1,m_z} + \rho A_{n_z,m_z} = F_{n_z,m_z}, \tag{48}$$

where: $A_{n_z,m_z} \equiv A_{n_z,m_z}(k_x,k_y,\omega)$, $F_{n_z,m_z} = \frac{i\hbar}{2\pi}\frac{1}{C}\delta_{n_z,m_z}$ and

$$\rho = \frac{M}{C}\omega^2 - 4\sin^2\frac{a_x k_x}{2} - 4\sin^2\frac{a_y k_y}{2} - 2. \tag{49}$$

At this stage of calculation we shall take into account the boundary conditions, consisting in the absence of the layers $n_z = -1$ and $n_z = N_z + 1$. These boundary conditions can be expressed as $u_{n_x,n_y,-1} = u_{n_x,n_y,N_z+1} = 0$. Due to these conditions, equation (48) goes over to the system of difference equations:

– for $n_z = 0$:

$$A_{1,m_z} + \rho A_{0,m_z} = F_{0,m_z}, \tag{50a}$$

– for $n_z = N_z$:

$$A_{N_z-1,m_z} + \rho A_{N_z,m_z} = F_{N_z,m_z}, \tag{50b}$$

– and for $1 \le n_z \le N_z$:

$$A_{n_z+1,m_z} + A_{n_z-1,m_z} + \rho A_{n_z,m_z} = F_{n_z,m_z}. \tag{50c}$$

The system of equations (50a) – (50c) is system of N_z + 1 nonhomogenous difference equations of the second order with nonlinear coefficients [54]. The solution of (50c) will be looked for in the form:

$$A_{n_z,m_z} = \sum_{\mu=\mu_0}^{N_z'} a_{\mu,m_z} \sin\left(n_z+1\right)\phi_\mu, \tag{51}$$

and after its substitution in (50c), we obtain expression determining the parameter ϕ_μ by the condition:

$$\sin\left(N_z+2\right)\phi_\mu = 0 \quad \Rightarrow \phi_\mu = \frac{\pi\mu}{N_z+2}; \qquad \mu = 1,2,...,N_z+1. \tag{52}$$

It should be pointed out that index μ may not take the value $\mu = 0$ since it leads to a trivial solution (51), i.e. $A_{n_z,m_z} = 0$. Besides, this index must take the same set of values as n_z and therefore maximal value of μ is N_z + 1.Since the set of values of index μ is determined, we finally conclude: the solution (51) with (52) fulfills all of N_z + 1 equations of the system of equations (50a) to (50c) and reduces them to a unique one:

$$\sum_{\mu=1}^{N_z+1} a_{\mu,m'}\left(2\cos\frac{\pi\mu}{N_z+2}+\rho\right)a_{\mu,m_z}\sin\left(n_z+1\right)\frac{\pi\mu}{N_z+2} = \frac{i\hbar}{2\pi}\frac{1}{C}\delta_{n_z,m_z}; \tag{53}$$
$$n_z = 0,1,2,...,N_z.$$

Now we shall introduce the standing waves representation of Kronecker's symbol:

$$\delta_{n_z,m_z} = \frac{2}{N_z+2}\sum_{\mu=1}^{N_z+1}\sin\left(n_z+1\right)\frac{\pi\mu}{N_z+2}\sin\left(m_z+1\right)\frac{\pi\mu}{N_z+2}. \tag{54}$$

Taking undetermined coefficient $a_{\mu,m'}$ in the form:

$$a_{\mu,m_z} = \frac{2}{N_z+2}\alpha\left(k_x,k_y,\mu,\omega\right)\sin\left(m_z+1\right)\frac{\pi\mu}{N_z+2}, \tag{55}$$

and substituting it in (53), we obtain:

$$\alpha\left(k_x,k_y,\mu,\omega\right) = \frac{i\hbar}{2\pi}\frac{1}{C}\left(\rho+2\cos\frac{\pi\mu}{N_z+2}\right)^{-1},$$

wherefrom, after the substitution of the parameter $\rho$from (49), it follows

$$\alpha\left(k_x,k_y,\mu,\omega\right)=\frac{i\hbar}{2\pi}\frac{1}{2\omega_{k_x,k_y,\mu}}\frac{1}{M}\left(\frac{1}{\omega-\omega_{k_x,k_y,\mu}}-\frac{1}{\omega+\omega_{k_x,k_y,\mu}}\right), \tag{56}$$

where

$$\omega_{k_x,k_y,\mu}=2\,\Omega\sqrt{\sin^2\frac{a_xk_x}{2}+\sin^2\frac{a_yk_y}{2}+\sin^2\frac{\pi\mu}{2\left(N_z+2\right)}}\,, \tag{57}$$

and $\Omega=\sqrt{C/M}$. Subsequently, combining (55) and (57), and substituting the result of combining into (11) we obtain:

$$\begin{aligned}A_{n_z,m_z}\left(k_x,k_y,\omega\right)&=\frac{i\hbar}{2\pi}\frac{1}{M}\frac{1}{N_xN_y}\frac{1}{N_z+2}\sum_{k_x,k_y}\sum_{\mu=1}^{N_z+1}\frac{1}{\omega_{k_x,k_y,\mu}}\times\\ &\times\left(\frac{1}{\omega-\omega_{k_x,k_y,\mu}}-\frac{1}{\omega+\omega_{k_x,k_y,\mu}}\right)\cdot\sin\left(n_z+1\right)\frac{\pi\mu}{N_z+2}\sin\left(m_z+1\right)\frac{\pi\mu}{N_z+2}.\end{aligned} \tag{58}$$

Consequently, the Green function given by the formula (47) is the following:

$$\begin{aligned}\Psi_{\vec{n},\vec{m}}\left(\omega\right)&=\frac{i\hbar}{2\pi}\frac{1}{M}\frac{1}{N_xN_y}\frac{1}{N_z+2}\sum_{k_x,k_y}\sum_{\mu=1}^{N_z+1}\frac{\mathrm{e}^{ik_xa_x\left(n_x-m_x\right)+ik_ya_y\left(n_y-m_y\right)}}{\omega_{k_x,k_y,\mu}}\times\\ &\times\left(\frac{1}{\omega-\omega_{k_x,k_y,\mu}}-\frac{1}{\omega+\omega_{k_x,k_y,\mu}}\right)\cdot\sin\left(n_z+1\right)\frac{\pi\mu}{N_z+2}\sin\left(m_z+1\right)\frac{\pi\mu}{N_z+2}.\end{aligned} \tag{59}$$

The spectral intensity of the function $\Psi_{\vec{m},\vec{n}}\left(\omega\right)$ is defined [41–43,53] by:

$$I_\Psi=\frac{\Psi_{\vec{n},\vec{m}}\left(\omega+i\delta\right)-\Psi_{\vec{n},\vec{m}}\left(\omega-i\delta\right)}{\mathrm{e}^{\hbar\omega/\theta}-1};\qquad\delta\to0^+;\qquad\theta=k_{\mathrm{B}}T\,.$$

After substitution (59) into this relation, we finally obtain the expression for spectral intensity of the function Ψ in the following form:

$$\begin{aligned}I_\Psi&=\frac{\hbar}{M}\frac{1}{N_xN_y}\frac{1}{N_z+2}\sum_{k_x,k_y}\sum_{\mu=1}^{N_z+1}\mathrm{e}^{ik_xa_x\left(n_x-m_x\right)+ik_ya_y\left(n_y-m_y\right)}\times\\ &\times\frac{\delta\left(\omega-\omega_{k_x,k_y,\mu}\right)-\delta\left(\omega+\omega_{k_x,k_y,\mu}\right)}{\mathrm{e}^{\hbar\omega/\theta}-1}\sin\left(n_z+1\right)\frac{\pi\mu}{N_z+2}\sin\left(m_z+1\right)\frac{\pi\mu}{N_z+2}\frac{1}{\omega_{k_x,k_y,\mu}}.\end{aligned} \tag{60}$$

By the definition of corresponding correlation function $<u_{\vec{m}}\left(0\right)u_{\vec{n}}\left(t\right)>$ [41–43,53]:

$$<u_{\vec{m}}\left(0\right)u_{\vec{n}}\left(t\right)>=\int_{-\infty}^{+\infty}d\omega\,\mathrm{e}^{-i\omega t}I_\psi\left(\omega\right), \tag{61}$$

we obtain:

$$< u_{\vec{m}}(0)\, u_{\vec{n}}(t) >= \frac{\hbar}{M}\frac{1}{N_x N_y}\frac{1}{N_z+2}\sum_{k_x,k_y}\sum_{\mu=1}^{N_z+1}\frac{e^{ik_x a_x(n_x-m_x)+ik_y a_y(n_y-m_y)-it\omega_{k_x,k_y,\mu}}}{\omega_{k_x,k_y,\mu}}\times$$
$$\times\left(\frac{e^{-i\omega_{k_x,k_y,\mu}t}}{e^{\hbar\omega_{k_x,k_y,\mu}/\theta}-1}-\frac{e^{i\omega_{k_x,k_y,\mu}t}}{e^{-\hbar\omega_{k_x,k_y,\mu}/\theta}-1}\right)\sin(n_z+1)\frac{\pi\mu}{N_z+2}\sin(m_z+1)\frac{\pi\mu}{N_z+2}. \qquad (62)$$

From the last formula we find the expression for the mean value of the square of atom displacements. Putting in (62) $\vec{m}=\vec{n}$ and $t=0$ we have:

$$< u_{\vec{n}}^2 >= \frac{\hbar}{M}\frac{1}{N_x N_y}\frac{1}{N_z+2}\sum_{k_x,k_y}\sum_{\mu=1}^{N_z+1}\frac{1}{\omega_{k_x,k_y,\mu}}\sin^2(n_z+1)\frac{\pi\mu}{N_z+2}\coth\frac{\hbar\omega_{k_x,k_y,\mu}}{2\theta}. \qquad (63)$$

This formula is very important since it is entered into the expressions for potential energy, crystal density and the other physical characteristics of the system.

II.2.3. *Green's function of the momentum type*

The momentum-momentum Green's function defined as [50–53]:

$$\Phi_{\vec{n},\vec{m}}(t)\equiv\Phi_{n_x,n_y,n_z;m_x,m_y,m_z}(t)=$$
$$=<< p_{\vec{n}}(t)\,|\,p_{\vec{m}}(0) >>=\Theta(t)<\left[p_{\vec{n}}(t),p_{\vec{m}}(0)\right]> \qquad (64)$$

is also important for defining physical characteristics of the film. It can be found by a procedure which is similar to that which was used for displacement-displacement Green's function in the previous paragraph. Defining: $\Pi_{\vec{n},\vec{m}}(t)\equiv<<\vec{u}_{\vec{n}}(t)\,|\,p_{\vec{m}}(0)>>$ and differentiating (64) with respect to time and using the equations of motion we find:

$$\frac{d}{dt}\Phi_{\vec{n},\vec{m}}(t)=C\left[\Pi_{\vec{n}+\vec{a}_x,\vec{m}}(t)+\Pi_{\vec{n}-\vec{a}_x,\vec{m}}(t)+\Pi_{\vec{n}+\vec{a}_y,\vec{m}}(t)+\right.$$
$$\left.+\Pi_{\vec{n}-\vec{a}_y,\vec{m}}(t)+\Pi_{\vec{n}+\vec{a}_z,\vec{m}}(t)+\Pi_{\vec{n}-\vec{a}_z,\vec{m}}(t)-6\Pi_{\vec{n},\vec{m}}(t)\right]. \qquad (65)$$

Differentiating the function Π with respect to time and using the equation of motion we have:

$$\frac{d}{dt}\Pi_{\vec{n},\vec{m}}(t)=i\hbar\delta_{\vec{n},\vec{m}}\,\delta(t)+\frac{1}{M}\Phi_{\vec{n},\vec{m}}(t).$$

After Fourier transformations time-frequency

$$\Phi_{\vec{n},\vec{m}}(t)=\int_{-\infty}^{+\infty}d\omega\, e^{-i\omega t}\Phi_{\vec{n},\vec{m}}(\omega);\quad \Pi_{\vec{n},\vec{m}}(t)=\int_{-\infty}^{+\infty}d\omega\, e^{-i\omega t}\Pi_{\vec{n},\vec{m}}(\omega);$$
$$\delta(t)=\frac{1}{2\pi}\int_{-\infty}^{+\infty}d\omega\, e^{-i\omega t},$$

in(67), this equation goes over to:

$$-i\omega\Phi_{\vec{n},\vec{m}}(\omega)=-\frac{C\hbar}{2\pi\omega}\Big(\delta_{\vec{n}+\vec{a}_x,\vec{m}}+\delta_{\vec{n}-\vec{a}_x,\vec{m}}+\delta_{\vec{n}+\vec{a}_y,\vec{m}}+\delta_{\vec{n}-\vec{a}_y,\vec{m}}+$$
$$+\delta_{\vec{n}+\vec{a}_z,\vec{m}}+\delta_{\vec{n}-\vec{a}_z,\vec{m}}-6\delta_{\vec{n},\vec{m}}\Big)-\frac{C}{iM\omega}\Big[\Phi_{\vec{n}+\vec{a}_x,\vec{m}}(\omega)+\Phi_{\vec{n}-\vec{a}_x,\vec{m}}(\omega)+ \tag{66}$$
$$+\Phi_{\vec{n}+\vec{a}_y,\vec{m}}(\omega)+\Phi_{\vec{n}-\vec{a}_y,\vec{m}}(\omega)+\Phi_{\vec{n}+\vec{a}_z,\vec{m}}(\omega)+\Phi_{\vec{n}-\vec{a}_z,\vec{m}}(\omega)-6\Phi_{\vec{n},\vec{m}}(\omega)\Big].$$

Due to the fact that translational symmetry is conserved in x and y directions we shall represent the function $\Phi_{n,m}(\omega)$ in the following way:

$$\Phi_{\vec{n},\vec{m}}(\omega)=\frac{1}{N_xN_y}\sum_{k_x,k_y}\mathrm{e}^{ik_xa_x(n_x-m_x)+ik_ya_y(n_y-m_y)}B_{n_z,m_z}(k_x,k_y,\omega),$$

whereunknown function: $B_{n_z,m_z}\equiv B_{n_z,m_z}(k_x,k_y,\omega)$ satisfies discrete equation:

$$B_{n_z+1,m_z}+B_{n_z-1,m_z}+\rho B_{n_z,m_z}=\frac{i\hbar}{2\pi}\frac{M^2}{C}\frac{2}{N_z+2}\times$$
$$\times\sum_{\mu=1}^{N_z+1}\omega^2_{k_x,k_y,\omega}\sin(n_z+1)\frac{\pi\mu}{N_z+2}\sin(m_z+1)\frac{\pi\mu}{N_z+2}. \tag{68}$$

where the parameter ρ is given by formula (49).

At this stage can be applied the boundary conditions, consisting in the absence of the layers $n_z = -1$ and $n_z = N_z + 1$, which can be expressed as $p_{n_x,n_y,-1}=p_{n_x,n_y,N_z+1}=0$. Due to these, the upon equation goes over to three subsystems:

- for $n_z = 0$:

$$B_{1,m_z}+\rho B_{0,m_z}=J_{0,m_z}; \tag{68a}$$

- for $n_z = N_z$:

$$B_{N_z,m_z}+\rho B_{N_z,m_z}=J_{N_z,m_z}, \tag{68b}$$

- and for $1 \le n_z \le N_z$:

$$B_{n_z+1,m_z}+B_{n_z-1,m_z}+\rho B_{n_z,m_z}=J_{n_z,m_z}, \tag{68c}$$

where we introduce notation:

$$J_{n_z,m_z}=\frac{i\hbar}{2\pi}\frac{M^2}{C}\frac{2}{N_z+2}\sum_{\mu=1}^{N_z+1}\omega^2_{k_x,k_y,\omega}\sin(n_z+1)\frac{\pi\mu}{N_z+2}\sin(m_z+1)\frac{\pi\mu}{N_z+2}.\cdot$$

The system of equations (68a) – (68c) has the same structure as the system of equations (50a) – (50c). For this reason it is not necessary to repeat the solving procedure, we will quote only the results of the solving. Consequently, taking:

$$B_{n_z,m_z}=\sum_{\mu=1}^{N_z+1}b_{\mu,m_z}\sin(n_z+1)\frac{\pi\mu}{N_z+2} \tag{69}$$

and

$$b_{\mu,m_z}=\frac{2}{N_z+2}\beta(k_x,k_y,\mu,\omega)\sin(m_z+1)\frac{\pi\mu}{N_z+2}, \tag{70}$$

we obtain that all the equations (68a) – (68c) are satisfied if equality is valid:

$$\beta\left(k_x,k_y,\mu,\omega\right)=\frac{i\hbar}{2\pi}\frac{M^2\omega_{k_x,k_y,\omega}^2}{C}\left(\rho+2\cos\frac{\pi\mu}{N_z+2}\right)^{-1}= \\ =\frac{i\hbar}{2\pi}\frac{M\omega_{k_x,k_y,\mu}}{2}\left(\frac{1}{\omega-\omega_{k_x,k_y,\mu}}-\frac{1}{\omega+\omega_{k_x,k_y,\mu}}\right). \tag{71}$$

Combining this and (70) with (69), it follows:

$$B_{n_z,m_z}\left(k_x,k_y,\omega\right)=\frac{i\hbar}{2\pi}\frac{M}{N_z+2}\sum_{\mu=1}^{N_z+1}\omega_{k_x,k_y,\mu}\left(\frac{1}{\omega-\omega_{k_x,k_y,\mu}}-\frac{1}{\omega+\omega_{k_x,k_y,\mu}}\right)\times \\ \times\sin\left(n_z+1\right)\frac{\pi\mu}{N_z+2}\cdot\sin\left(m_z+1\right)\frac{\pi\mu}{N_z+2}. \tag{72}$$

Now, introducing this result into requested function, we obtain:

$$\Phi_{\vec{n},\vec{m}}\left(\omega\right)=\frac{i\hbar}{2\pi}M\frac{1}{N_xN_y}\frac{1}{N_z+2}\sum_{k_x,k_y}\sum_{\mu=1}^{N_z+1}\mathrm{e}^{ik_xa_x\left(n_x-m_x\right)+ik_ya_y\left(n_y-m_y\right)}\omega_{k_x,k_y,\mu}\times \\ \times\left(\frac{1}{\omega-\omega_{k_x,k_y,\mu}}-\frac{1}{\omega+\omega_{k_x,k_y,\mu}}\right)\sin\left(n_z+1\right)\frac{\pi\mu}{N_z+2}\cdot\sin\left(m_z+1\right)\frac{\pi\mu}{N_z+2}. \tag{73}$$

By the definition of the spectral intensity of momentum-momentum Green's function $\Phi_{n,m}(\omega)$ [41–43]:

$$I_\Phi=\left.\frac{\Phi_{\vec{n},\vec{m}}\left(\omega+i\delta\right)-\Phi_{\vec{n},\vec{m}}\left(\omega-i\delta\right)}{\mathrm{e}^{\frac{\hbar\omega}{\Theta}}-1}\right|_{\delta\to0^+},$$

we give:

$$I_\Phi\left(\omega\right)=\hbar M\frac{1}{N_xN_y}\frac{1}{N_z+2}\sum_{k_x,k_y}\sum_{\mu=1}^{N_z+1}\mathrm{e}^{ik_xa_x\left(n_x-m_x\right)+ik_ya_y\left(n_y-m_y\right)}\times \\ \times\omega_{k_x,k_y,\mu}\sin\left(n_z+1\right)\frac{\pi\mu}{N_z+2}\sin\left(m_z+1\right)\frac{\pi\mu}{N_z+2}\times \\ \times\left(\mathrm{e}^{\hbar\omega/\theta}-1\right)^{-1}\left[\delta\left(\omega-\omega_{k_x,k_y,\mu}\right)-\delta\left(\omega+\omega_{k_x,k_y,\mu}\right)\right]. \tag{74}$$

From definition of the correlation function [50–53]:

$$<p_{\vec{m}}\left(0\right)p_{\vec{n}}\left(t\right)>=\int_{-\infty}^{+\infty}d\omega\,\mathrm{e}^{-i\omega t}I_\Phi\left(\omega\right),$$

after substitution (78), we obtain:

$$< p_{\vec{m}}(0)\ p_{\vec{n}}(t) >= \hbar M \frac{1}{N_x N_y} \frac{1}{N_z+2} \sum_{k_x,k_y} \sum_{\mu=1}^{N_z+1} \mathrm{e}^{ik_x a_x (n_x-m_x)+ik_y a_y (n_y-m_y)-it\omega_{k_x,k_y,\mu}} \times$$
$$\times\ \omega_{k_x,k_y,\mu} \left(\frac{\mathrm{e}^{-i\omega_{k_x,k_y,\mu} t}}{\mathrm{e}^{\hbar\omega_{k_x,k_y,\mu}/\theta}-1} - \frac{\mathrm{e}^{i\omega_{k_x,k_y,\mu} t}}{\mathrm{e}^{-\hbar\omega_{k_x,k_y,\mu}/\theta}-1} \right) \tag{75}$$
$$\times \sin(n_z+1)\frac{\pi\mu}{N_z+2} \sin(m_z+1)\frac{\pi\mu}{N_z+2}.$$

Finally, putting: $\vec{m}=\vec{n}$ and $t=0$ in (74), we obtain the expression of the square of the momentum of oscillations in the following form:

$$< p_{\vec{n}}^2 >= \frac{\hbar M}{N_x N_y (N_z+2)} \sum_{k_x,k_y} \sum_{\mu=1}^{N_z+1} \omega_{k_x,k_y,\mu} \sin^2(n_z+1)\frac{\pi\mu}{N_z+2} \coth\frac{\hbar\omega_{k_x,k_y,\mu}}{2\theta}. \tag{76}$$

The square of momentum enables us to find diffusion tensor [41–43], kinetic energy and other characteristics of the film connected with them.

II.3. Kinetic and Thermodynamic Properties of Thin Phonon Films

For better understanding of thin films physics it is necessary to emphasize their main feature: the physical characteristics of thin ideal (nonperturbed) films are spatially dependent [55–61]. This spatial dependence is the consequence of non-equivalency spatial distribution of their crystallographic points. As far as we know, this obvious fact was not theoretically reproduced. The formal reason for the need for the existence of theory of broken symmetry structures is the lack of procedures for calculating the Green's functions which depend on two spatial coordinates. In the theory of broken symmetry structures, up to now, Green's functions have been used depending on the difference of two spatial coordinates (this approach is correct only in the case of ideal structures) or the Green's functions with diagonal spatial coordinates [50–53]. In this work the calculation techniques for the Green's functions depending on two spatial coordinates are developed separately [54]. These unique correct techniques of calculation immediately reproduced the expected physical result, i.e. the spatial dependence of the broken symmetry structure properties.

II.3.1. *Energy Spectra of Phonons in Thin Films*

We shall start from the dispersion law of thin film phonons. It is obtained by solving algebraic equations – polynomial identity (Chebychev's) of the second type and order N_z + 1, which represents the developed form of the determinant system of difference equations (50a) –(50c) and/or (68a) –(68c) and zero [28–30]. The setting of this identity is the result of seeking singularity of the Green's functions (real parts of singularity pose potential energy of elementary excitations [50–53]). The roots of the determinants of the mentioned systems of equations have solutions of the form: $\rho \equiv \rho_{kxky,\mu}, \mu = 1, 2, 3, \ldots, N_z + 1$, where, by means of the relation (49), phonon energies can be expressed as $E \equiv E_{kx,ky,\mu}$. Consequently, the energy of thin film phonons is given by:

$$E_{k_x,k_y,\mu} = 2\hbar\Omega\sqrt{\sin^2\frac{a_x k_x}{2} + \sin^2\frac{a_y k_y}{2} + \sin^2\frac{\pi\mu}{2(N_z+2)}}\,. \tag{77}$$

These energy spectra can be represented graphically (Figure 10), for example, as in [49], where it is marked:

$$\varepsilon_\mu \equiv \frac{E_{k_x,k_y,\mu}}{2\hbar\,\Omega}\,; \quad R_{xy} \equiv \sin^2\frac{a_x k_x}{2} + \sin^2\frac{a_y k_y}{2} \in [0,\,2]\,;$$

$$S_\nu = \sin^2\frac{\pi\nu}{2(N_z+2)}\,; \quad \nu = 1,2,3,\cdots,N_z+1\,,$$

since we observe the first Brillouin zone with: $a_x k_x \wedge a_y k_y \in [-\pi/a, +\pi/a]$.

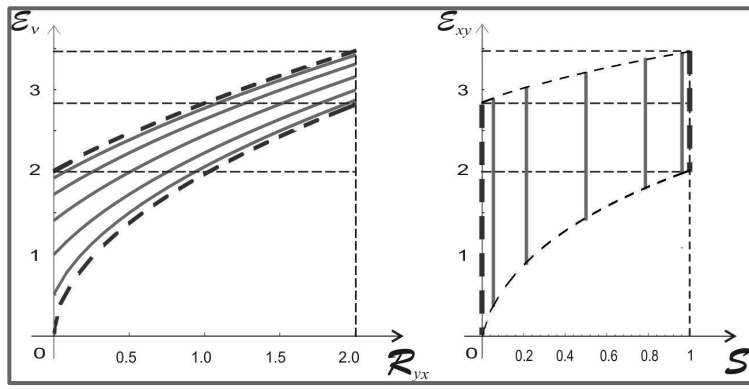

Figure 10: Energy spectra of phonons in the thin ideal crystalline film model

The physically most interesting energetic states are those with the lowest energy. Since minimal values of k_x and k_y, as well as the function R, are equal to zero (center of the first 2D Brillouin zone), while the minimal value of μ is equal to 1, the minimal energy of thin film phonons is:

$$E_{\min} \equiv \min E_{k_x,k_y,\mu} = E_{0,0,1} = 2\hbar\,\Omega\,\sin^2\frac{\pi}{2(N_z+2)}\,. \tag{78}$$

These minimal values are given in the Table 1 for films containing 3, 7 and 11 layers and $\hbar\Omega = 200\ k_B$, i.e. for $T_D = 200$ K.

Table 1: Values of the energy gaps of phonons in thin films

N_z	$E_{\min}$ [$k_B T$]	$E_{\min}$ [meV]
2	153,1	13,2
6	78,0	6,7
10	52,2	4,5

It is seen from this table that excitation of collective mechanical oscillations requires heat quanta corresponding to the temperatures T_3 = 153 K, T_7 = 78 K and T_{11} = 520 K, respectively. It means that up to the quoted temperatures the collective mechanical waves (acoustical phonons) cannot appear. Up to these temperatures atoms oscillations are mutually independent. Consequently, for a film with three layers the temperature of 153 K practically represents the absolute zero. From the point of view superconductive behavior of crystals this means that three-layer film has the critical superconductive temperature equal to 153 K. This conclusion points out to extraordinary superconductive properties of thin films.

Now we shall calculate the mean values of possible energies of phonons per atom in different layers of the film. The mean value of kinetic energies per atom is given by:

$$< T_{\vec{n}} >= \frac{1}{2M} < p_{\vec{n}}^2 > . \tag{79}$$

Substituting $< p_{\vec{n}}^2 >$ from (76) and going over in this formula from sums over k_x and k_y to integrals, in accordance with the formula:

$$\sum_{k_x,k_y} \to \frac{N_x N_y a^2}{(2\pi)^2} \int_0^{2\pi} d\varphi \int_0^{k_{\max}} dk\, k ,$$

After the use of small wave vectors approximation we obtain:

$$\begin{aligned} < T_{\vec{n}} >= & \frac{\hbar\Omega}{4\pi} \frac{1}{N_z+2} \sum_{\mu=1}^{N_z+1} \sin^2\left(n_z+1\right) \frac{\pi\mu}{N_z+2} \sin^2 \frac{\pi\mu}{N_z+2} \times \\ \times \int_0^{2\sqrt{\pi}} & dq\, q \sqrt{q^2 + 4\sin^2 \frac{\pi\mu}{2\left(N_z+2\right)}} \coth \frac{\hbar\Omega}{2\theta} \sqrt{q^2 + 4\sin^2 \frac{\pi\mu}{2\left(N_z+2\right)}} . \end{aligned} \tag{80}$$

The potential energy per atom is given by:

$$W_{\vec{n}} = \frac{C}{2} \left[\left(u_{\vec{n}} - u_{\vec{n}-\vec{a}_x}\right)^2 + \left(u_{\vec{n}} - u_{\vec{n}-\vec{a}_y}\right)^2 + \left(u_{\vec{n}} - u_{\vec{n}-\vec{a}_z}\right)^2 \right]. \tag{81}$$

Keeping in mind that the X and Y planes of film represent ideal structure, we can write:

$$\left(u_{\vec{n}+\vec{a}_{x/y}} - u_{\vec{n}}\right)^2 = \left(1 - \mathrm{e}^{-iak_{x/y}}\right)^2 u_{\vec{n}}^2 ,$$

and taking into account that boundaries k_x and k_y are symmetrical and that phonons dispersion law is even function, we can write the mean value of potential energy as:

$$\begin{aligned} < W_{\vec{n}} >= & \frac{C}{2} \left[\left(4\sin^2 \frac{ak_x}{2} + 4\sin^2 \frac{ak_y}{2} \right) < u_{\vec{n}}^2 > + < u_{n_x,n_y,n_z}^2 > + \right. \\ & \left. + < u_{n_x,n_y,n_z-1}^2 > -2 < u_{n_x,n_y,n_z} u_{n_x,n_y,n_z-1} > \right]. \end{aligned} \tag{82}$$

After application (68a) and going over from sums over k_x and k_y to integrals we obtain (assuming the small values of k) the following results:

$$< W_{\vec{n}} >= \frac{\hbar\Omega}{4\pi}\frac{1}{N_z+2}\left\{\sum_{\mu=1}^{N_z+1}\left[J_1(\mu)+J_3(\mu)\right]\sin^2(n_z+1)\frac{\pi\mu}{N_z+2}+\right.$$
$$\left.+\sum_{\mu=1}^{N_z+1}J_1(\mu)\left[\sin n_z\frac{\pi\mu}{N_z+2}-2\sin(n_z+1)\frac{\pi\mu}{N_z+2}\right]\sin n_z\frac{\pi\mu}{N_z+2}\right\}, \tag{83}$$

where

$$J_s(\mu)=\int_0^{2\sqrt{\pi}} dq\, q^s \frac{\coth\left(\frac{\hbar\Omega}{2\theta}\sqrt{q^2+4\sin^2\frac{\pi\mu}{2(N_z+2)}}\right)}{\sqrt{q^2+4\sin^2\frac{\pi\mu}{2(N_z+2)}}}.$$

The mean value of the full energy per atombeing the sum of kinetic and potential energy,

$$< E_{\vec{n}} >=< T_{\vec{n}} > + < W_{\vec{n}} >, \tag{84}$$

was calculated for ultrathin film consisting of two layers, i.e. three crystalline planes (N_z = 2). These values were numerically calculated (using the software package *Mathematica*) at the temperatures 0, 100, 200 and 300 K. The given results are exposed in the Table 2.

Based on the data obtained from Table 2 it is seen that mean energy per atom in the film depends on the index n_z labeling the layers. The differences of energies are the most distinguished in the thinnest film since the increasing of thickness means, in fact, bringing it closer to an ideal structure.

Table 2: Calculated mean value of kinetic, potential and total energy of phonons per atomin ultrathin film (N_z = 2)

n_z	T [K]	$10^{21}<T_{nz}>$ [J]	$10^{21}<W_{nz}>$ [J]	$10^{21}<E_{nz}>$ [J]
0	0	1,92504	1,68318	3,60822
	100	1,95277	1,70871	3,66148
	200	2,20640	1,92974	4,13614
	300	2,67865	2,34079	5,01944
1	0	1,91858	1,91291	3,83149
	100	1,94905	1,93935	3,88840
	200	2,20524	2,18644	4,39168
	300	2,67822	2,64978	5,32800
2	0	1,92504	1,90308	3,82812
	100	1,95277	1,92637	3,87914
	200	2,20640	2,16296	4,36936
	300	2,67865	2,61439	5,29304

II.3.2. *Comparison toPhonon Bulk Energies*

At this stage of the analysis, the comparison of the film mean energies per atom to corresponding mean energies of an ideal structure seems to be suitable. For this reason we shall calculate the mean energy per atom of a bulk structure. These mean energies are equal for all atoms due to translational invariance of an ideal structure.

We shall start from the expression for atom displacement and the corresponding momentum in ideal structure [41–43]:

$$u_{\vec{n}} = \sum_{\vec{k}} \sqrt{\frac{\hbar}{2MN\omega_{\vec{k}}}} \left(b_{\vec{k}}\, \mathrm{e}^{i\vec{k}\vec{n} - i\omega_{\vec{k}} t} + b_{\vec{k}}^{+}\, \mathrm{e}^{-i\vec{k}\vec{n} + i\omega_{\vec{k}} t} \right);$$
$$p_{\vec{n}} = M\, \dot{u}_{\vec{n}} = -i \sum_{\vec{k}} \sqrt{\frac{\hbar}{2MN\omega_{\vec{k}}}} \left(b_{\vec{k}}\, \mathrm{e}^{i\vec{k}\vec{n} - i\omega_{\vec{k}} t} - b_{\vec{k}}^{+}\, \mathrm{e}^{-i\vec{k}\vec{n} + i\omega_{\vec{k}} t} \right). \tag{85}$$

In this formula $b_{\vec{k}}$ and $b_{\vec{k}}^{+}$ are the Bose operators annihilating and creating phonons. The frequency ω_k will be taken in small wave vectors approximation: $\omega_{\vec{k}} = \hbar\Omega\, k$; $k = \left|\vec{k}\right|$.The mean kinetic energy per atom of the bulk structure is given by:

$$< T_{\vec{n}} >_{\mathrm{b}} = \frac{1}{2M} < p_{\vec{n}}^{2} > = \frac{\hbar\Omega\, a}{4N_x N_y N_z} \sum_{k_x, k_y, k_z} k \left(1 + 2 < b_{\vec{k}}^{+} b_{\vec{k}} > \right), \tag{86}$$

where $< b_{\vec{k}}^{+} b_{\vec{k}} > = \left(\mathrm{e}^{\hbar\Omega a k/\theta} - 1 \right)^{-1}$. Going over from sums to integrals according the standard rule

$$\frac{1}{N_x N_y N_z} \sum_{k_x, k_y, k_z} \rightarrow \frac{N_x N_y N_z a^3}{(2\pi)^3} \int d^3\vec{k}\,,$$

we obtain the following expression for the mean kinetic energies per atom of the ideal structure:

$$< T >_{\mathrm{b}}^{T=0} = \frac{9\pi^2}{32} \hbar\Omega + \frac{3}{2} \frac{1.08232}{\pi^2} \frac{\theta^4}{(\hbar\Omega)^3}, \tag{87}$$

where $1.08232 = \sum_{n=1}^{\infty} n^{-4}$ represents Riemann zeta-function with argument 4.

The potential energy per atom of the bulk structure after the use of the formulas

$$\left(u_{\vec{n} - \vec{a}_j} - u_{\vec{n}} \right)^2 = \left(1 - \mathrm{e}^{-iak_j} \right)^2 u_{\vec{n}}^2, \tag{88}$$

where*j* stands for *x*, *y* and *z*. The mean value of potential energy per atom of the ideal structure can be obtained after substitution u_n from the formula (85) and application of the unit operator $\left(N_x N_y N_z \right)^{-1} \sum_{k_x, k_y, k_z}$. The described procedure leads to the result:

$$< W_{\vec{n}} >_{\mathrm{b}} = \frac{9\pi^2}{32}\hbar\Omega + \frac{3}{2}\,\frac{1.08232}{\pi^2}\,\frac{\theta^4}{(\hbar\Omega)^3}\,. \tag{89}$$

From the formulae (87) and (89) we obtain the mean energy per atom of the bulk structure in the following form:

$$< E_{\vec{n}} >_{\mathrm{b}} \equiv < T_{\vec{n}} >_{\mathrm{b}} + < W_{\vec{n}} >_{\mathrm{b}} = \frac{9\pi^2}{16}\hbar\Omega + \frac{3\cdot 1.08232}{\pi^2}\,\frac{\theta^4}{(\hbar\Omega)^3}\,. \tag{90}$$

It should be pointed out that the first term in this expression comes from zero oscillations. Using (90) the values $<E_n>_{\mathrm{b}}$ are calculated at the temperatures T = 0, 100, 200 and 300 K. The results are given in the Table 3.

Table 3: Calculated mean value of total energy of phonons per atomin bulk structure

T [K]	0	100	200	300
$10^{21}\cdot E_{\mathrm{b}}$[J]	15,3226	15,3793	16,2306	19,9194

Comparing these results with corresponding ones from the Table 2, we can conclude that the mean energies per atom of the bulk structure are about two times higher than those of the film.

II.3.3. *Phonon Diffusion and Ultrathin Film Density*

The phonon diffusion of thin films will be determined with the help of correlation function (75). In the [54] the diffusion tensor is defined as follows:

$$D_{\vec{n}\vec{m}} = \left| \lim_{\varepsilon\to 0} \int_0^\infty dt\, \mathrm{e}^{-\varepsilon t}\, \frac{< p_{\vec{m}}(0)\, p_{\vec{n}}(t) >}{M^2} \right|. \tag{91}$$

Substituting (80) and solving the integral, we obtain:

$$D_{n_x,n_y,n_z;m_x,m_y,m_z} = \frac{\hbar}{2M}\delta_{n_x,m_x}\delta_{n_y,m_y}\delta_{n_z,m_z}\,. \tag{92}$$

It is seen that the phonon diffusion tensor is the diagonal one, with the same values along the diagonal. Consequently this diffusion tensor can be treated as diffusion coefficient whose value is $\hbar/(2M)$. It is interesting that the phonon diffusion coefficient does temperature independent. This result was obtained in [30,56] by a noticeably different approach.

The next step of analysis will be the calculation of film densities and their comparison to the densities of an ideal structure. The changes of the density of the "frozen" bulk structure

$$\rho_{\mathrm{b}} = \frac{M}{a^3} = 313.125\ \frac{\mathrm{kg}}{\mathrm{m}^3}, \tag{93}$$

where $M = 12 \cdot 1.67 \cdot 10^{-27}$ kg $= 2 \cdot 10^{-27}$ kg, corresponds to carbon atom and $a = 4\cdot 10^{-10}$ m can be obtained by dividing ρ_{b} with relative correction of elementary cell volume which is given by

$$\left[\frac{a(T)}{a(0)}\right]^3 = 1 + 3\,\frac{< u_{\vec{n}}^2 >}{a^2}. \tag{94}$$

By applying the already used formula, of the same form as the one given under the expression (63), where sums over k_x and k_y are substituted with the corresponding integrals and the small wave vectors approximation is taken, we obtain the corrections Δa^3 for three-layer (ultrathin) film. The densities of three-layer film at different temperatures: 0, 100, 200 and 300 K, are given in Table 4.

It is seen from this table that the central layer of the film has the minimal density. It is also very important to emphasize that the densities for film can be determined in one layer only. By convention we can define the density of the whole film as the arithmetical mean value of layer densities. The fourth row of the Table 4 is the result of the mentioned convention.

Table 3.4: Calculated value of density per atomof ultrathin film

n_z	$\rho_f(0)\left[\frac{\text{kg}}{\text{m}^3}\right]$	$\rho_f(100)\left[\frac{\text{kg}}{\text{m}^3}\right]$	$\rho_f(200)\left[\frac{\text{kg}}{\text{m}^3}\right]$	$\rho_f(300)\left[\frac{\text{kg}}{\text{m}^3}\right]$
0	312,193	312,184	312,132	312,049
1	312,188	312,176	312,116	312,025
2	312,193	312,184	312,132	312,049
$\overline{\rho}_f$	312,191	312,181	312,126	312,041

II.3.4. *Comparison to Bulk Density*

Using the formula (41) for bulk structure displacement we obtain

$$\frac{< u_{\vec{n}}^2 >}{a^2} = \frac{3}{8}\frac{\hbar}{M\Omega a^2} + \frac{1}{2\pi^2}\frac{\zeta(2)}{\hbar M\Omega^3 a^2}\theta^2, \tag{95}$$

where $\zeta(2) = \sum_{n=1}^{\infty}\frac{1}{n^2} = \frac{\pi^2}{6} = 1.6432$ is Riemann's function with argument 2. Using the last two formulae, we can find the densities of the ideal structure at the temperatures T = 0, 100, 200 and 300 K. Those values are given in Table 5.

Table 5: Calculated value of density per atomof bulk structure

$\rho_b(0), \left[\frac{\text{kg}}{\text{m}^3}\right]$	$\rho_b(100), \left[\frac{\text{kg}}{\text{m}^3}\right]$	$\rho_b(200), \left[\frac{\text{kg}}{\text{m}^3}\right]$	$\rho_b(300), \left[\frac{\text{kg}}{\text{m}^3}\right]$
309,028	309,004	308,933	308,814

Comparing the densities of the film to those of the ideal structure we can conclude that the densities of film are higher. The differences between film and ideal structure densities are not too high.

II.3.5. *Phonon Contribution to Thermodynamics of Ideal Films*

The next important characteristic of the film is the internal energy. It is quite clear that the internal energy of the film is the sum of internal energies of all layers of the film [49]. If the energy of one atom of the layer labeled with n_z at the temperature T is $E_{nz}(T)$ then the internal energy of this film is given by:

$$U_f(T) = N_x N_y \sum_{n_z=0}^{N_z} E_{n_z}(T). \tag{96}$$

This value is small compared to the internal energy of the ideal, i.e. unbounded three-dimensional structure [41–43]. The internal energy of the three dimensional ideal structure is given by:

$$U_n = \frac{9\pi^2}{16}\hbar\Omega + \frac{3\cdot 1.08232}{\pi^2}\frac{\theta^4}{(\hbar\Omega)^3}. \tag{97}$$

Since $N_x N_y N_z$ is of the order 10^{24} while $N_x N_y$is of the order 10^{16} the comparison between (90) and (97) is not interesting, but when it is calculated according to one molecule, then they can easily be compared. The more interesting characteristics are specific heat of the film and the corresponding ideal structure. Unit specific heat o f the b ulk-structure is defined in the standard way [41–43]:

$$C_V^{(b)} \equiv \frac{1}{\mathsf{M}}\frac{\partial U}{\partial T} = \frac{12\cdot 1.08232}{\pi^2}\frac{k_B}{M}\frac{\theta^3}{(\hbar\Omega)^3}, \tag{98}$$

where$\mathsf{M}$ is the structure mass, $\mathsf{M}\equiv N_x N_y N_z M$.

The formula for internal energy of the film is not suitable for differentiating with respect to T. Therefore, average $C_V^{(f)}$ will be taken:

$$C_{n_z}(T_2) = \frac{E_{n_z}(T_2) - E_{n_z}(T_1)}{\mathsf{M}(T_2 - T_1)}. \tag{99}$$

It is important to note that the unit specific heat in films can be found for layers, only. Since the unit specific heat of the whole film cannot be defined, we can use as convention that arithmetic mean value represents the specific heat of the film. This value is given as

$$\overline{C}(T_2) = \sum_{n_z=0}^{N_z} \frac{E_{n_z}(T_2) - E_{n_z}(T_1)}{(N_z+1)\,\mathsf{M}(T_2 - T_1)}. \tag{100}$$

The values of unit specific heats of the bulk-structure as well as the adequate average unit specific heats of three-layer film are given in Table 6. It is seen that at these relatively high temperature bulk specific heats are higher than those of film but theydo not differ substantially. The difference between ideal structure specific heats and mean values of film specific heats increases with the increase of the temperature.

Table 6: Calculated value of specific heats per atom of bulk and three-layer film-structure

T, [K]	100	200	300
$C_{\mathrm{b}}\left[\frac{\mathrm{J}}{\mathrm{kg\,K}}\right]$	112,72	467,887	708,75
$C_{\mathrm{f}}\left[\frac{\mathrm{J}}{\mathrm{kg\,K}}\right]$	113,27	906,160	3058,29

It is seen that at low temperature the specific heat of the film is about 3000 times smaller than those of the ideal structure. It means that the film heat isolation of thin films at the low temperatures is noticeably higher.

It can be shown that the film specific heat is lower than the one of the ideal structure up to the temperature of 80 K. In the temperature interval [80 K, 97 K], the specific heat of the bulk structure is lower than that of the film. For the temperatures $T > 97$ K, the specific heat of the bulk structure is again higher than that of the film. The behavior of specific heats is represented in Figure 11. It should be pointed out that the similar or almost the same results were obtained in the refs. [30–33,49].

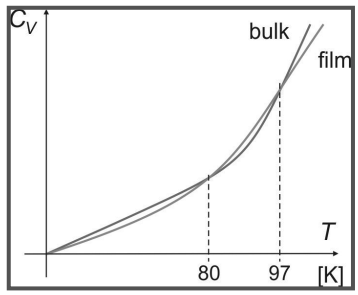

Figure 11: Unit specific heat per atom of bulk and ultrathin film

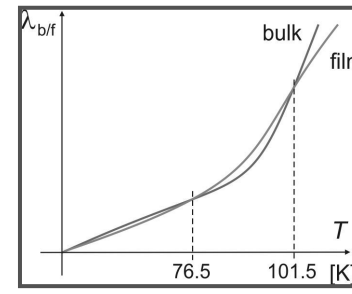

Figure 12: Unit thermal conductivity heat coefficient of bulk and ultrathin film

We will finish these analyses by examination of the thermal conductivity coefficient, which is one of the main kinetic parameters. It is a standard defined as [41–43]:

$$\lambda = D \cdot C_V \cdot \rho \,. \tag{99}$$

Using the results obtained for the diffusion coefficient, specific heat and density, we calculated the thermal conductivity coefficient for three-layer films and the corresponding bulk structures for 100, 200 and 300 K(Table 7).

It is seen that at 100 K the thermal conductivity of film is higher than that of the bulk structure. At 200 K and 300 K the thermal conductivity of the film is lower than the thermal conductivity of the bulk structure. On the basis of the Table 7 we can easily conclude that at the low temperatures thermal conductivity of the film is lower than that of bulk structure. It is the additional proof that at low temperatures thermal insulation properties of films are extremely better than those of the bulk structure.

Table 7: Calculated value of coefficient of thermal conductivity per atomof ideal three layer film-structure

$N_z = 2$	$10^5 \cdot \lambda_n \left[\frac{\mathrm{W}}{\mathrm{m} \cdot \mathrm{K}}\right]$		
$n_z \downarrow$ | $T\ [\mathrm{K}] \rightarrow$	100	200	300
0	9,04636	37,2159	56,3479
1	9,60036	39,1769	59,1758
2	9,06466	38,6136	58,6393
$\overline{\lambda}$	9,23713	38,3355	58,0543
λ_b	9,20668	73,6353	248,422

The coefficient of thermal conductivity of the film can be calculated for layers only, as well as the specific heat. The dependence of film specific heat and of the film thermal conductivity of spatial coordinates is given in Figure 12.

In these figures, unit-specific heat and the coefficient of thermal conductivity, as well as temperature, are expressed as dimensionless quantities – relative to the relation of their characteristic values on the Debye level.Ending the analyses of this section, we emphasize the qualitatively new effect appearing in films: at the temperatures of 4.88 K the film thermal conductivity becomes negative, which can be understood as the reflection of thermal flux propagating through the film.

II.4. Phonons in Perturbed Ultrathin Films

The thermally or mechanically caused atomic oscillations around their equilibrium positions in crystal were studied, where the breaking of translational symmetry is expressed by space limitation along one crystalographic direction. The phonon dispersion law, which was evaluated by the method of two-time temperature dependent Green's functions, is distinctly discrete and finite and posseses the top and bottom gap. Analyzing the influence of the magnitude of surface parameters on the energy spectra, the condition for the appearance and existence of the localized phonon states was found and graphically presented.

The scope of our study in this part is limited to the analysis of the phonon behaviour in more realistic – ultrathin layered structures, i.e. in perturbed crystalline nanofilms [62,63], which implies the existence of two boundary surfaces perpendicular to a prefered direction. The existence of the finite structure width along that direction introduces additional boundary conditions into the analysis of the phonon behaviour [64,65]. One of the most important aims is to study if the minimal frequencies of the phonons in the film are non-vanishing (i.e. does the phonon energy spectrum possess the gap), as well as to find the condition for the appearance of the localized phonon states.

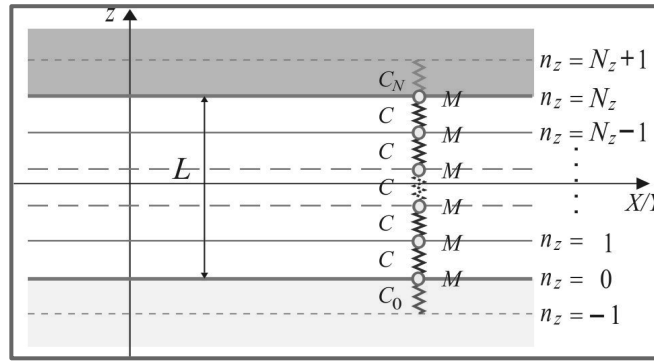

Figure 13: Model of perturbed ultrathin crystalline film

The starting point of our study is the standard Hamiltonian of the phonon system in the nearest neighbours approximation [66,67]:

$$
\begin{aligned}
H = T + W = \frac{M}{2} \sum_{n_x n_y;\alpha} \sum_{n_z=0}^{N_z} \dot{u}^2_{n_x n_y n_z;\alpha} + \\
+ \frac{C}{4} \sum_{n_x n_y;\alpha} \left\{ \sum_{n_z=1}^{N_z-1} \dot{u}^2_{n_x n_y n_z;\alpha} \left[\left(u^\alpha_{n_x n_y n_z} - u^\alpha_{n_x+1, n_y n_z} \right)^2 + \left(u^\alpha_{n_x n_y n_z} - u^\alpha_{n_x-1, n_y n_z} \right)^2 + \right. \right. \\
+ \left(u^\alpha_{n_x n_y n_z} - u^\alpha_{n_x n_y+1, n_z} \right)^2 + \left(u^\alpha_{n_x n_y n_z} - u^\alpha_{n_x n_y-1, n_z} \right)^2 + \\
\left. + \left(u^\alpha_{n_x n_y n_z} - u^\alpha_{n_x n_y n_z+1} \right)^2 + \left(u^\alpha_{n_x n_y n_z} - u^\alpha_{n_x n_y n_z-1} \right)^2 \right] + \\
+ (1+\varepsilon) \left(u^\alpha_{n_x n_y 0} \right)^2 + \left(u^\alpha_{n_x n_y 0} - u^\alpha_{n_x n_y 1} \right)^2 + \\
\left. + (1+\gamma) \left(u^\alpha_{n_x n_y N_z} \right)^2 + \left(u^\alpha_{n_x n_y N_z} - u^\alpha_{n_x n_y N_z-1} \right)^2 \right\},
\end{aligned}
\tag{101}
$$

where $u_{n_x n_y n_z}$ is displacement of the atom at the crystal site $\vec{n} \equiv (n_x, n_y, n_z)$, while $C \equiv C^{\alpha\alpha}_{\vec{n},\vec{m}}$ is Hooke's elastic constant between sites $\vec{n}$ and $\vec{m}$, except boundary ones: $C_0 \equiv (1+\varepsilon) C$ and $C_N \equiv (1+\gamma) C$, where boundary coeficients $\varepsilon, \gamma \in (-0.5, 1.0)$. The fact that the film is of finite dimension along all *z*-directions (orthogonal to the film boundary surfaces) is expressed in terms of the conditions: $n_z = 0, 1, 2, ..., N_z$, $N_z \leq 10$; $n_\alpha \in \left[-\frac{N_\alpha}{2}, +\frac{N_\alpha}{2} \right]$, $N_\alpha \sim 10^8$, $\alpha = (x, y)$.

II.4.1. *Dispersion Law of Phonons in Perturbed Crystalline Films*

We have decided to use the approach of Green's function method [50–52] for the determination of possible frequencies of phonons. For that purpose, we study phonon, two-time commutator Green's function:

$$G^{\alpha\alpha}_{\vec{n},\vec{m}}(t) \equiv \langle\langle u^{\alpha}_{\vec{n}}(t) \mid u^{\alpha}_{\vec{m}}(0\ )\rangle\rangle = \Theta(t)\langle\left[u^{\alpha}_{\vec{n}}(t), u^{\alpha}_{\vec{m}}(0\ )\right]\rangle_0 . \tag{102}$$

Following the standard procedure, using equations of motion for the Green's function and performing the temporal and partial spatial (*XY*) Fourier-transformation we obtain the system of N_z+1 nonhomogeneous algebraic-difference equations:

$$G_{n_z-1} + \left(\rho - \varepsilon\,\delta_{n_z,0} + \gamma\,\delta_{n_z,N_z}\right)G_{n_z} + G_{n_z+1} = K_{n_z}, \tag{103}$$

where: $G_{n_z} \equiv G_{n_z,m_z}(k_x k_y, \omega)$, $K_{n_z} \equiv \dfrac{i}{4\pi\,\Omega}\,\delta_{n_z,m_z}$, $\Omega = \sqrt{C/M}$ and

$$\rho = \frac{\omega^2}{\Omega^2} - 4\left(\sin^2\frac{a_x k_x}{2} + \sin^2\frac{a_y k_y}{2}\right) - 2 . \tag{104}$$

The determination of Green's function poles, which define the spectrum of possible phonon energies, turns into the calculation of the roots of the determinant of the system of equations (3), i.e. to condition:

$$D_{N_z+1}(\rho) = \begin{vmatrix} \rho-\varepsilon & 1 & 0 & 0 & \cdots & 0 & 0 & 0 & 0 \\ 1 & \rho & 1 & 0 & \cdots & 0 & 0 & 0 & 0 \\ 0 & 1 & \rho & 1 & \cdots & 0 & 0 & 0 & 0 \\ \vdots & \vdots & \vdots & \vdots & \ddots & \vdots & \vdots & \vdots & \vdots \\ 0 & 0 & 0 & 0 & \cdots & 1 & \rho & 1 & 0 \\ 0 & 0 & 0 & 0 & \cdots & 0 & 1 & \rho & 1 \\ 0 & 0 & 0 & 0 & \cdots & 0 & 0 & 1 & \rho-\gamma \end{vmatrix}_{N_z+1} \equiv 0 . \tag{105}$$

In the general case, this equation is not anallytically solvable (anallytically solvable cases arise for $\varepsilon, \gamma = 0, -1$ [66–68]), so numerical methods must be applied. For given numerical values of the parameters N_z and ε, γ from the equation (105), one can obtain the numerical values for $\rho_\nu \equiv \rho_\nu(\varepsilon, \gamma)$, $\nu = 1, 2, 3, \ldots, N_z+1$. Their substitution into (104) leads to the phonon dispersion law in the following form:

$$\begin{gathered} E_{xy}(\nu) \equiv \frac{\omega_{xy}(\nu)}{2\,\Omega} = \sqrt{F_{xy} + G_\nu}\ ; \\ F_{xy} \equiv \sin^2\frac{a_x k_x}{2} + \sin^2\frac{a_y k_y}{2}\ ; \quad G_\nu \equiv \frac{\rho_\nu + 2}{4}, \end{gathered} \tag{106}$$

which is presented on Figure 14.

Studying the influence of the surface parameters ε and γonto the energy spectrum for different film width (N_z), one concludes that (similar to the case of ideal crystalline film)

the energy spectra of phonons are discrete with the finite number of energy levels (N_z+1) and that they possess a top and a bottom energy gap:

$$b \equiv \sqrt{G_\nu^{min}} = \sqrt{G_{\nu=1}(\varepsilon,\gamma)}\,; \qquad t \equiv 1-\sqrt{G_\nu^{max}} = 1-\sqrt{G_{\nu=N_z+1}(\varepsilon,\gamma)}\,. \qquad (107)$$

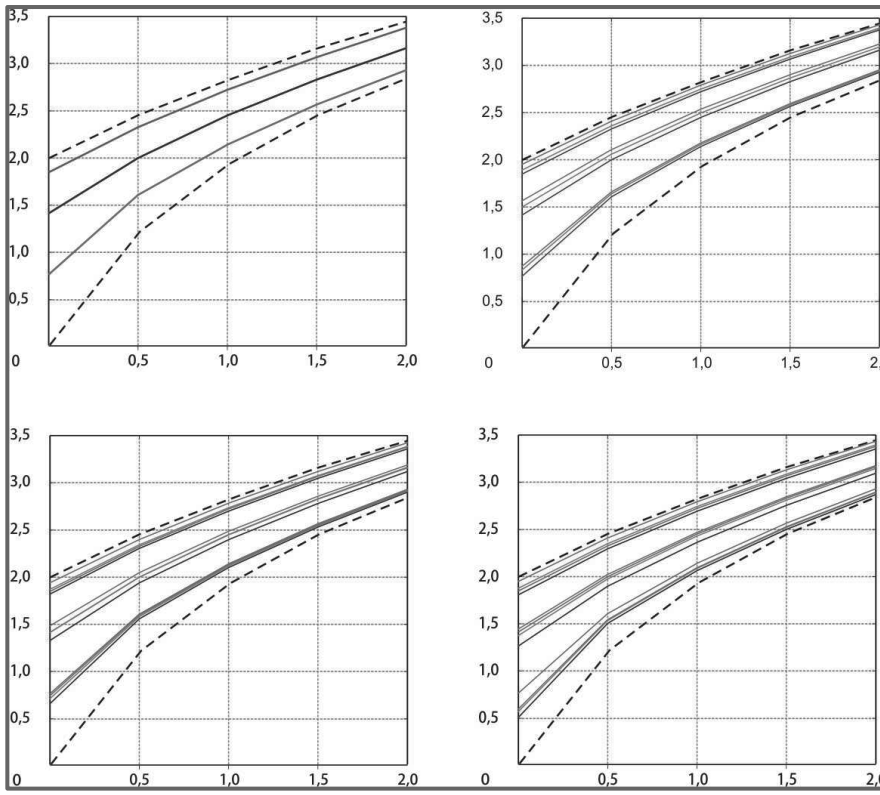

Figure 14: Energy specta of perturbed ultrathin films

Analyzing the energy gap dependance on the film width and the boundary parameter, one obtains the existence of the localized phonon states for some values of $\varepsilon,\gamma:\ t<0$, i.e. $E_{max}^F > E_{max}^B = 1$, for $k_x = k_y = 0$.

Energy levels out of the continuum band of the allowed energies of an infinite crystal correspond to the complex values of quasimomentum, i.e. there arise the localized phonon states at the surface film layers.

The condition for the appearance of the localized states is determined from the equation (106) by substituting: $\omega_{max} > 2\Omega$, with $\rho > 2$ and $D_n = n+1$ and for. It is interesting to note that in this case we obtain the condition:

$$\varepsilon > 2\,; \quad \omega_{max} > 2\Omega\,.$$

Increasing the film width, the energies of the localized states approach to the bulk band boundary, so in the limiting case ($N_z \to \infty$) they coincide with it.

Results of these analyses confirm the essential differences in dispersion law of phonons in film structures in comparison with unbounded ones, which is as an exclusive consequence of boundaries existence.

- Energy spectrum of phonons in the crystalline film is a discrete one with the finite number of possible energy levels equal to the number of atomic planes in the film along *z*-direction.
- The consequence of the spectrum discreteness is the existence of the top and bottom energy gap which decrease with the increase of the film width.
- Increasing the magnitude of the boundary elastic constants, the energy spectrum shifts towards higher energies (the increase of the bottom gap and the decrease of the top gap).
- Depending on the values of the parameter of surface interactions, certain energy levels can lie outside the energy band of the ideal crystal, so there appear the surface localized states of phonons.
- Increasing the film width, the energy of the localized states shifts towards the bulk band boundary, coinciding with it for $N_z \to \infty$. In this limit the localized states, as well as the energy gaps vanish, while the spectrum turns in the quasicontinual spectrum of the ideal infinite crystal.

II.4.2. *Calculating diffusion tensor of phonon system*

Diffusion tensor according to Kubo formula [69,70] is defined as

$$D_{ij}^{f}(k) = \lim_{\delta \to 0+} \int_0^\infty dt\, \mathrm{e}^{-\delta t} \langle \hat{v}_i(0) \hat{v}_j(t) \rangle, \tag{108}$$

where $\hat{v}_i$ and $\hat{v}_j$ are velocity operators (in Heisenberg's representation) oscillation of the molecules in the crystal along the crystallographic direction $i, j \in (x, y, z)$, δ perturbation parameter. To find the correlation function that exists in the expression for the diffusion coefficient, we start from Green's functions of type impulse - impulse $\langle\langle p_i(t) \mid p_j(0) \rangle\rangle$ because $\hat{v}_{i/j} = \hat{p}_{i/j} / m$.

Using the calculating procedure of Green's functions represented in the introductory part we get the equation

$$\begin{aligned} \frac{d}{dt} \langle\langle p_f(t) \mid p_g(0) \rangle\rangle &= C_H \langle\langle u_{f+1}(t) \mid p_g(0) \rangle\rangle + \\ &+ C_H \langle\langle u_{f-1}(t) \mid p_g(0) \rangle\rangle - 2C_H \langle\langle u_f(t) \mid p_g(0) \rangle\rangle. \end{aligned} \tag{109}$$

In this equation Green's functions of the type shift- impulse appear. When they are calculated we obtain

$$\begin{aligned} \frac{d}{dt} \langle\langle u_f(t) \mid p_g(0) \rangle\rangle &= i\hbar \delta_{f,g} \delta(t) + \frac{1}{M} \langle\langle p_f(t) \mid p_g(0) \rangle\rangle; \\ \frac{d}{dt} \langle\langle u_{f+1}(t) \mid p_g(0) \rangle\rangle &= i\hbar \delta_{f+1,g} \delta(t) + \frac{1}{M} \langle\langle p_{f+1}(t) \mid p_g(0) \rangle\rangle \end{aligned} \tag{110}$$

$$\frac{d}{dt}\langle\langle u_{f-1}(t)\,|\,p_g(0)\rangle\rangle = i\hbar\delta_{f-1,g}\delta(t) + \frac{1}{M}\langle\langle p_{f-1}(t)\,|\,p_g(0)\rangle\rangle.$$

Here $\delta_{f,g};\delta_{f\pm1,g};$ are Kronecker's operators, and $\delta(t)$ Dirac's delta function.Fourier's transformations frequency-time are introduced

$$\begin{aligned}
\langle\langle p_f(t)\,|\,p_g(0)\rangle\rangle &= \int_{-\infty}^{\infty} d\omega\, \mathrm{e}^{-i\omega t}\,\langle\langle p_f\,|\,p_g\rangle\rangle_\omega;\\
\langle\langle u_f(t)\,|\,p_g(0)\rangle\rangle &= \int_{-\infty}^{\infty} d\omega\, \mathrm{e}^{-i\omega t}\,\langle\langle u_f\,|\,p_g\rangle\rangle_\omega;\\
\langle\langle u_{f\pm1}(t)\,|\,p_g(0)\rangle\rangle &= \int_{-\infty}^{\infty} d\omega\, \mathrm{e}^{-i\omega t}\,\langle\langle u_{f\pm1}\,|\,p_g\rangle\rangle_\omega
\end{aligned} \tag{111}$$

when Fourier's character $\langle\langle u_f\,|\,p_g\rangle\rangle_\omega$ is replaced in the equation for $\langle\langle p_f\,|\,p_g\rangle\rangle_\omega$ we obtain the final with the crystal films of the case $f = g$:

$$\begin{aligned}
\langle\langle p_f\,|\,p_f\rangle\rangle_\omega = \frac{i\hbar C_H}{\pi\omega^2} + \frac{C_H}{M\omega^2}\Big(2\langle\langle p_f\,|\,p_f\rangle\rangle_\omega -\\
-\langle\langle p_{f+1}\,|\,p_f\rangle\rangle_\omega - \langle\langle p_{f-1}\,|\,p_f\rangle\rangle_\omega\Big).
\end{aligned} \tag{112}$$

The system of difference equations for Green's functions follows from here

$$\begin{aligned}
\langle\langle p_{f+1}\,|\,p_f\rangle\rangle_\omega + \langle\langle p_{f-1}\,|\,p_f\rangle\rangle_\omega +\\
+\left(\frac{M\omega^2}{C_H} - 2\right)\langle\langle p_f\,|\,p_f\rangle\rangle_\omega = \frac{i\hbar M}{\pi}.
\end{aligned} \tag{113}$$

Solving this system of difference equations, Green's functions which figure in it are found. Appropriate correlation function is given by:

$$\langle p_f(t)p_f(0)\rangle = \frac{\hbar C_H}{\omega_k}\left(\frac{\mathrm{e}^{-i\omega_k t}}{\mathrm{e}^{\hbar\omega_k/\theta}-1} - \frac{\mathrm{e}^{i\omega_k t}}{\mathrm{e}^{-\hbar\omega_k/\theta}-1}\right), \tag{114}$$

If we go back to the formula that defines the diffusion coefficient of phonon system we obtain

$$D_{ij}^f(k) = \lim_{\delta\to0^+}\frac{\hbar C_H}{M^2\omega_k}\int_0^\infty\left(\mathrm{e}^{-\delta t}\frac{\mathrm{e}^{-i\omega_k t}}{\mathrm{e}^{\hbar\omega_k/\theta}-1} - \mathrm{e}^{-\delta t}\frac{\mathrm{e}^{-i\omega_k t}}{\mathrm{e}^{-\hbar\omega_k/\theta}-1}\right)dt, \tag{115}$$

which gives a final result

$$D_{ij}^f(k) = \left|i\frac{\hbar C_H}{M^2\omega_k^2}\right|. \tag{116}$$

Therefore, the calculation results are the following:

- Diffusion tensor of phonon system is diagonal

$$D_{ii}^f(k) = \frac{\hbar C_H}{M^2\omega_k^2}. \tag{117}$$

- It is larger at lower frequencies
- Is independent of the temperature

This third view is very important because it justifies the macroscopic theory of heat conduction in which it is assumed that the diffusion coefficient is independent of the temperature.

II.5. Phonon Contribution to Thermodynamics of Perturbed Films

Forasmuch as the properties of anisotropic structures are conditioned by the change of dispersion law, it is necessary to observe behavior of certain thermodynamic properties towards obtainment of better understanding about those properties. Phonon participation in thermodynamic properties (or heat capacitance temperature behavior, i.e. generally -- in heat transferring) in thin film was found in our previous paper [47–49].

Getting that, when $k \to 0$ (in long-wave approximation):

$$4\left[\sin^2\left(ak_x/2\right)+\sin^2\left(ak_y/2\right)\right] \approx a^2k^2,\ k^2 = k_x^2 + k_y^2,$$

energies of all three phonon branches have non-zero values, it can be utilized dispersion relations (77), i.e. (106), in somewhat simplified form:

$$E(\vec{k}) = \sqrt{a^2k^2E_0^2 + \Delta_f^2}, \tag{118}$$

where: $\Delta_f = ak_z^{min}E_0;\ E_0 \equiv \hbar\sqrt{\frac{C_\alpha}{M}}.$

It should be specifically emphasized that verification of phonon dispersion law at very low values of k is virtually impossible, so that verification of existence of phonon gap detects itself in measurement of low temperature thermal capacitances in film and corresponding ideal structure.

II.5.1. *Thermal capacitance of ultrathin crystalline film*

The thermal capacitance is analyzed, whereby at first internal energy is calculated in terms of standard form [69–71]:

$$U_f = 3\sum_{k_x,k_y,k_z} E(\vec{k})\left[\mathrm{e}^{E(\vec{k})/\theta} - 1\right]^{-1}. \tag{119}$$

Going over from sum in last expression to integral in accordance with the formula:

$$\sum_{k_x,k_y,k_z} \to 3(N_z+1)\sum_{k_x,k_y} \to \frac{3N_xN_y(N_z+1)a^2}{4\pi^2}\int_0^{2\pi} d\phi \int_0^{k_{\max}} k\,dk,$$

and taking $k_{\max} \approx k_D = \sqrt[3]{6\pi^2}$, after suitable notations:

$$\eta \equiv \sqrt{\frac{N_z^2}{3} + N_z + 1}; \quad \zeta \equiv \sqrt{1 + \left(\frac{N_z + 2}{\pi} \sqrt[3]{6\pi^2} \right)^2}$$

and adequate operations, expression for internal energy has been obtained in form:

$$\begin{aligned} U_f(x) = \frac{3N_f}{4\pi^2} \frac{\Delta_f^4}{E_0^3} x^2 \left\{ \left[Z_2\left(\frac{1}{x}\right) - \eta^2 Z_2\left(\frac{\eta}{x}\right) + \eta^2\zeta^2 Z_2\left(\frac{\eta\zeta}{x}\right) - \zeta^2 Z_2\left(\frac{\zeta}{x}\right) \right] + \right. \\ + 4x \left[Z_3\left(\frac{1}{x}\right) - \eta Z_3\left(\frac{\eta}{x}\right) + \eta\zeta Z_3\left(\frac{\eta\zeta}{x}\right) - \zeta Z_3\left(\frac{\zeta}{x}\right) \right] + \\ \left. + 6x^2 \left[Z_4\left(\frac{1}{x}\right) - Z_4\left(\frac{\eta}{x}\right) + Z_4\left(\frac{\eta\zeta}{x}\right) - Z_4\left(\frac{\zeta}{x}\right) \right] \right\}, \end{aligned} \tag{120}$$

where the symbol x is introduced for reduced temperature: $x = \theta / \Delta_f$, $N_f = N_x N_y (N_z + 1)$ and $Z_r(X) = \sum_{j=1}^{\infty} j^{-r} \mathrm{e}^{-jX}$ -- the functions are called Dyson's functions.

For finding of expression for the thermal capacitance per a unit cell (here: per an atom), the standard definitional form [69–71] is used:

$$C_f = \frac{1}{N_f} \frac{\partial U_f}{\partial T} \equiv \frac{k_B}{N_f} \frac{\partial U_f}{\partial \theta} = \frac{1}{\Delta_f} \frac{k_B}{N_f} \frac{\partial U_f}{\partial x}. \tag{121}$$

In accordance with that it is obtained:

$$\begin{aligned} C_f(x) = \frac{3k_B}{4\pi^2} \left(\frac{\Delta_f}{E_0} \right)^3 \left\{ \left[Z_1\left(\frac{1}{x}\right) - \eta^3 Z_1\left(\frac{\eta}{x}\right) + \eta^3\zeta^3 Z_1\left(\frac{\eta\zeta}{x}\right) - \zeta^3 Z_1\left(\frac{\zeta}{x}\right) \right] + \right. \\ + 6x \left[Z_2\left(\frac{1}{x}\right) - \eta^2 Z_2\left(\frac{\eta}{x}\right) + \eta^2\zeta^2 Z_2\left(\frac{\eta\zeta}{x}\right) - \zeta^2 Z_2\left(\frac{\zeta}{x}\right) \right] + \\ + 18x^2 \left[Z_3\left(\frac{1}{x}\right) - \eta Z_3\left(\frac{\eta}{x}\right) + \eta\zeta Z_3\left(\frac{\eta\zeta}{x}\right) - \zeta Z_3\left(\frac{\zeta}{x}\right) \right] + \\ \left. + 24x^3 \left[Z_4\left(\frac{1}{x}\right) - Z_4\left(\frac{\eta}{x}\right) + Z_4\left(\frac{\eta\zeta}{x}\right) - Z_4\left(\frac{\zeta}{x}\right) \right] \right\}. \end{aligned} \tag{122}$$

It is known that the phonon part in thermal capacitance of the system is described with cubic temperature dependence. By introducing nondimensional reduced temperature, this dependence amounts to: $C_b(x) = \frac{12}{5} \pi^4 N_b k_B \left(\frac{\Delta_f}{E_D} \right)^3 x^3$. For comparison of these dependencies, these and expression (122) are divided by the constant: $C_0 = \frac{k_B}{2} \left(\frac{\Delta_f}{E_D} \right)^3$, whose dimension is equal to dimension of thermal capacitance, and nondimensional

properties are compared: $C_{f/b} \equiv \frac{C_{f/b}}{C_0}$. On Fig.15 are shown relative (nondimensional) thermal capacitances of bulk (*b*) and film-structure (*f*) subject to the relative temperature *x* in low (a) and very low temperature region.

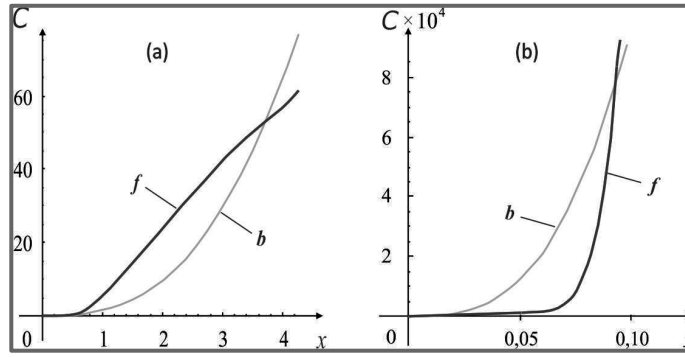

Figure 15: Thermal capacitance vs. temperature at low and extremely low temperatures

On Fig.16 are shown relative (nondimensional) thermal capacitances of bulk (*b*) and film-structure (*f*) samples versus relative temperature *x*, for ultrathin -- $N_z = 3$ (a), thin $N_z = 8$ (b) and thick $N_z = 48$ (c) film-structures, in comparatione with bulk ones.

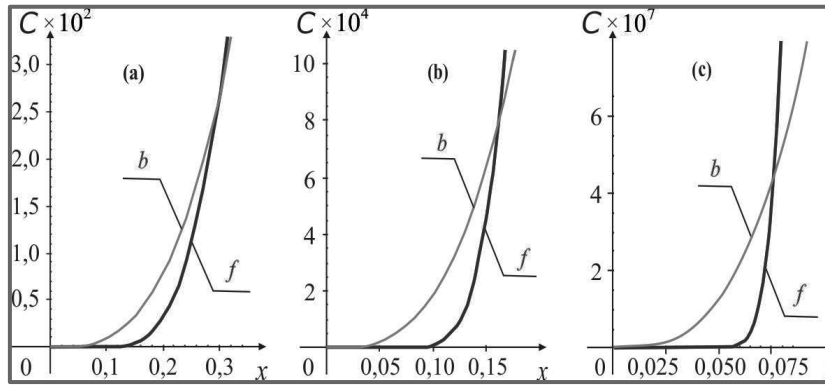

Figure 16: Thermal capacitance in low temperature regime for ultrathin, thin, thick films

It can be seen that in low-temperature region (Fig.15) thermal capacitance of film is lower than that of massive specimens, whereas at the intermediate temperatures situation is reversed [12]. Intersect point of two curves at low temperatures is moving -- with increase of film-thickness -- towards lower temperatures (Fig.16 a – c). Besides, it is noticeable that thermal capacitance of film with decrease of temperature declines faster than that of corresponding ideal structure, or slowly rises with the increase of temperature – to a certain upper temperature. Hence, for film heating from certain lower to a certain upper temperature, it is necessary to use more thermal energy per mass unit than for heating the same quantity of corresponding (with the identical crystallographical parameters) unbounded structure to the same temperature. It is in accordance with the fact that phonons in film have non-zero excitation energy.

II.5.2. *Thermal conductivity of ultrathin crystalline film*

Using the formula

$$\kappa = DC\rho_M, \tag{123}$$

where κ is the coefficient of the thermal conductivity, D the diffusion coefficient, C the specific heat and ρ_M the density, we shall determine the coefficient thermal conductivity of thin film. The analysis of the coefficient is the great practical interest, since it determines the heat isolation and a number of other properties of these structures [71].

The diffusion coefficient D (strictly speaking the diffusion tensor D_{ij}) is founded via the use of Kubo's formula, and expressed by formula (117), while the specific heat – by formula (122).

To determine the density, we first calculate the density correction caused by molecular vibrations. Starting with the standard expression [47–49]:

$$\vec{u}_{\vec{n}} = \sum_{j,\vec{k}} \sqrt{\frac{\hbar}{2MN\omega_{\vec{k}}^{j}}} \left[b_j^{+}(\vec{k}) \mathrm{e}^{-i(\vec{k}\vec{n}-\omega_{\vec{k}}^{j}t)} + b_j(\vec{k}) \mathrm{e}^{i(\vec{k}\vec{n}-\omega_{\vec{k}}^{j}t)} \right] \vec{e}_j(\vec{k}), \tag{124}$$

$j \in (x, y, z)$, for molecular displacements, we can find the averages of square displacements:

$$\sum_{\vec{n}} \langle u_{\vec{n}}^2 \rangle \equiv N_f \langle u^2 \rangle = \sum_{j,\vec{k}} \frac{\hbar}{2M\omega_{\vec{k}}^{j}} \left[1 + 2\langle \hat{n}_{\vec{k}} \rangle \right]; \quad \langle \hat{n}_{\vec{k}} \rangle = \frac{1}{\mathrm{e}^{E_{\vec{k}}/\theta} - 1}. \tag{125}$$

Introduction of the notation $\langle u_0^2 \rangle = \frac{1}{N} \sum_{\vec{k}} \frac{\hbar}{2M\langle \omega_{\vec{k}} \rangle}$, one can find in (125):

$$\langle u^2 \rangle - \langle u_0^2 \rangle = \frac{3}{2\pi} \frac{\hbar}{M\omega_D} \frac{\Delta_f^2}{E_0^2} \left\{ Z_1\left(\frac{1}{x}\right) - \eta Z_1\left(\eta \frac{1}{x}\right) + \frac{1}{x} \left[Z_2\left(\frac{1}{x}\right) - \eta Z_2\left(\eta \frac{1}{x}\right) \right] \right\}. \tag{126}$$

The density of the film is given by the formula:

$$\rho_M = \frac{M}{\langle (a_0 + u)^3 \rangle} = \frac{M}{\langle a_0^3 \rangle} \frac{1}{1 + 3\dfrac{\langle u^2 \rangle}{\langle a_0^2 \rangle}} \rho_M \approx \rho_0^M \left(1 - \frac{3\langle u^2 \rangle}{\langle a_0^2 \rangle} \right). \tag{127}$$

Using Debye's approximation [26] we shall substitute $\langle u^2 \rangle$ in (127) with $\langle u^2 \rangle - \langle u_0^2 \rangle$ from formula (126). Thus, we obtain:

$$\frac{\rho_M}{\rho_0^M}=1-\frac{3}{2\pi}\frac{\hbar^2\Delta_f^2 x}{M\langle a_0\rangle^2 E_D E_0^2}\left\{Z_1(\frac{1}{x})-\right.$$
$$\left.-\eta Z_1(\eta\frac{1}{x})+\frac{1}{x}\left[Z_2(\frac{1}{x})-\eta Z_2(\eta\frac{1}{x})\right]\right\}. \tag{128}$$

Substituting (117), (122) and ρ_M from (128) into (123) we finally obtain be expression for the thermal conductivity coefficient of thin film structures:

$$\kappa_f=\frac{3k_B}{2\pi}\frac{\hbar\Omega^{\alpha 2}}{M\langle\omega_k^2\rangle}\left(\frac{\Delta_f}{E_0}\right)^2\left\{\frac{1}{x}\left[\left(\mathrm{e}^{1/x}-1\right)^{-1}-\eta^3\left(\mathrm{e}^{\eta/x}-1\right)^{-1}\right]+\right.$$
$$+3\left[Z_1(\frac{1}{x})-\eta^2 Z_1(\eta\frac{1}{x})\right]+6x\left[Z_2(\frac{1}{x})-\eta Z_2(\eta\frac{1}{x})\right]$$
$$\left.+6x^2\left[Z_3(\frac{1}{x})-Z_3(\eta\frac{1}{x})\right]\right\}\rho_0^M\left(1-\frac{3}{2\pi}\frac{\hbar^2}{M\langle a_0\rangle^2 E_D}\left(\frac{\Delta_f}{E_0^2}\right)^2\times\right. \tag{129}$$
$$\left.\times\left\{Z_1(\frac{1}{x})-\eta Z_1(\eta\frac{1}{x})+x\left[Z_2(\frac{1}{x})-\eta Z_2(\eta\frac{1}{x})\right]\right\}x\right).$$

Formula (129) was analyzed numerically as a function of the scaled temperature $x=\theta/\Delta_f$.

The notation: $\lambda_{b/f}\equiv\frac{\kappa_{b/f}(x)}{\kappa_0}$; $\kappa_0=\frac{8}{9}\left(6\pi^2\right)^{-2/3}\frac{\hbar}{a^3}\left(\frac{\Delta_f}{E_0}\right)^3$, represent scaled thermal conductivity, is introduced into formula (129). The dependence of scaled thermal conductivity on the scaled temperature is given in Fig.17.

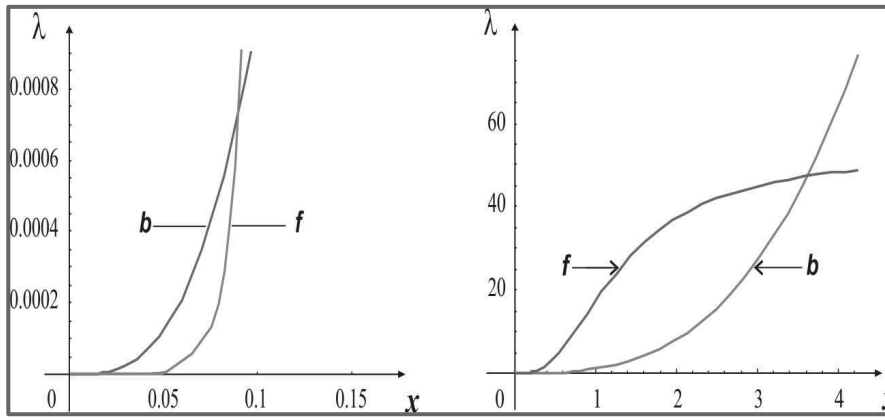

Figure 17: Thermal conductivity versus temperature

a) at extremely low temperature (up to 5 K) – left;

b) at higher temperature (in the range $T>5$ K) – right.

It can be seen from figures quoted that, at extremely low temperatures $T \leq 4$ K and at temperatures $T \geq 180$ K, the thermal conductivity of a film is lover than that of a bulk. In the temperature range $4 < T < 180$ K the thermal conductivity of a bulk is lower than that of a film.

At the end of this section we would like to point out an important fact: since Eqs. (77) and (107) does not have solution $k_z = 0$, all phonon energies in film have a gap. Consequently, to excite the phonons in films some activation energy is necessary.

Studying and comparing the phonon spectra and states in the ideal unbounded and nondeformed (bulk) structures and the structures with broken translational symmetry (films) we have reached the following conclusions.

- Mechanical vibrations in bulk structures are plane waves in all directions, while in the films they represent the superposition of the standing waves in z-directions (perpendicular to the boundary surfaces) and plane waves in XY-planes (parallel to boundary surfaces).
- The amplitude of phonon displacements in the films depends on the film width and it is $\sim 10^4 \sqrt{2/N_z}$ times higher than in the ideal structures. This indicates their larger elastic "maneuvering space" without any negative effect to the mechanical properties of the given material (for example no breaking of interatomic bonds) which leads to higher resistance and higher melting point of the films with respect to bulk samples.
- All three acoustic frequencies in bulk structures vanish for $\vec{k} \to 0$, while in the films they tend toward some minimal value depending on the film width. This means that phonons in the films possess the energy gap, that for their excitation (creation) one should spend certain energy, i.e. heat them up to certain – activation temperature, meaning that the system up to that temperature behaves as the "frozen" one, as if the phonons were not present.
- Phonon gap, besides depending on the film width, depends also on the type of the atoms and their distribution along$z$-direction and also on the stoichiometric relation of the atoms injected in the films.
- The densities of phonon states and Debye's frequencies have lower values in the films than in the corresponding bulk structures. This implies that in the films, phonon excitations are more "difficult" to appear, that they are less "present" and that created acoustic phonons of the optical type (above the activation temperature) are energetically "softer" than the classical ones which appear in the bulk structures.
- Since phonons with Debye's frequencies define thermal and electrical properties of the materials, this means that films are worse thermal and electrical conductors.

These analyzes show that the films are better superconductors than the corresponding bulk samples, made from the same material with the same crystalline structure. This statement, which is an experimental fact is supported by the following of our results.

- In the films there appear standing phonon waves along z-directions, the collective property specific for the macroscopic quantum-mechanical state which is the characteristics of the superconductors. In the ideal structures, where there exist only plane phonon waves, there is no such property.

- The appearance of the energy gap in the phonon spectrum of the films means that up to the activation temperature these systems behave as completely frozen, i.e. without any mechanical vibrations which would cause the real resistance to the electrical current conduction.
- Lower values of Debye's frequencies in the films could result in the higher values of (BCS) matrix elements of the effective electron-electron interaction. The attraction between paired electrons is stronger, and one must spend more energy for their destruction, so the critical temperature of these systems is higher.

Since phonons with Debye's frequencies are responsible for electrical and thermal induced transport properties of material [69–73], it follows that the nanofilm-structure will be inferior electrical and thermic conductor in contrast with the relative massive structures, providing there is no chemical and structural differences between them.

On the other hand, it is well known fact that the more inferior electrical conductor materials is (under normal conditions), the better superconductor it becomes [26,71]. Due to that, the experimental fact can be concluded and justified, that in spatially very confined structures more qualitative superconductive properties have been achieved.

In the region of low temperatures, the thermal capacitance of film is lower than in massive structures, while in medium temperatures it is reversed. Intersect point of two curves at low temperatures is moving – with increase of film-thickness -- towards lower temperatures. Besides, it is noticeable that thermal capacitance of film with decrease of temperature declines faster than that of corresponding ideal structure, or slowly rises with the increase of temperature – to a certain upper temperature.

Hence, for film heating from certain lower to a certain upper temperature, it is necessary to use more thermal energy per mass unit than for heating the same quantity of corresponding (with the identical crystallographical parameters) unbounded structure to same temperature.

It is well known that poorer electric conductors are better superconductors, so that in ultrathin films it is possible to achieve much better superconducting properties!

The results obtained show that the thermal conductivity coefficient of a film is considerably lower than that of a bulk at low temperature, where the thermal conductivity of bulk decreases as T^3. This result is practically applicable: sandwich of several films would be a better thermal insulator than the bulk structure of the same thickness.

In accordance with the Wiedemann - Franz law, the electrical conductivity is proportional to thermal conductivity. This leads to conclusion that films are worse electrical conductors than bulk structures of the same material.

It could be interesting to estimate the superconductive properties, since worse conductors are, in principle, better superconductors.

The results obtained here are compared to theoretical results as well as to the experimental data from Ref [74–80].

References

[1] B.S.Tošić, J.P.Šetrajčić, R.P.Đajić and D.Lj.Mirjanić, Phonons in Broken-Symmetry Structures, *Phys.Rev.*B **36**, 9094 (1987).

[2] J.P.Šetrajčić, R.P.Đajić, D.Lj.Mirjanić and B.S.Tošić, Phonon Spectra in Superconducting Ceramics, *Physica Scripta***42**, 732 (1990).

[3] J.P.Šetrajčić, I.D.Vragović i S.Lazarev, Termodinamika superprovodnih kvazi 2D kristalnih nanostruktura, *Fullerenes and Nanotubes Review***1**/4, 39 (1997).

[4] J.P.Šetrajčić, Makroskopski kvantni efekti kod superprovodnih materijala, *Zbornik radova – Satelitski simpozijum „Epoha kvanta"*, 78 (2001).

[5] J.P.Šetrajčić, S.K.Jaćimovski, D.Raković and D.I.Ilić, Phonon Spectra in Crystalline Nanostructures, *Proceedings 2nd WSEAS International Conference on Nanoelectronicsand ElectroMagnetic Compatibility (ICONEMC)***1**, 1091 (2002).

[6] D.I.Ilić, S.K.Jaćimovski, J.P.Šetrajčić, V.D.Sajfert, S.M.Vučenović and D.Raković, Phonon Spectra And Possible States In Ultra-Narrow Wires, *Proceedings 1st International Workshop on Nanosciences & Nanotechnology (IWON)*, 160 (2005).

[7] B.S.Tošić, V.D.Sajfert, D.Popov, J.P.Šetrajčić i D.Ćirić, Analiza teoretica proprietilor specifice ale nano-structurilor, ISBN 978-973-625-475-8, ps.224, *Editura Politehnica*, Timioara (Romania) 2007.

[8] I.J.Šetrajčić, D.Rodić, I.Mandić, S.Armaković, N.V.Delić and J.P.Šetrajčić, Fononski udeo u superprovodnim karakteristiikama ultratankih film-struktura, *Tehnika – Novi materijali***20**(2), 189 (2011).

[9] S.K.Jaćimovski, D.Lj.Mirjanić and J.P.Šetrajčić, Participation of Mechanical Oscillations in Thermodynamics of Crystals With Superlattice, *Physica Macedonica***61**, 21 (2012).

[10] J.P.Šetrajčić and S.K.Jaćimovski, Review of Results of Theoretical Approaches to Phonon Engineering of Thermodynamic Properties for Different Quantum Structures, *NBP***20**/3, 67 (2015).

[11] J.P.Šetrajčić: Matematička fizika – integralne transformacije, autorizovana skripta, *Departman za fiziku PMF*, Novi Sad 2000 – 2006. (I – IV izdanje).

[12] Đ.Mušicki, Uvod u teorijsku fiziku I: Teorijska mehanika, *Naučna knjiga*, Beograd 1980.

[13] J.P.Šetrajčić i D.Lj.Mirjanić, Fononi u kristalnim lancima, Spomenica akademika Veselina Perića, ISBN 978-99938-21-29-8, str.45-55, *ANURS*, Banja Luka 2011.

[14] I.Supek, Teorijska fizika i struktura materije, *Školska knjiga*, Zagreb 1992.

[15] B.S.Tošić, Statistička fizika, *Institut za fiziku PMF UNS*, Novi Sad 1978.

[16] P.G.de Gennes: Superconductivity of Metals and Allovs, *Benjamin*, New York 1966.

[17] M.Tinkham: Introduction to Superconductivity, *Mc Graw-Hill*,Kogamusha 1975.

[18] V.V.Shmidt: Vvedenie v fiziku sverhprovodnikov,*Nauka*, Moskva 1982.

[19] J.P.Šetrajčić, Superprovodnost, ISBN 86-489-0318-1, *Zmaj*, Novi Sad 2001.

[20] Ajay Kumar Saxena: High-Temperature Superconductors, *Springer*, Berlin 2010.

[21] A.S.Davydov, Solid State Theory,*Nauka*, Moskva 1976, in Russian.

[22] Ch.Kittel, Introduction to Solid State Physics, 7th ed., *Wiley*, New York 2006.

[23] A.M.Kosevich, The Crystal Lattice, *Wiley*, Weinheim 2005.

[24] Y.K.Godovskii, Thermophysics of Polymers, *Himiya*, Moskva 1982. – in Russian

[25] M.Mijatović, K. Trenčevski, *Proc. XII Yugoslav Symp.CondensMatter Phys.*(Skopje), 43 (1992).

[26] J.Callaway, Quantum Theory of the Solid State, 2nd ed., *Academic*, Boston 1991.

[27] T. M. Tritt, Thermal Conductivity Theory, Properties and Applications, *KluwerPlenum*, New York 2004.

[28] Zh.M.Zhang, Nano/Microscale Heat Transfer, *Mc Graw Hill*, New York 2007.

[29] W-Q.Huang, K-Q.Chen, Z.Shuai, L.Wang, W.Hu,B.S.Zou, Acoustic-phonon transmission and thermal conductance in a double-bend quantum waveguide, *J.Appl.Phys*. **98**, 093524 (2005).

[30] J.-S.Wang, J.Wang, J.T.Lü, Quantum thermal transport in nanostructures, *Eur.Phys.J.* B **62**, 381 (2008).

[31] A.A.Balandin, D.L.Nika, Phononics in Low-Dimensionals Materials, *Materials Today***15**/6, 266 (2012).

[32] D.L.Nika, E.P.Pokatilov, A.A.Balandin, V.M.Fomin, A.Rastelli, O.G.Schmidt, Reduction of Lattice Thermal Conductivity in One-Dimensional Quantum-Dot Superlattices due to Phonon Filtering, *Phys.Rev*.B **84**, 165415 (2011).

[33] D.L.Nika, A.I.Cocemasov, C.I.Isacova, A.A.Balandin, V.M.Fomin, O.G.Schmidt, Suppression of Phonon Heat Conduction in Cross-Section-Modulated Nanowires, *Phys.Rev.*B **85**, 205439 (2012).

[34] M. Rieth, Nano-Engineering in Science and Technology – An Introduction to the World of Nano-Design, *World Scientific*, Singapore 2003.

[35] Introduction to Nano – Basics to Nanoscience and Nanotechnology, Eds. A.Sengupta, Ch.K.Sarkar, *Springer-Verlag*, New York 2015.

[36] Handbook of Theoretical and Computational Nanotechnology (10-Volume Set**)**, Eds. M. Rieth, and Wolfram Schommers, *World Scientific*, Singapore 2006.

[37] W.Kelley, A.Peterson, Difference Equations – An Introduction with Applications, *Academic Press*, London 2001.

[38] B.S.Tošić, V.D.Sajfert, D.Popov, J.P.Šetrajčić i D.Ćirić, Primena diferencnog računa u analizi nanostruktura, ISBN 86-85889-00-6, *VANU*, Novi Sad 2005.

[39] V.D.Sajfert and B.S.Tošić, The Research of Nanoscience Progress, *J.Comput.Theor.Nanosci*. **7**/1, 15–84 (2010).

[40] J.P.Šetrajčić, S.K.Jaćimovski, V.D.Sajfert, I.J.Šetrajčić, Specific Quantum Mechanical Solution of Difference Equation of Hyperbolic Type, *Commun.Nonlinear Sci.Numer.Simulat*. **19**/5, 1313 (2014).

[41] J.P.Šetrajčić, D.I.Ilić, B.Markoski, A.J.Šetrajčić, S.M.Vučenović, D.Lj.Mirjanić, B.Škipina, S.S.Pelemiš, Adapting and Application of the Green's Functions Method onto Research of the Molecular Ultrathin Film Optical Properties, *Physica Scripta*T **135**, 014043: 1-4 (2009).

[42] J.P.Šetrajčić, V.D.Sajfert, D.Lj.Mirjanić, S.M.Vučenović, Operator Method for Solving the Difference Equations, *Proceedings 5th WSEAS International Conference on Applied Mathematics*, **488**/148, 1-4 (2004).

[43] J.P.Šetrajčić, Exact Microtheoretical Approach to Calculation of Optical Properties of Ultralow Dimensional Crystals, *Arxiv*, eprint arXiv:1004.2387 (04/2010).

[44] J.W.Kim, Ho-S.Yang, Y.Ha Jun, K.Ch.Kim, Interfacial effect on thermal conductivity of diamond-like carbon films, *J Mech.Sci.Technol*. **24**/7, 1511-1514 (2010).

[45] K.M.F.Shahil, A.A.Balandin, Thermal Properties of Graphene and Multilayer Graphene: Applications in Thermal Interface Materials, *Solid State Commun*. **152**/15, 1331 (2012).

[46] G.Zhang, H.Zhang, Thermal Conduction and Rectication in Few-Layer Graphene Y Junctions, *Nanoscale***3**, 4604 (2011).

[47] S.Lazarev, D.Lj.Mirjanić, M.Pantić, B.S.Tošić and J.P.Šetrajčić, Phonons in Ultrathin Layered Structures, *J.Phys.Chem.Sol.***60**, 849 (1999).

[48] J.P.Šetrajčić, V.M.Zorić, S.M.Vučenović, D.Lj.Mirjanić, V.D.Sajfert, S.K.Jaćimovski and D.I.Ilić, Phonon Thermodynamics in Crystalline Nanofilms, *Materials Science Forum***555**, 291 (2007).

[49] J.P.Šetrajčić, S.K.Jaćimovski, V.D.Sajfert, Phonon Engineering Theory of Crystalline Layered Nanostructures, ISBN: 978-3659-80775-6, *LAP Lambert Academ.Publ.*, Saarbrücken 2015.

[50] E.N.Economou, Green's Functions in Quantum Physics, *Springer*, Berlin 1949.

[51] G.Rickayzen, Green's Functions and Condensed Matter, *Academic Press*, London 1980.

[52] S.Doniach, E.H.Sondheimer, Green's Functions for Solid State Physicists, *Imperial College Press*, London 1999.

[53] J.P.Šetrajčić, V.D.Sajfert, and S.K.Jaćimovski, Fundamental Preferences Of The Phonon Engineering For Nanostructural Samples, *Rev.Theor.Sci*. **4**/4, 353-401 (2016); doi:10.1166/rits.2016.1067.

[54] V.M.Agranovich, M.D.Galanin, Migration of Electron Energy Excitations in CondensedMatter, *Nauka*, Moscow 1978 (In Russian).

[55] B.S.Tošić, V.D.Sajfert, D.Popov, J.P.Šetrajčić, D.Ćirić,Application of Difference Calculus to Nanostructure analysis, *Academy of Sciences and Arts*, Novi Sad 2005 (in Serbian).

[56] S.K.Jaćimovski, Phonon Thermodynamics of Layered Nanostructures, Dr.Dissertation, *Faculty of Electrical Engineering*, Belgrade 2003 (in Serbian).

[57] Nanoscale Energy transport and Hardvesting – A Computational Study, Ed. G.Zhang, *Taylor & Francis*, New York 2015.

[58] W.E.Bies, R.Radke, H.Ehrenreich, Phonon Dispersion Effect and Thermal Conductivity Reduction in GaAs/AlAs Superlattices, *http://xxx.lanl.gov./find/cond.mat*. No 0005028 (2000).

[59] Electron-Phonon Interactions in Low-Dimensional Structures, Ed. L.Challis, *University Press*, Oxford 2003.

[60] L.C.Jackson, Low Temperature Physics, *Wiley & Sons*, New York 1962.

[61] M.A.Stroscio, M.Dutta, Phonons in Nanostructures, *Cambridge*, Cambridge 2001.

[62] J.P.Šetrajčić, V.M.Zorić, N.V.Delić, D.Lj.Mirjanić and S.K.Jaćimovski, Phonon Participation in Thermodynamics and Superconductive Properties of Thin Ceramic Films, Chapter 15, pp. 317-348, In „Thermodynamics", Ed.M.Tadashi, ISBN: 978-953-307-544-0, *InTech*, Vienna (Austria) 2011.

[63] S.Lazarev, M.Pantić, S.K.Jaćimovski and J.P.Šetrajčić, Phonons in Thin Layered Structures, *Solid State Phenomena***61-62**, 193 (1998).

[64] S.K.Jaćimovki, J.P.Šetrajčić, M.S.Jaćimovski and V.V.Stojanović, Phonon Contribution in Thermodynamics And Transport Properties Of Ultrathin Ceramic Films, *Acta Phys.Pol.* A **126**/3, 811 (2014).

[65] B.S.Tošić, J.P.Šetrajčić, D.Lj.Mirjanić and Z.V.Bundalo, Low-Temperature Properties of Thin Films, *Physica* A **184**, 354 (1992).

[66] J.P.Šetrajčić, I.D.Vragović, D.Lj.Mirjanić and S.K.Jaćimovski, Appearance of Localized Phonon States in Thin Bounded Crystal-Structures, *Bal.Phys.Lett.***5**, 418 (1998).

[67] J.P.Šetrajčić, R.P.Đajić, D.Lj.Mirjanić and B.S.Tošić, Phonon Spectra in Superconducting Ceramics, *Physica Scripta***42**, 732 (1990).

[68] V.D.Sajfert, J.P.Šetrajčić, S.K.Jaćimovski and D.Popov, Theoretical Basis for Phonon Engineering of Nanostructures, *Quantum Matter* – accepted (2016).

[69] G.D.Mahan, Condensed Matter in a Nutshell, *University Press*, Princeton 2011.

[70] W.Jones, N.H.March, Theoretical Solid State Physics (I and II), *Dover*, New York 1985.

[71] A.A.Maradudin, Physics of Phonons, *Proceedings of the XXIII Winter School of Theoretical Physics (Lecture Notes in Physics)*, held in Karpacz, February 1987, ISBN-13 978-3540182443.

[72] D.Popov, S.K.Jaćimovski, B.S.Tošić and J.P.Šetrajčić, Kinetics of Thin Films Mechanical Oscillations. *Physica* A **317**/1, 129 (2003).

[73] P.Hylgaard, G.Mahan, Thermal Conductivity, Vol. 23, *Tehnomic*, Lancaster1996.

[74] A.J.Bullen, K.E.O'Hara, D.G.Cahill, Thermal conductivity of amorphous carbon thin films, *http://xxx.lanl.gov/find/cond.mat*. No:0008084 (2001).

[75] D.H.Santamore, M.C.Cross, The effect of surface roughness on universal thermal conductance, *http://xxx.lanl.gov/find/cond.mat*. No:0011473,324-333 (2001).

[76] W.E.Bies, R.Radke, H.Ehrenreich, Phonon dispersion effect and the thermal conductivity reduction in GaAs/AlAs superlatices, *http://xxx.lanl.gov/find/cond.mat*. No:0005028 (2000).

[77] S.K.Jaćimovski, D.I.Raković, J.P.Šetrajčić, S.Armaković and V.M.Zorić, Thermal Conductivity Clasical and High-Tc-Superconductors, *Proceedings 4th International Congress: "Contemporary Materials"*, 21-34 (2011).

[78] V.D.Sajfert, J.P.Šetrajčić, S.K.Jaćimovski and D.Popov, Application of Difference Calculus and Difference Equations to Investigation of Specific Nanostructure Properties, *Quantum Matter***3**/4, 307-314 (2014); doi:10.1166/qm.2014.112.

[79] J.P.Šetrajčić, I.J.Šetrajčić, S.K.Jaćimovski, B.Markoski and S.Markoski, Phonons in the Crystal Nanofilm-Structure, *Proceedings ETAI*-2015 **13**-3, 1-5 (2015).

[80] J.P.Šetrajčić, S.K.Jaćimovski and V.D.Sajfert, Phonon Contribution to Heat Capacitance of Nanolayered Crystalline Structures, *Mod.Phys.Lett.* B **29**(4), 1550008 [13 pages] (2015); doi: 10.1142/S0217984915500086.

III. PHONONS IN CRYSTALLINE SUPERLATTICES

Unlike in the previous part, here we will try to observe the difference between the characteristics of single (solo) nano-crystalline films and composite films, i.e. superlattices. We were interested in whether the quantum size effects (quantum confinement), quantum (de)coherence and influence of boundary conditions, observed in nanofilms, strengthen or weaken in superlattices.

Application of superlattices requires a knowledge of their thermodynamic characteristics [1,2]. Regardless of the type of superlattice, the thermodynamics of their subsystems (electrons, excitons, spin waves, etc.) is determined when the subsystem is in thermodynamic equilibrium with phonons [3,4–6]. Therefore the thermodynamic analysis of phonon subsystems is the first step in investigations of superlattice properties.

III.1. Model of crystalline superlattice

It will be assumed that symmetry is disturbed along the z direction. Translational symmetry of cubic structure is conserved in *XY*planes. On the Figure 1 the superlattice is presented schematically in the *z*-direction only.

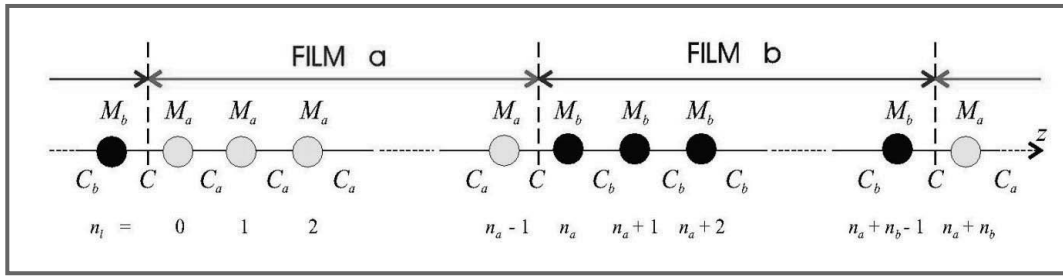

Figure 1: Schematic representation of simple superlattice model

The standard Hamiltonian of phonon subsystem [7–9] in the nearest neighbors approximation can be written as follows:

$$H = \sum_{\vec{n},\, i=1,2} \sum_{\alpha=x,y,z} \sum_{n_l=0}^{n_a+n_b-1} \left\{ \frac{\left[p^{(i)}_{\vec{n},n_l;\alpha} \right]^2}{2M_i} + \right.$$

$$+ \frac{C_i^{\alpha}}{4} \left[\left(u_{n_x,n_y,n_z;n_l} - u_{n_x+1,n_y,n_z;n_l} \right)^2 + \left(u_{n_x,n_y,n_z;n_l} - u_{n_x-1,n_y,n_z;n_l} \right)^2 + \right. \tag{1}$$

$$+ \left(u_{n_x,n_y,n_z;n_l} - u_{n_x,n_y+1,n_z;n_l} \right)^2 + \left(u_{n_x,n_y,n_z;n_l} - u_{n_x,n_y-1,n_z;n_l} \right)^2 +$$

$$\left. \left. + \left(u_{n_x,n_y,n_z;n_l} - u_{n_x,n_y,n_z+1;n_l} \right)^2 + \left(u_{n_x,n_y,n_z;n_l} - u_{n_x,n_y,n_z-1;n_l} \right)^2 \right] \right\},$$

where $\vec{u}_{\vec{n}}^{\alpha}$ are the small movements of atom in the place $\vec{n}$ from their equilibrium position in the α direction, and $\vec{p}_{\vec{n}}^{\alpha}$ is the corresponding momentum; M_i, where $i = a, b$ – is the mass of the corresponding atoms in the elementary cell and C_i^{α} are the straining constants (negligible relative to the torsion Hooke's elastic constants).

The symbolic notation will be introduced:

$$\vec{n} \equiv \{n_x, n_y, n_z\}; \quad n_{x/y/z} \in \left[-\frac{N_{x/y/z}}{2}, +\frac{N_{x/y/z}}{2} \right], \; N_{x/y} \sim 10^8, \; N_z \sim 10; \qquad n_l \in \begin{cases} [0,\, n_a - 1] & -\text{for } a\text{-film}; \\ [n_a,\, n_a + n_b - 1] & -\text{for } b\text{-film}, \end{cases} \tag{2}$$

where: $n_{x/y}$ is the counter of lattice nodes in X and Y direction, n_z is the counter of positions along the basic motive of superlattice or atoms of film (z-direction), n_l is the counter of node positions in the basic motive of superlattice.

Taking into account that superlattice is the periodical crystal structure the cyclic conditions are valid along $x$and $y$direction for any configuration function, i.e.

$$f_{m_x m_y m_z m_l + N_{x/y}} = f_{m_x m_y m_z m_l} \Rightarrow \mathrm{e}^{iN_{x/y}k_{x/y}a_{x/y}} = \mathrm{e}^{2\pi i \nu_{x/y}} \tag{3a}$$

Analogously, the cyclic condition in z-direction is:

$$f_{m_x m_y m_z m_l + (n_a + n_b)N_z} = f_{m_x m_y m_z m_l} \Rightarrow \mathrm{e}^{i(n_a + n_b)N_z k_z a_z} = \mathrm{e}^{2\pi i \nu_z} \tag{3b}$$

Allowed values of z-component of wave vector $k_z$are defined by integer $\nu_z \in 0, \pm 1, \pm 2, \ldots, \pm N_z/2$. In this way the boundaries of the first Brillouin zone in z-direction are defined:

$$k_z \in -\left[\frac{\pi}{(n_a + n_b)\tilde{a}}, + \frac{\pi}{(n_a + n_b)\tilde{a}} \right]; \qquad \tilde{a} \equiv \frac{(n_a - 1)a_a + (n_b - 1)a_b + 2a}{n_a + n_b}, \tag{4}$$

where the notation $\tilde{a}$is introduced for the average value of lattice constant in the z-direction.

III.2. Phonon dispersion law in superlattice

The phonon dispersion law will be found with the help of the Green's function [10–12]:

$$G_{\vec{n},n_l;\vec{m},m_l}(t - t') \equiv \langle\langle u_{\vec{n},n_l}(t) \,|\, u_{\vec{m},m_l}(t') \rangle\rangle = \Theta(t - t') \langle [u_{\vec{n},n_l}(t),\, u_{\vec{m},m_l}(t')] \rangle, \tag{5}$$

having equation of the motion of the form:

$$-M_i \omega^2 G_{\vec{n},n_l;\vec{m},m_l}(\omega) = -\frac{i\hbar}{2\pi} \delta_{\vec{n},\vec{m}} \, \delta_{n_l,m_l} + \frac{1}{i\hbar} \langle\langle \left[p_{\vec{n},n_l}, H \right] \Big| u_{\vec{m},m_l} \rangle\rangle_{\omega}, \tag{6}$$

where$M_i \in (M_a, M_b)$.

The next step is an evaluation of commutators figuring in a higher order Green's function (the procedure is presented in [7,8]). After a substitution of found commutators and the application of the partial configuration Fourier transformation (due to the disturbance of

translational symmetry of considered system, this transformation is applied to coordinates x,y and z, but not to coordinate l, where the translational symmetry is disturbed), one obtains the system of non-homogeneous algebraic-differential equations:

a) $n_l = 0$:

$$M_a\,\omega^2 G_{n_x,n_y,n_z,0;\vec{m},m_l} = \frac{i\hbar}{2\pi}\delta_{\vec{n},\vec{m}}\,\delta_{0,m_l} + \Big[\Big(2C_a^x + 2C_a^y + C_a^z + C\Big)G_{n_x,n_y,n_z,0;\vec{m},m_l} + \\ + C_a^x\Big(G_{n_x+1,n_y,n_z,0;\vec{m},m_l} + G_{n_x-1,n_y,n_z,0;\vec{m},m_l}\Big) + C_a^y\Big(G_{n_x,n_y+1,n_z,0;\vec{m},m_l} + G_{n_x,n_y-1,n_z,0;\vec{m},m_l}\Big) + \\ + C_a^z\,G_{n_x,n_y,n_z,1;\vec{m},m_l} + C\,G_{n_x,n_y,n_z-1,n_a+n_b-1;\vec{m},m_l}\Big], \tag{7a}$$

b) $1 \le n_l \le n_a - 2$:

$$M_a\,\omega^2 G_{n_x,n_y,n_z,0\;\vec{m},m_l} = \frac{i\hbar}{2\pi}\delta_{\vec{n},\vec{m}}\,\delta_{n_l,m_l} + \Big[2\Big(C_a^x + C_a^y + C_a^z\Big)G_{n_x,n_y,n_z,n_l;\vec{m},m_l} + \\ + C_a^x\Big(G_{n_x+1,n_y,n_z,n_l;\vec{m},m_l} + G_{n_x-1,n_y,n_z,n_l;\vec{m},m_l}\Big) + C_a^y\Big(G_{n_x,n_y+1\,n_z,n_l;\vec{m},m_l} + G_{n_x,n_y-1\,n_z,n_l;\vec{m},m_l}\Big) + \\ + C_a^z\Big(G_{n_x,n_y,n_z,n_l+1\;\vec{m};m_l} + G_{n_x,n_y,n_z,n_l-1;\vec{m},m_l}\Big]\Big), \tag{7b}$$

c) $n_l = n_a - 1$:

$$M_a\,\omega^2 G_{n_x,n_y,n_z,n_a-1;\vec{m},m_l} = \frac{i\hbar}{2\pi}\delta_{\vec{n},\vec{m}}\,\delta_{n_a-1,m_l} + \Big[\Big(2C_a^x + 2C_a^y + C_a^z + C\Big)G_{n_x,n_y,n_z,n_a-1;\vec{m},m_l} + \\ + C_a^x\Big(G_{n_x+1,n_y,n_z,n_a-1;\vec{m},m_l} + G_{n_x-1,n_y,n_z,n_a-1;\vec{m},m_l}\Big) + C_a^y\Big(G_{n_x,n_y+1,n_z,n_a-1;\vec{m},m_l} + G_{n_x,n_y-1,n_z,n_a-1;\vec{m},m_l}\Big) + \\ + C_a^z\,G_{n_x,n_y,n_z,n_a-2;\vec{m},m_l} + C\,G_{n_x,n_y,n_z,n_a;\vec{m},m_l}\Big], \tag{7c}$$

d) $n_l = n_a$:

$$M_b\,\omega^2 G_{n_x,n_y,n_z,n_a;\vec{m},m_l} = \frac{i\hbar}{2\pi}\delta_{\vec{n},\vec{m}}\,\delta_{n_a,m_l} + \Big[\Big(2C_b^x + 2C_b^y + C_b^z + C\Big)G_{n_x,n_y,n_z,n_a;\vec{m},m_l} + \\ + C_b^x\Big(G_{n_x+1,n_y,n_z,n_a;\vec{m},m_l} + G_{n_x-1,n_y,n_z,n_a;\vec{m},m_l}\Big) + C_b^y\Big(G_{n_x,n_y+1\,n_z,n_a;\vec{m},m_l} + G_{n_x,n_y-1\,n_z,n_a;\vec{m},m_l}\Big) + \\ + C_b^z\,G_{n_x,n_y,n_z,n_a+1\;\vec{m};m_l} + C\,G_{n_x,n_y,n_z,n_a-1;\vec{m},m_l}\Big], \tag{7d}$$

e) $n_a + 1 \le n_l \le n_a + n_b - 2$:

$$M_b\,\omega^2 G_{n_x,n_y,n_z,n_l;\vec{m},m_l} = \frac{i\hbar}{2\pi}\delta_{\vec{n},\vec{m}}\,\delta_{n_a,m_l} + \Big[2\Big(C_b^x + C_b^y + C_b^z\Big)G_{n_x,n_y,n_z,n_l;\vec{m},m_l} + \\ + C_b^x\Big(G_{n_x+1,n_y,n_z,n_l;\vec{m},m_l} + G_{n_x-1,n_y,n_z,n_l;\vec{m},m_l}\Big) + C_b^y\Big(G_{n_x,n_y+1\,n_z,n_l;\vec{m},m_l} + G_{n_x,n_y-1\,n_z,n_l;\vec{m},m_l}\Big) + \\ + C_b^z\,G_{n_x,n_y,n_z,n_l+1\;\vec{m};m_l} + C\,G_{n_x,n_y,n_z,n_l-1;\vec{m},m_l}\Big], \tag{7e}$$

f) $n_l \le n_a + n_b - 1$:

$$M_b\,\omega^2 G_{n_x,n_y,n_z,n_a+n_b-1;\vec{m},m_l} = \frac{i\hbar}{2\pi}\delta_{\vec{n},\vec{m}}\,\delta_{n_a,m_l} + \Big[2\Big(C_b^x + C_b^y + C_b^z\Big)G_{n_x,n_y,n_z,n_a+n_b-1\;\vec{m},m_l} + \\ + C_b^x\Big(G_{n_x+1,n_y,n_z,n_a+n_b-1;\vec{m},m_l} + G_{n_x-1,n_y,n_z,n_a+n_b-1;\vec{m},m_l}\Big) + C_b^y\Big(G_{n_x,n_y+1,n_z,n_a+n_b-1;\vec{m},m_l} + G_{n_x,n_y-1,n_z,n_a+n_b-1;\vec{m},m_l}\Big) + \\ + C_b^z\,G_{n_x,n_y,n_z,n_a+n_b-2;\vec{m},m_l} + C\,G_{n_x,n_y,n_z+1,0;\vec{m},m_l}\Big]. \tag{7f}$$

Due to the disturbance of translational symmetry of considered system the partial configuration Fourier transformation is introduced (this transformation is applied to coordinates x, y and z but not to coordinate l, where the translational symmetry is disturbed):

$$G_{\vec{n},n_l;\vec{m},m_l}(\omega)=\frac{1}{N}\sum_{\vec{k}} G_{n_l;m_l}\,\mathrm{e}^{i[a_xk_x(n_x-m_x)+a_yk_y(n_y-m_y)]}\,\mathrm{e}^{i[\tilde{a}(n_a+n_b)k_z(n_z-m_z)+J]}, \tag{8}$$

where $N=N_xN_yN_z$, $\vec{k}\equiv\{k_x,k_y,k_z\}$ and:

$$J=\begin{cases}1.\ \ a_ak_z(n_l-m_l) & , \quad n_l-m_l<n_a\\ 2.\ \ a_ak_z(n_a-1)+ak_z & , \quad n_l-m_l=n_a\\ 3.\ \ a_ak_z(n_a-1)+a\ _zk+a^bk_z(n_l-m_l-n_a) & , \quad n_a<n_l-m_l<n_a+n_b\\ 4.\ \ a_ak_z(n_a-1)+a^bk_z(n_b-1)+2a\ _zk & , \quad n_l-m_l=n_a+n_b\end{cases} \tag{9}$$

We will apply the transformation (8), first to the equation of motion (7a), i.e. in the case of $n_l=0$. In this way and after some simplification, this equation becomes:

$$\left[\omega^2-4\left(\Omega_{a_x}^2\sin^2\frac{a_xk_x}{2}+\Omega_{a_y}^2\sin^2\frac{a_yk_y}{2}\right)-\Omega_{a_z}^2-\Omega_a^2\right]G_{0;m_l}+$$
$$+\,\Omega_{a_z}^2\,\mathrm{e}^{ia_ak_z}G_{1;m_l}+\Omega_a^2\,\mathrm{e}^{iak_z}G_{n_a+n_b-1;m_l}=\frac{i\hbar}{2\pi M_a}\,\delta_{0,m_l}, \tag{10}$$

where the notations are introduced: $C_a^{x/y/z}/M_a\equiv\Omega_{a_{x/y/z}}^2$ and $C/M_a\equiv\Omega_a^2$. By repeating of the same evaluation procedure for every layer and introducing the notations analogous to those: $C_b^{x/y/z}/M_b\equiv\Omega_{b_{x/y/z}}^2$ and $C/M_b\equiv\Omega_b^2$, for $n_l\in(n_a,n_a+n_b-1)$, the system of n_a+n_b non-homogeneous algebraic-differential equations for Green's functions is obtained:

$$\left(\rho_i-1\right)G_{n_l;m_l}+k_i^2\,\mathrm{e}^{ia_ik_z}\,G_{n_l+1;m_l}+\mathrm{e}^{-ia\,k_z}\,G_{n_l-1;m_l}=\frac{i\hbar}{2\pi C_i}\,\delta_{n_l,m_l}, \tag{11}$$

where: $\Omega_i=\sqrt{C/M_i}$, $\Omega_{i;\alpha}=\sqrt{C_i^\alpha/M_i}$, $k_i=(\Omega_{i;\alpha}/\Omega_i)^2$,

$$\rho_i\equiv\rho_i^\alpha(k)=\frac{\omega^2-F_{xy}^{\ i}}{\Omega_i^2}-k_i \tag{12}$$

and $F_{xy}^i=4\left[\Omega_{i_x}^2\sin^2\left(a_xk_x/2\right)+\Omega_{i_y}^2\sin^2\left(a_yk_y/2\right)\right]+\Omega_{i_z}^2$.

These models can be reduced to the models of simple cubic lattices (and in this way simplified) with the help of following substitutions: $a_x^{a/b}=a_y^{a/b}=a_z=a$. Thus, we obtained the solvable systems of algebraic-difference equations. The unknown Green's functions are given by the formula: $G_{n;m}=D_m/D$, where D_m is the variable determinant and D is the determinant of the system. The poles of Green's functions, determining the dispersion laws of phonons, are found by setting the value of determinant D to zero. Expanding the determinant through numerical calculations only [7–9], we provide the adequate number of values for ρ, i.e. for frequencies ω_k. In this way, we determined the dispersion law of phonons in two-layered crystalline nano-structures.

Therefore, since the condition $D = 0$ is not analytically solvable, numerical analysis for some specific cases were performed here. Different combinations of numbers of n_a and n_b atoms were observed, as well as the changes in the relationship of the elastic constants between and within the films. During further analysis, superlattices built of films with the same atoms ($C_a = C_b \neq C$) were observed, but from n_a and n_b layers, namely in two cases:

- When the bond between the atoms within the layers is weaker than the bonds between the atoms from the boundary areas of films ($\alpha \equiv C_{a/b}/C = 0.5$);
- When the bond between the atoms within the layers is stronger than the bonds between the atoms from the boundary areas of films ($\alpha = 1.5$).

These two cases are shown graphically in Figures 2a–d and 3a–d, respectively, where the reduced phonon frequencies (ω/Ω) are given on the ordinates, and the reduced wave vectors along the z-direction ak_z $(n_a + n_b)/\pi$ are given on the abscissae. Only the center of the first Brillouin zone was considered ($k_x = k_y = 0$). Numbers of atoms in corresponding layers are given in parentheses (n_a, n_b).

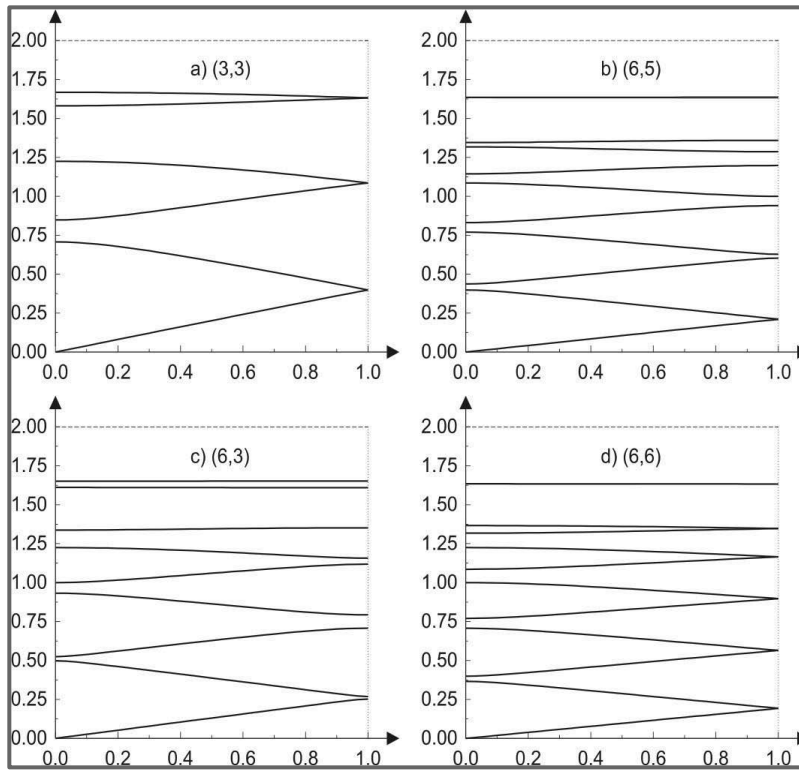

Figure 2: Phonon dispersion law for α = 0.5

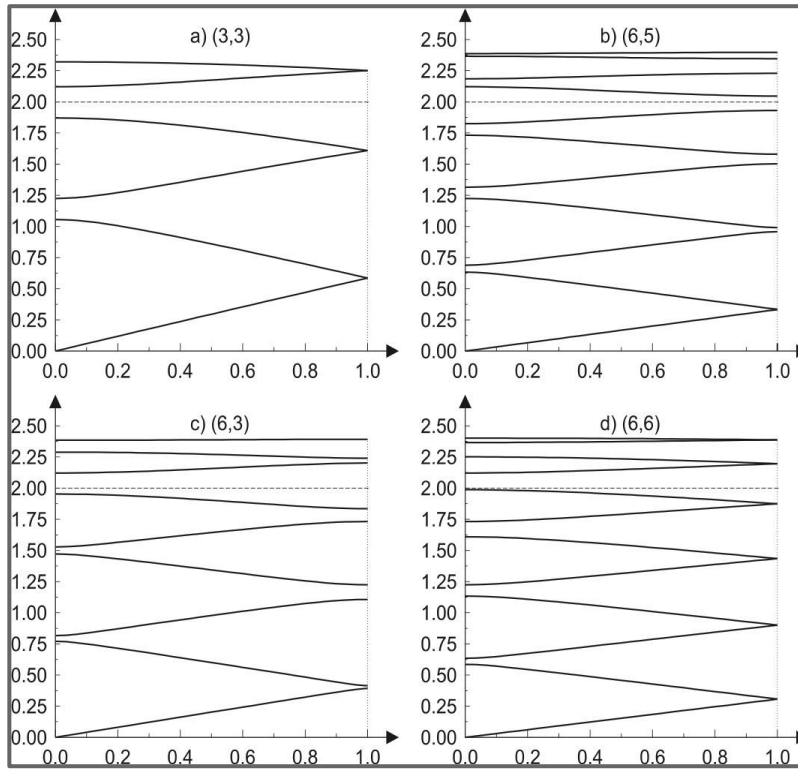

Figure 3: Phonon dispersion law for α = 1.5

During the analysis of the given figures, the following characteristics of the dispersion law of phonons in superlattices were observed:

- With an increase in the energy (reduced phonon frequency), phonon states thicken for all the observed values of a combination of numbers of atoms in the layers of the superlattices, as well as the parameters α and β, with the phenomenon being more pronounced in the case of stronger-bonded films ($\alpha = 0.5$).
- In the case of stronger bonds between the layers of superlattices ($\alpha = 0.5$), there is a suppression of energy levels within the bulk zone ($\omega/\Omega \approx 2$) for about 1/8 of its width, regardless of the total number of atoms $n_a + n_b$ within the basic motive of the superlattice. If the bond between the layers is weaker ($\alpha = 1.5$), the energy levels are thrown over the bulk zone for roughly the same amount. In this case, the number of dispersion branches N outside the zone is approximately given in the relations:
  - If $n_a + n_b$ is even $\Rightarrow N = (n_a + n_b - 2)/2$,
  - If $n_a + n_b$ is odd $\Rightarrow N = (n_a + n_b - 3)/2$.
- In the case of symmetric superlattices ($n_a = n_b$), dispersion branches are to be merged at the boundary of the first Brillouin zone.
- For the same values of the sum of the numbers of atoms in the layer of superlattice ($n_a + n_b$), the convergence of the highest dispersion branch is bigger, if the difference between the n_a and n_b is smaller.
- On the basis of the performed analysis, no symmetry of dispersion branches were observed, and there was no more pronounced regularity in the arrangement and breadth of the allowed. i.e. the forbidden energy zones.

The general formula for phonon frequencies can be expressed in the form:

$$\omega_k = \Omega \sqrt{A + B\,a^2 k^2}\ , \tag{13}$$

where $\Omega = \sqrt{C_{a/b} / M_{a/b}}$. The text below the formula (12) explains a procedure for obtaining the root (ρ_k) of the system determinants of difference equations (11). From the equations (12), phonon frequencies can be expressed in the form of:

$$\omega_k^2 \equiv \omega_k^2(\rho_k) \ \Rightarrow\ \omega_k = \omega_k(\rho_k^{1/2})\,.$$

Further elaboration leads to the anticipated form of the dispersion law, where:

$$k = \sqrt{k_x^2 + k_y^2}\ ; \quad A = \rho + 2\alpha\ ; \quad B = \alpha\ .$$

It is evident that the acoustic phonon dispersion law, i.e. phonon state energies in nanostructures is different to bulk ones. The most significant difference is related to the occurrence of an energy gap [1,7,8], which is a feature of the optical phonons. The size of the gap depends on the boundary conditions on the structure (nano-sample) surfaces and on (low) dimensions of these samples, the consequences of which are the quantum size and confinement effects. Consequently, spatial confinement of acoustic phonons in nanostructures affects their dispersion. It modifies acoustic phonon properties such as phonon group velocity, polarization, density of states, and changes the way acoustic phonons interact with other phonons, defects and electrons [13–17]. Such changes create opportunities for engineering phonon spectrum in nanostructures for improving electrical or thermal properties.

The interest in the subject substantially increased when it was pointed out that the confinement-induced changes in the acoustic phonon dispersion can strongly affect the thermal conductivity energy [18–20].

III.3. Phonon participation in superlattice thermodynamics

We will now put the analysis of the dispersion law aside, which can be found, for example, in our papers [7–9,21], and address the role of phonons in the process of heat transport, which are in such nanostructures significantly modified compared to bulk-structures. In Section 3, significant differences in ultrathin films have been shown, and here we are most interested in whether in superlattices, such as sandwich composite nanofilms, these effects are increased or not, and whether there are new signs as a result of the multiplicity of boundary surfaces.

In this regard, we will examine temperature behavior of the free and the internal energy, and using them we will be able to determine the role of phonons in the arrangement of the system in the processes of heat conduction.

Internal energy can be calculated using the standard formula [21–23]:

$$U_{\mathrm{SL}} = \sum_{k\alpha} \hbar\omega_{k\alpha} \left(\mathrm{e}^{\frac{\hbar\omega_{k\alpha}}{\theta}} - 1 \right)^{-1}\ , \tag{14}$$

where index α denotes three phonon polarizations and $\theta \equiv k_B T$. Going over in this formula from sum to integral [13–16], after long but elementary calculations, the following expression for internal energy is obtained:

$$U_{SL} = \frac{3N}{2\pi}\left(\frac{\Delta_m}{E_0}\right)^2 \theta \left\{\left[Z_1(\frac{\Delta_m}{\theta}) - \varepsilon^2 Z_1(\frac{\Delta_n}{\theta})\right] + \right.$$
$$\left. + 2\frac{\theta}{\Delta_m}\left[Z_2(\frac{\Delta_m}{\theta}) - \varepsilon Z_2(\frac{\Delta_n}{\theta})\right] + 2\left(\frac{\theta}{\Delta_m}\right)^2\left[Z_3(\frac{\Delta_m}{\theta}) - Z_3(\frac{\Delta_n}{\theta})\right]\right\}, \quad (15)$$

where: $E_0 = \hbar\Omega$, $\Delta_m = \hbar\Omega\sqrt{A + B\,ak_{\min}}$, $\Delta_n = \hbar\Omega\sqrt{A + B\,ak_{\max}}$, $\varepsilon = \frac{\Delta_n}{\Delta_m}$ and $Z_r(X) = \sum_{j=1}^{\infty} j^{-r}\,\mathrm{e}^{-jX}$ are the Dyson's functions. Differentiating this expression over absolute temperature [19–25] we obtain the expression for specific heat:

$$C_{SL} = \frac{3k_B}{2\pi}\left(\frac{\Delta_m}{E_0}\right)^2 \left\{\frac{\Delta_m}{\theta}\left[\left(\mathrm{e}^{\frac{\Delta_m}{\theta}} - 1\right)^{-1} - \varepsilon^3\left(\mathrm{e}^{\frac{\Delta_n}{\theta}} - 1\right)^{-1}\right] + \right.$$
$$+ 3\left[Z_1(\frac{\Delta_m}{\theta}) - \varepsilon^2 Z_1(\frac{\Delta_n}{\theta})\right] + 6\frac{\theta}{\Delta_m}\left[Z_2(\frac{\Delta_m}{\theta}) - \varepsilon Z_2(\frac{\Delta_n}{\theta})\right] + \quad (16)$$
$$\left. + 6\left(\frac{\theta}{\Delta_m}\right)^2\left[Z_3(\frac{\Delta_m}{\theta}) - Z_3(\frac{\Delta_n}{\theta})\right]\right\}.$$

As it is seen, whether the acoustical phonons were investigated in superlattice, the internal energy as well as the specific heat is exponentially small at low temperatures. The practical aspects of this effect were discussed in the previous section.

At the end of this section the phonon contribution into specific heat of superlattice (in accordance with last formula), film and bulk structures (in accordance with data from [26–28]) will be numerically analyzed. Film and superlattice are considered for "cut off" case, i.e. the deformations of boundary parameters of the system were not taken into account.

This analysis has shown that superlattice and film in the temperature range from zero to 35 K have practically equal specific heats. Their values are considerable lower than those of the bulk structure in the temperature range from zero to 7.5 K. At the temperature of 7.5 K the intersection of specific heat curves occurs and specific heats of film and superlattice become higher than the corresponding one of the bulk structure. This behavior of specific heats takes place up to 65 K for films and to 80 K for superlattice. At the temperatures above 35 K the specific heats of film and superlattice differ. The specific heat of superlattice is higher than that of the film. At the temperature about 65 K the specific heat of the bulk becomes higher than that of the film, but it is still lower than that superlattice. Finally, at the temperature of 80 K specific heat of the bulk structure exceeds the specific heat of the superlattice. After this temperature, the specific heat of the bulk is the highest, and then comes superlattice specific heat and finally specific heat of the film.

Exposed numerical estimates of the specific heat are presented in Fig.4. The relative specific heat is denoted with C, while x denotes relative temperature:

$$C_{\mathrm{b/f/s}} \equiv \frac{C_{\mathrm{b/f/s}}}{C_0}; \quad C_0 = \frac{k_{\mathrm{B}}}{2}\left(\frac{\Delta}{E_0}\right)^3; \quad x \equiv \frac{\theta}{\Delta}; \quad \Delta \approx 50\,k_{\mathrm{B}}.$$

(b – denotes bulk structure, while f – is related to the film and s –is related to the superlattice).

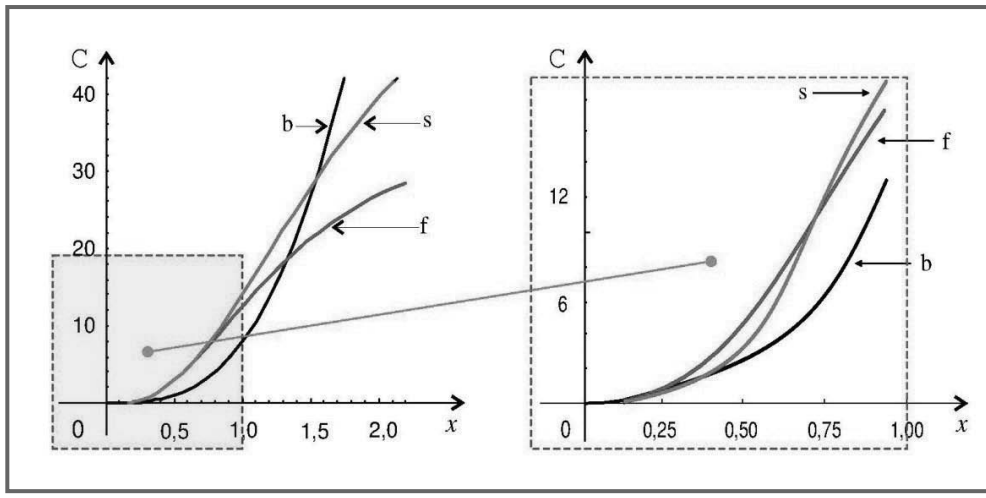

Figure 4: Temperature (left) and low-temperature (right) behavior of specific heats

The analysis of low-temperature thermodynamic properties has shown that it is expected for films and superlattices to be better superconductors than the corresponding bulk structures. It should be pointed out that at lower temperatures film and superlattice behave identically. Experimental confirmation of this statement can be found in [26 – 35]. At the temperatures below 10 K and above 80 K the specific heat of the bulk structure is higher than those of film and superlattice. It means that in the temperature ranges quoted, bulk possesses higher thermal conductivity, and consequently, in accordance with Wiedemann-Franz's law, the higher electrical conductivity. This conclusion is of some practical interest, because between 10 and 80 K films and superlattices have lower electrical resistance, which means that they can be used to save electric energy.

It is seen in Fig. 4 that the superlattice above 35 K has higher specific heat than film. It means that its thermal conductivity is higher. So, it can be concluded that metallic superlattices have the best chances for practical applications since at extremely low temperatures their superconductive properties are the same as those of films, but at higher temperatures they are better conductors than films. It is also evident from these figures that in the mid-temperature and high-temperature areas, the heat capacitances as well as the thermal conductivities of nanostructures are significantly lower that the same quantities in the bulk structures at the same temperatures.

References

[1] M.G.Cottam, D.R.Tilley, Introduction to Surface and Superlattice Excitations, *University Press*, Cambridge, 1989.

[2] B.S.Tošić, V.D.Sajfert, D.Popov, J.P.Šetrajčić, D.Ćirić,Application of Difference Calculus to Nanostructure analysis, *Academy of Sciences and Arts*, Novi Sad 2005 (in Serbian).

[3] C.Kittel, Quantum Theory of Solids, *Wiley*, New York 1963.

[4] C.Kittel, Introduction to Solid State Physics, *Wiley*, New York 1986.

[5] H.Ibach, H.Lüth, Solid–State Physics: An Introduction to Principles of Material Science, *Springer*, Berlin 2003.

[6] G.Strobl, Condensed Matter Physics: Crystals, Liquid Crystals, and Polymers, *Springer*, Berlin 2004.

[7] S.K.Jaćimovski, J.P.Šetrajčić, B.S.Tošić, V.D.Sajfert, Thermodynamics of Mechanical Oscillations in Superlattices, *Materials Science Forum***453-454**, 33-36 (2004).

[8] S.K.Jaćimovski, B.S.Tošić, J.P.Šetrajčić, V.M.Zorić, V.D.Sajfert, D.I.Ilić, Thermodynamics of Mechanical Oscillations in Crystalline Superlattices, *Int.J.Mod.Phys.*B **21**(6), 917-930 (2007).

[9] S.K.Jaćimovski, J.P.Šetrajčić, M.S.Jaćimovski and V.V.Stojanović, Phonon Contribution in Thermodynamics and Transport Properties of Ultrathin Ceramic Films, *Acta Phys.Pol.* A **126**/3, 811 (2014).

[10] E.N.Economou, Green's Functions in Quantum Physics, *Springer*, Berlin 1949.

[11] G.Rickayzen, Green's Functions and Condensed Matter, *Academic Press*, London 1980.

[12] S.Doniach, E.H.Sondheimer, Green's Functions for Solid State Physicists, *Imperial College Press*, London 1999.

[13] O.Manasreh, Semiconductor Heterojunctions and Nanostructures, *McGraw-Hill*, New York 2005.

[14] C.Delerue, M.Lannoo, Nanostructures -- Theory and Modelling, *Springer*, Berlin 2009.

[15] H.E.Schaefer, Nanoscience – The Science of the Small in Physics, Engineering, Chemistry, Biology and Medicine, *Springer*, Berlin 2010.

[16] M.C.Tringides, M.Jałochovski, E.Bauer, Quantum Size Effect in Metallic Nanostructures, *Physics Today*, April 2007, pp. 50–54.

[17] A.A.Balandin, D.L.Nika, Phononics in Low-Dimensionals Materials, *Materials Today***15**/6, 266 (2012).

[18] Nanoscale Energy transport and Hardvesting – A Computational Study, Ed. G.Zhang, *Taylor & Francis*, New York 2015.

[19] W.E.Bies, R.Radke, H.Ehrenreich, Phonon Dispersion Effect and Thermal Conductivity Reduction in GaAs/AlAs Superlattices, *http://xxx.lanl.gov./find/cond.mat*. No 0005028 (2000).

[20] Electron-Phonon Interactions in Low-Dimensional Structures, Ed. L.Challis, *University Press*, Oxford 2003.

[21] D.Popov, S.K.Jaćimovski, B.S.Tošić, J.P.Šetrajčić, Kinetics of Thin Films Mechanical Oscillations, *Physica* A **317**, 129-139 (2003).

[22] G.D.Mahan, Condensed Matter in a Nutshell, *University Press*, Princeton 2011.

[23] J.M.Ziman, Electrons and Phonons: The Theory of Transport Phenomena in Solids, *Oxford University Press*, New York 2001.

[24] M.A.Stroscio, M.Dutta, Phonons in Nanostructures, ISBN 0-521-79279-7; *University Press*, Cambridge 2004.

[25] L.C.Jackson, Low Temperature Physics, *Wiley & Sons*, New York 1962.

[26] B.S.Tošić, J.P.Šetrajčić, R.P.Đajić, D.Lj.Mirjanić, Phonons in Broken-Symmetry Structures, *Phys.Rev.*B **36**, 9094-9097 (1987).

[27] B.S.Tošić, J.P.Šetrajčić, D.Lj.Mirjanić, Z.V.Bundalo, Low temperature Properties of Thin Films, *Physica*A**184**, 354-366 (1992).

[28] D.Popov, V.Sajfert, B.S.Tošić, Thermodynamic and Kinetic Properties of Mechanical Oscillations in Thin Films, *Int.J.Mod.Phys.*B**20**/24, 3507-3532 (2006).

[29] S.K.Jaćimovski, Phonon Thermodynamics of Layered Nanostructures, Dr.Dissertation, *Faculty of Electrical Engineering*, Belgrade 2003 (in Serbian).

[30] J.P.Šetrajčić and S.K.Jaćimovski, Review of Results of Theoretical Approaches to Phonon Engineering of Thermodynamic Properties for Different Quantum Structures, *NBP***20**/3, 67 (2015).

[31] J.P.Šetrajčić, S.K.Jaćimovski, V.D.Sajfert, Phonon Contribution to Heat Capacitanceof Nanolayered Crystalline Structures, *Mod.Phys.Lett.*B **29**/4, 1550008 (2015); doi: 10.1142/S0217984915500086.

[32] J.P.Šetrajčić, V.M.Zorić, N.V.Delić, D.Lj.Mirjanić, S.K.Jaćimovski, Phonon Participation in Thermodynamics and Superconductive Properties of Thin Ceramic Films, Ch.15, pp.317-348, In Thermodynamics, Ed. M.Tadashi, *InTech*, Vienna 2011.

[33] J.P.Šetrajčić, S.K.Jaćimovski, D.Raković, D.I.Ilić, Phonon Spectra in Crystalline Nanostructures, in Electrical and Computer Engineering Series: Advances in Simulation, Systems Theory and Systems Engineering, Eds. N.E.Mastorakis, V.V.Kluev, Dj.Koruga, *WSEAS Press*, 2003; pp. 146-151.

[34] J.P.Šetrajčić, S.K.Jaćimovski, V.D.Sajfert, I.J.Šetrajčić, Specific Quantum Mechanical Solution of Difference Equation of Hyperbolic Type, *Commun.Nonlinear Sci.Numer.Simulat*. **19**/5, 1313 (2014).

[35] S.K.Jaćimovski, M.Bukurov, J.P.Šetrajčić, D.I.Raković, Phonon Thermal Conductivity of Graphene, Superlattices and Microstructures, http://dx.doi.org/10.1016/j.spmi.2015.09.027 – In Press (2015).

Appendix

GENERAL SOLUTION FOR DIFFERENCE EQUATIONS OF BOUNDED CRYSTALLINE STRUCTURE THEORY

General difference equation of condensed matter physics is solved using the operator method. The solution has general character, but only some concrete applications are discussed. This method gives the compact solution if the variable coefficient is of exponential type and it can be applied to the problem of founding atom displacements in crystalline chain with finite length. It is shown that the atom displacement represents the specific superposition of harmonic functions depends on space position.

A.1. *Introduction*

Difference equations [1 – 3] play important roll in condensed matter physics, especially in the problems connected with crystal structures. Probability amplitudes in one-particle wave function as well as Green's functions are the solutions of systems of difference equations. General type of difference equations defining mentioned quantities ,are the following:

$$Y_{n+1} + Y_{n-1} + xY_n = 0, \tag{1}$$

where integer n denotes place of atom or molecule, while x is parameter consisting physical characteristic of system.

If crystal structure is translational invariant [4,5], parameter x does not depend on integer n [6 – 9]. In the cases of broken symmetry (impurities, presence of boundaries etc), this parameter is dependent on molecule position. In the mentioned cases difference equation (1) goes over to equation with variable coefficient $x \equiv x_n$, i.e.

$$Y_{n+1} + Y_{n-1} + x_n Y_n = 0. \tag{2}$$

In the next section the general procedure of solving the equation (1) will be exposed. A particular example will be solved, too.

A.2. *General operator solution*

The homogeneous difference equation of second kind (2), will be solved using operator's method. The application of this method requires introduction of translation operators $\hat{T}_l$ ($l \in \mathbb{N}$) obeying the following rules:

$$\begin{aligned} &\hat{T}_l f_n = f_{n+l}; \quad \hat{T}_l = \left(\hat{T}_1\right)^l \equiv \hat{T}_1^l; \\ &\hat{T}_l \cdot \hat{T}_k = \hat{T}_{l+k}; \quad \hat{T}_{-l} = \hat{T}_1^{-l}; \quad \hat{T}_0 = 1. \end{aligned} \tag{3}$$

Taking this into account, the equation (2) can be written in the form:

$$\left(\hat{T}_1 + \hat{T}_{-1} + x_n\right) Y_n = 0. \tag{4}$$

Operator's solving requires that at least one of the left-hand side operators in (4) give zero acting to the constant. It is easily seen that no one of operators, i.e. $\hat{T}_1 + \hat{T}_{-1}$ and x_n satisfies this requirement. Therefore we shall transform (4) in the following way:

$$\left[\left(\hat{T}_1 + \hat{T}_{-1}\right) - 2 + \left(x_n + 2\right)\right] Y_n = 0, \tag{5}$$

where it is seen now that translational operator acting to constant gives zero.

In order to make calculations more clear and compact, we shall introduce the following notations: $\hat{a} \equiv \hat{T}_1 + \hat{T}_{-1} - 2$ and $\hat{b}_n \equiv x_n + 2$. The equation (5) now has the form:

$$\left(\hat{a} + \hat{b}_n\right) Y_n = 0. \tag{6}$$

In this way the operator form in (5) is prepared for application of operator method. The operator's method gives the solution of homogeneous difference equation expressed over two linearly independent solutions of the corresponding non-homogeneous equation:

$$\left(\hat{a} + \hat{b}_n\right) y_n = \Phi_n, \tag{7}$$

for a suitable function Φ_n. Really, if (7) has two linearly independent solutions $y_n^{(1)}$ and $y_n^{(2)}$, then the following is valid:

$$\begin{aligned} \left(\hat{a} + \hat{b}_n\right) y_n^{(1)} &= \Phi_n, \\ \left(\hat{a} + \hat{b}_n\right) y_n^{(2)} &= \Phi_n. \end{aligned}$$

Subtracting these equations and comparing this result with (6) we conclude:

$$\begin{aligned} &\left(\hat{a} + \hat{b}_n\right)\left(y_n^{(1)} - y_n^{(2)}\right) = 0 \\ &\Rightarrow \quad Y_n \equiv y_n^{(1)} - y_n^{(2)}. \end{aligned} \tag{8}$$

The further question is how to find the functions $y_n^{(1)}$ and $y_n^{(2)}$? The formal solution of (7) is:

$$y_n = \left(\hat{a} + \hat{b}_n\right)^{-1} \Phi_n. \tag{9}$$

Now, it can be shown that there do exist two independent forms of the inverse operator:

$$\left(\hat{a} + \hat{b}_n\right)^{-1} = \begin{cases} \left[\hat{b}_n\left(1 + \hat{b}_n^{-1}\hat{a}\right)\right]^{-1} = \left(1 + \hat{b}_n^{-1}\hat{a}\right)^{-1}\hat{b}_n^{-1} = \\ \qquad = \sum_{k=0}^{\infty}(-1)^k\left(\hat{b}_n^{-1}\hat{a}\right)^k \hat{b}_n^{-1}, \\ \left[\hat{a}\left(1 + \hat{a}^{-1}\hat{b}_n\right)\right]^{-1} = \left(1 + \hat{a}^{-1}\hat{b}_n\right)^{-1}\hat{a}^{-1} = \\ \qquad = \sum_{k=0}^{\infty}(-1)^k\left(\hat{a}^{-1}\hat{b}_n\right)^k \hat{a}^{-1}. \end{cases}$$

Taking this into account we can write:

$$\begin{aligned} y_n^{(1)} &= \left(1 - \hat{b}_n^{-1}\hat{a} + \hat{b}_n^{-1}\hat{a}\hat{b}_n^{-1}\hat{a} - \cdots\right)\hat{b}_n^{-1}\Phi_n, \\ y_n^{(2)} &= \left(1 - \hat{a}^{-1}\hat{b}_n + \hat{a}^{-1}\hat{b}_n\hat{a}^{-1}\hat{b}_n - \cdots\right)\hat{a}^{-1}\Phi_n. \end{aligned} \tag{10}$$

Until now, Φ_n has been suitable. But, if we take that $\Phi_n \equiv \hat{b}_n$, then (10) gives:

$$\begin{aligned} y_n^{(1)} &= 1, \\ y_n^{(2)} &= \hat{a}^{-1}\hat{b}_n - \hat{a}^{-1}\hat{b}_n\hat{a}^{-1}\hat{b}_n + \hat{a}^{-1}\hat{b}_n\hat{a}^{-1}\hat{b}_n\hat{a}^{-1}\hat{b}_n - \cdots \end{aligned} \tag{11}$$

Taking into account formulas (10) and (11), we conclude that the solution of homogeneous equation (8) is given as follows:

$$Y_n = \sum_{k=0}^{\infty}(-1)^k\left(\hat{a}^{-1}\hat{b}_n\right)^k. \tag{12}$$

We can find now the explicit form of the operator $\hat{a}^{-1} \equiv \left(\hat{T}_1 + \hat{T}_{-1} - 2\right)^{-1}$:

$$\hat{a}^{-1} = \begin{cases} \left\{-2\left[1 - \frac{1}{2}\left(\hat{T}_1 + \hat{T}_{-1}\right)\right]\right\}^{-1} = \\ \quad = -\sum_{k=0}^{\infty} 2^{-(k+1)}\left(\hat{T}_1 + \hat{T}_{-1}\right)^k, & \text{(a)} \\ \left\{\left(\hat{T}_1 + \hat{T}_{-1}\right)\left[1 - 2\left(\hat{T}_1 + \hat{T}_{-1}\right)^{-1}\right]\right\}^{-1} = \\ \quad = \sum_{k=0}^{\infty} 2^k\left(\hat{T}_1 + \hat{T}_{-1}\right)^{-(k+1)}. & \text{(b)} \end{cases} \tag{13}$$

One can see that the down expression figures power of the operator $\left(\hat{T}_1 + \hat{T}_{-1}\right)^{-1}$. This operator can be written in two ways:

$$\left(\hat{T}_1 + \hat{T}_{-1}\right)^{-1} = \begin{cases} \left[\hat{T}_1\left(1 + \hat{T}_{-2}\right)\right]^{-1} = \sum_{k=0}^{\infty}(-1)^k\hat{T}_{-(2k+1)}, & \text{(a)} \\ \left[\hat{T}_{-1}\left(1 + \hat{T}_2\right)\right]^{-1} = \sum_{k=0}^{\infty}(-1)^k\hat{T}_{2k+1}. & \text{(b)} \end{cases} \tag{14}$$

Now, all necessary elements for application for operator method are given.

A.3. *Applying the general solution*

The exposed method will be applied on the particular example: phonon subsystem in crystalline chain. One dimensional propagation of mechanical waves in condensed matter physics describes, in the nearest neighbor approximation [4,5], by consideration of difference equation:

$$u_{n+1} + u_{n-1} + \rho u_n = 0 \tag{15}$$

valid for small displacements u_n of atom/molecule from its equilibrium site $n \in [0, N]$. For ultra-short ($L = Na$) crystalline chain [10 – 12], the quantity: $\rho \equiv \rho_n = 2(\cos n\xi - 1)$, $\xi \equiv \xi(\omega)$. The expression (15) is equivalent to (2) and we can apply described operator method. It is seen from (5) and (6) that $b_n = \mathrm{e}^{in\xi} + \mathrm{e}^{-in\xi}$.

At the beginning, we shall look for the function $\hat{a}^{-1}\mathrm{e}^{in\xi}$ representing the operator $\hat{a}^{-1}$ by the formula (13a). Since

$$\left(\hat{T}_1+\hat{T}_{+1}\right)^{-1}\mathrm{e}^{in\xi}=2\,\mathrm{e}^{in\xi}\cos\xi,$$

it follows:

$$\begin{aligned}\hat{a}^{-1}\mathrm{e}^{in\xi} &= -\frac{1}{2}\mathrm{e}^{in\xi}-\frac{1}{2^2}\left(\hat{T}_1+\hat{T}_{-1}\right)^{+1}\mathrm{e}^{in\xi}-\frac{1}{2^3}\left(\hat{T}_1+\hat{T}_{-1}\right)^{+2}\mathrm{e}^{in\xi}-\cdots= \\ &= -\left(\frac{\mathrm{e}^{in\xi}}{2}+\frac{\mathrm{e}^{in\xi}}{2}\cos\xi+\frac{\mathrm{e}^{in\xi}}{2}\cos^2\xi+\cdots\right)= \\ &= -\frac{\mathrm{e}^{in\xi}}{2}\sum_{k=0}^{\infty}\cos^k\xi=\frac{-\mathrm{e}^{in\xi}}{2(1-\cos\xi)}.\end{aligned}$$

In further we have calculated

$$\begin{aligned}\left(\hat{a}^{-1}\mathrm{e}^{in\xi}\right)^2 &= \hat{a}^{-1}\mathrm{e}^{in\xi}\,\frac{-\mathrm{e}^{in\xi}}{2(1-\cos\xi)}= \\ &= \frac{\mathrm{e}^{2in\xi}}{2^2(1-\cos\xi)(1-\cos 2\xi)},\end{aligned}$$

wherefrom it can be easily concluded

$$\left(\hat{a}^{-1}\mathrm{e}^{in\xi}\right)^k=\frac{(-1)^k\,\mathrm{e}^{kin\xi}}{2^k\prod_{q=1}^{k}(1-\cos q\xi)};\quad k=1,2,3,\cdots \tag{16}$$

On the basis the general story exposed in the previous section, we must look for the solution $u_n(\xi)$ by (16), which satisfies the difference equation:

$$\left(\hat{a}+\mathrm{e}^{in\xi}\right)u_n(\xi)=0. \tag{17}$$

If we multiply this equation by $\mathrm{e}^{-2in\xi}$ from left-hand site, and to the obtained equation add (17), we obtain:

$$\left(\hat{\alpha}_n+b_n\right)u_n(\xi)=0, \tag{18}$$

where: $\hat{\alpha}_n\equiv\left(1+\mathrm{e}^{-2in\xi}\right)\hat{a}$ and $b_n\equiv 2\cos n\xi$. From (12), the solution of the upper equation goes over to:

$$u_n(\xi)=\sum_{k=0}^{\infty}(-1)^k\left(\hat{\alpha}^{-1}b_n\right)^k. \tag{19}$$

It is easy to prove that is: $\hat{\alpha}^{-1}b_n\equiv\hat{a}^{-1}\mathrm{e}^{in\xi}$, so from (16) and (19), the searched solution is:

$$u_n(\omega)\equiv u_n(\xi)=\sum_{k=0}^{\infty}\frac{\mathrm{e}^{in\xi(\omega)}}{2^k\prod_{q=1}^{k}\left[1-\cos q\xi(\omega)\right]}. \tag{20}$$

It is seen that atom displacement represents the specific superposition of harmonic function depends on space position. Physically, it represents by the superposition of progressive plane and standing waves.

References

[1] Abdul J.Jerri, Linear Difference Equations with Discrete Transforms Method, *Kluwer Ac. Publ*., Dordrecht 1996.

[2] Saber N.Elaydi, S.Axler, F.W.Gehring, K.A.Ribet, An Introduction to Difference Equations, *Springer-Verlag*, New York 1999.

[3] L.Brand, Differential and Difference Equations, *J.Wiley & Sons*, New York 1966.

[4] G.Mahan, Many Particle Physics, *Plenum Press*, New York 1990.

[5] G.Rickayzen, Green's Functions and Condensed Matter, *Academic Press*, London 1980.

[6] S.G.Davison and M.Steslicka, Basic Theory of Surface States, *Clarendon Press*, Oxford 1996.

[7] M.Pruton, Introduction to Surface Physics, *Clarendon Press*, Oxford 1995.

[8] I.D.Vragović, R.Fürstenberg, S.M.Stojković, J.P.Šetrajčić, D.Lj.Mirjanić, Phonon Spectra of Quantum Wires, *Novi Sad J.Math*. **30**/3, 185 (2000).

[9] S.K.Jaćimovski, D.I.Ilić, I.K.Junger, J.P.Šetrajčić, Microtheoretical and Numerical Calculation of Phonon Spectra in Superlattices, *Novi Sad J.Math*. **31**/1, 55 (2001).

[10] J.P.Šetrajčić, B.S.Tošić, S.K.Jaćimovski, V.D.Sajfert, V.M.Zorić, S.M.Vučenović, Difference Equations of Atom Displacements in Space-Bounded Crystalline Chains, *General Conference of Serbia & Montenegro Physicians*, Petrovac 2004.

[11] J.P.Šetrajčić, B.S.Tošić, Mathematical Physics: Difference Equations and Green's Functions, *Faculty of Sciences*, Novi Sad 2004.

[12] S.Lazarev, D.Lj.Mirjanić, M.Pantić, B.S.Tošić and J.P.Šetrajčić, Phonons in Ultrathin Layered Structures, *J.Phys.Chem.Sol.***60**, 849 (1999).

IV. CONCLUSION AND DISCUSSION

Temperature analysis of phonon contribution to the thermodynamic characteristics behavior of nano-layered structures (ultrathin films and superlattices) was carried out in detail. The main results follow.

The results of the analyses of phonons in ultrathin films can be summarized as follows:

1. The method of calculation of Green functions in broken symmetry structures (these Green functions depend on two spatial coordinates separately) is formulated. The analyses with help of this Green function method reproduced a physically sound fact: the properties of broken symmetry structure are spatially dependent.
2. The density of three-layer film is minimal at the middle of the film. The kinetic energy is also minimal at the middle of the film and maximal at boundary layers. This is physically acceptable since the boundary atoms are semi free.
3. The energies per atom in film depend on the index labeling film layers. It is maximal in the middle of the film. It means that the potential energy in films is more significant than the kinetic one. The most practically important result is the presence of energy gap in phonon spectra of ultrathin films.
4. Comparing the specific heat of film with the specific heat of ideal structure we found that the specific heat curves have two intersections points and these intersections are quoted in this work. From $T = 0$ K up to first intersection point specific heat of film is several orders of magnitude less than the specific heat of the ideal structures. The same is valid for thermal conductivities: the low temperature thermal conductivity of the film is noticeably less than that of the ideal structure. It emphasizes that at the low temperatures the films process thermal insulation properties extremely well.

At the temperatures higher than the second intersection temperature point the thermal conductivity of the film is less than that of the ideal structure but their differences are not extremely high.

In the temperature interval, which lies in domain (50 – 100 K) approximately, the specific heat of the film as well as thermal conductivity is insignificantly higher than these characteristics of the ideal structure.

It was shown that phonon transport in superlattices can be significantly modified due to formation of mini-bands and emergence of the mini-umklapp process, a new type of umklapp scattering processes associated with transitions between the mini-Brillouin zones. The modification of phonon transport comes from the crystal lattice periodicity in the direction of superlattice layering. In such a case, the mini-reciprocal lattice vectors associated with superlattice mini-zones give rise to mini-processes that contribute to the thermal resistance.

The situation is quite different in ultrathin films, which are either free standing or embedded into material with distinctively different elastic properties [29]. Here, the phonon dispersion changes due to the phonon spatial confinement induced by the boundaries. This affects all phonon relaxation rates, and makes the thermal transport properties different from those of superlattices. In this paper, we address the issue of how spatial confinement of acoustic phonon modes directly modifies the lattice thermal conductivity in a nanofilm and corresponding superlattice.

It was very interesting for us, and a bit unexpected, that the differences in the corresponding thermodynamic quantities, relative to the bulk-structure, are more pronounced in single (solo) ultrathin films, than in multilayered films – superlattices. This is imposed as a very important conclusion. Effects of dimensional quantization and confinement, which are important for nano-films (in parallel films, i.e. superlattices, they are amplified), are damped and their behavior is closer to the behavior of corresponding quantities in bulk-structures.

At the temperatures below 10 K and above 80 K the heat capacitance of the bulk-structure is higher than those of ultrathin films and superlattices. It means that in the temperature ranges quoted bulk possesses higher thermal conductivity, and consequently, in accordance with Wiedemann-Franz's law, the higher electrical conductivity. This conclusion is of some practical interest, because between 10 and 80 K ultrathin films and superlattices have lower electrical resistance, which means that they can be used for the storage of electric energy.

The general conclusion of higher-temperature analysis presented here is that the main thermodynamic characteristics of both nano-structures (ultrathin films and superlattices) are considerably lower than those of the bulk-structure. Consequently, their superconductive characteristics are better than the superconductive characteristics of corresponding bulk-structures. Experimental confirmation of this statement can be found in cited Refs. This analysis of temperature behavior of thermodynamic properties has shown that it is expected for ultrathin films to be better superconductors than the corresponding superlattice-structures and much better than bulk ones.

Consequently, the paper shows that the apparent changes in the dispersion law of acoustic phonons in nanostructures caused by quantum size and confinement effects have a direct implication on the significant reductions of their thermal characteristics in relation to the ones in the bulk structures. The volume of the reduction certainly depends on the boundary conditions of nanostructures: for films – on the thickness, i.e. the number of crystallographic planes, as well as on the values of boundary parameters (phonon interactions) on the surface-planes, and for superlattices – on the period, the transmission ratio and the value of boundary parameters (phonon interactions) on the surfaces of the primitive cell. These dependencies are not presented in the paper because this is an ongoing research and their impact is being tested and will be the subject of our next report. Here we focus only on the general guidelines and outlined tendencies and analytical application of the Green's functions method to the testing of the share of phonons in thermal behavior of nanostructures, and qualitative indicators of possible effects of the fundamental confinement effects to the macroscopic properties of the samples have been obtained.

Since phonons with Debye frequencies are responsible for electrically and thermally induced transport properties of material, it follows that the nanowire will be inferior electrical and thermic conductor in contrast with the relative massive structures, providing there are no chemical and structural differences between them. On the other hand, it is a well-known fact that the more inferior electrical conductor material is (under normal conditions), the better superconductor it becomes. Due to that, the experimental fact can be concluded and justified, that in spatially very confined structures more qualitative superconductive properties have been achieved.

Acknowledgements

The greatest thanks the author owes to his teacher, mentor and friend, unfortunately, recently deceased Academician, Prof. Dr. Bratislav S. Tošić. His proper and quality oriented suggestions had crucial impact on the value and importance of this work.

This paper was in part supported by the Serbian Ministry of Education, Science and Technological Development (Grants: ON-171039 and TR-34019) and Ministry of Science and TechnologyOf Republic of Srpska (Grants: 19/6-020/961-15/16) as well as the Vojvodina Provincial Secretariat for Science and Technological Development (Grant 114-451-2092/2016).

AUTHOR INDEX

CIP – Каталогизација у публикацији
Народна библиотека Србије, Београд

66.017/.018:538.945
544.223.22
621.315.5

ŠETRAJČIĆ, Jovan P., 1951-
Phonon Engineering Theory of Crystalline Layered Nanostructures / Jovan P. Šetrajčić, Stevo K. Jaćimovski, Siniša M. Vučenović. - Belgrade : Academy of Criminalistic and Police Studies, 2016 (Belgrade : Pekograf). - 112 str. : ilustr. ; 24 cm

Tiraž 100. - Bibliografija uz svako poglavlje. - Registar. - Sadrži i: General Solution for Difference Equations of Bounded Crystalline Structure Theory.

ISBN 978-86-7020-370-9
1. Jaćimovski, Stevo K., 1955- [аутор] 2. Vučenović, Siniša M., 1971- [аутор]
a) Наноматеријали - Суперпроводљивост b) Суперпроводници
COBISS.SR-ID 228288268